

1

2       **The enteric nervous system of the *C. elegans* pharynx is specified by**  
3       **the Sine oculis-like homeobox gene *ceh-34***

4

5       Berta Vidal, Burcu Gulez, Wen Xi Cao, Eduardo Leyva-Diaz, Molly B Reilly, Tessa  
6       Tekieli and Oliver Hobert

7       Department of Biological Sciences, Columbia University, Howard Hughes Medical Institute,  
8       New York, NY, USA

9

10   **ABSTRACT**

11       Overarching themes in the terminal differentiation of the enteric nervous system, an  
12   autonomously acting unit of animal nervous systems, have so far eluded discovery. We  
13   describe here the overall regulatory logic of enteric nervous system differentiation of the  
14   nematode *Caenorhabditis elegans* that resides within the foregut (pharynx) of the worm. A *C.*  
15   *elegans* homolog of the *Drosophila* Sine oculis homeobox gene, *ceh-34*, is expressed in all  
16   14 classes of interconnected pharyngeal neurons from their birth throughout their life time,  
17   but in no other neuron type of the entire animal. Constitutive and temporally controlled *ceh-34*  
18   removal shows that *ceh-34* is required to initiate and maintain the neuron type-specific  
19   terminal differentiation program of all pharyngeal neuron classes, including their circuit  
20   assembly. Through additional genetic loss of function analysis, we show that within each  
21   pharyngeal neuron class, *ceh-34* cooperates with different homeodomain transcription factors  
22   to individuate distinct pharyngeal neuron classes. Our analysis underscores the critical role of  
23   homeobox genes in neuronal identity specification and links them to the control of neuronal  
24   circuit assembly of the enteric nervous system. Together with the pharyngeal nervous system  
25   simplicity as well as its specification by a Sine oculis homolog, our findings invite speculations  
26   about the early evolution of nervous systems.

27

28

## 29 INTRODUCTION

30 Across animal phylogeny, enteric nervous systems constitute a self-contained,  
31 autonomously acting neuronal network that detects physiological conditions to control the  
32 peristaltic movement of food through the digestive tract (Ayali, 2004; Copenhaver, 2007;  
33 Fung and Vanden Berghe, 2020; Hartenstein, 1997; Laranjeira and Pachnis, 2009). Because  
34 of structural and functional autonomy, the enteric nervous system has been referred to as a  
35 “second brain” (Gershon, 1998). In mammals, the enteric nervous system is composed of  
36 around 20 different neuron types, categorized into intrinsic sensory, inter- or motor neurons,  
37 which line the interior lumen of different sections of the digestive system (Drokhlyansky et al.,  
38 2020; Furness, 2000). While progress has been made in understanding early developmental  
39 patterning events that establish the fate of neurons in the enteric nervous system of  
40 mammals (Nagy and Goldstein, 2017; Sasselli et al., 2012), fish (Ganz, 2018) and flies  
41 (Copenhaver, 2007; Myers et al., 2018), much less is known about terminal differentiation  
42 programs of enteric neurons, both in vertebrate and invertebrate models (Copenhaver, 2007;  
43 Hao and Young, 2009; Memic et al., 2018; Morarach et al., 2021; Rao and Gershon, 2018).  
44 Specifically, it has remained unclear as to whether there are common unifying themes in how  
45 enteric neurons acquire their terminally differentiated state. This is particularly interesting  
46 from an evolutionary standpoint. The function of enteric neurons in controlling feeding  
47 behavior is an ancient one that may precede the evolution of the bilaterian central nervous  
48 system (Cook et al., 2020; Furness and Stebbing, 2018; Gilbert, 2019; Koizumi, 2007).  
49 Understanding how enteric neurons acquire their terminal features may therefore provide  
50 novel insights into nervous system evolution.

51 The nematode *C. elegans* contains an autonomously acting nervous system in its  
52 foregut, the pharynx, composed of 20 synaptically interconnected neurons that fall into 14  
53 anatomically distinct classes, (Albertson and Thomson, 1976; Cook et al., 2020; Mango,  
54 2007)(**Fig.1**). Due to its association with the digestive tract of the worm, the pharyngeal  
55 nervous system can be considered to be the enteric nervous system of *C. elegans*. Apart  
56 from this anatomical association, the pharyngeal nervous system shares functional features  
57 of enteric nervous systems of more complex animals. It is required for movement of food  
58 through the digestive tract of the worm and functions in an entirely autonomous manner, even  
59 if removed from the rest of the animal (Albertson and Thomson, 1976; Avery, 2012; Cook et  
60 al., 2020; Mango, 2007). Like other enteric nervous systems, the nematode pharyngeal



nervous system constitutes a non-centralized neuronal network isolated from the rest of the nervous system and, in rough analogy to the vagus nerve, is connected to the remainder of the nervous system through a single nerve fiber, that of the bilateral RIP neuron pair (Albertson and Thomson, 1976; Cook et al., 2020; Cook et al., 2019; White et al., 1986). Like vertebrate enteric neurons (Fung and Vanden Berghe, 2020), pharyngeal neurons have sensory, inter- and motorneuron function (Avery and Horvitz, 1989; Cook et al., 2020; Trojanowski et al., 2014).

Our recent re-analysis of pharyngeal nervous system anatomy has shown that rather than segregating these functions over distinct neurons as vertebrates do (Fung and Vanden Berghe, 2020), most pharyngeal neurons each combine sensory, inter- and motorneuron function, i.e. are polymodal (Cook et al., 2020). The 14 distinct pharyngeal neurons types are defined by their unique anatomy, i.e. axonal projections, morphology, synaptic connectivity (**Fig.1B,C**)(Cook et al., 2020) and unique functional features (Avery and Horvitz, 1989; Trojanowski et al., 2014). This anatomical and functional classification has recently been further extended by the description of their unique molecular fingerprint, determined by scRNA transcriptomic analysis (Taylor et al., 2021)(**Fig.1D**). For example, each pharyngeal neuron class is uniquely defined by characteristic signatures of neurotransmitter systems, from acetylcholine (ACh), glutamate (Glu) to serotonin, and by unique combinations of neuropeptide-encoding genes (**Fig.1E**). While pharyngeal neurons are clearly different from one another, scRNA profiling has shown that their molecular signatures are more similar to each other than to other neurons in the nervous system (Taylor et al., 2021)(**Fig.1D**).

One fascinating aspect of the *C. elegans* pharyngeal nervous system is that it has an appearance of what one could imagine an ancestral, primitive nervous system to have looked like. Primitive nervous systems are generally thought to have emerged in the context of monolayers of epithelial cells, with individual cells in such layers specializing into primitive sensory-motor-type neurons (Arendt, 2008; Mackie, 1970; Varoqueaux and Fasshauer, 2017). These diffusely organized neurons may have sensed the environment and relayed such sensory information to the other primitive cell type thought to have arisen early in evolution, namely, contractile “myoepithelial” cells that were able to generate motion. The organization of the *C. elegans* pharynx reveals some striking parallels to such a presumptive primitive nervous system: It is also essentially a single monolayer of cells that is organized into a tubular structure and the vast majority of constituent cells are myoepithelial cells

93 (pharyngeal muscle) and polymodal, interconnected sensory/motor neurons (Cook et al.,  
94 2020; Mango, 2007; Portereiko and Mango, 2001). Pharyngeal neurons combine sensory,  
95 inter- and motor neuron features and are also not localized to ganglia but rather diffusely  
96 localized, resembling the architecture of more ancient nerve nets (Albertson and Thomson,  
97 1976; Watanabe et al., 2009). The interconnectivity of pharyngeal neurons displays also less  
98 selectivity than non-pharyngeal neurons, such that mere physical proximity is an almost  
99 sufficient criterion for connectivity (Cook et al., 2020). Moreover, pharyngeal neurons are  
100 closely related to non-neuronal pharyngeal cells by lineage; for example, some muscle and  
101 neurons derive from a common mother cell (Sulston et al., 1983). The idea of enteric neurons  
102 being reflective of an early, primitive state of the nervous system has also been brought  
103 forward in the context of comparing enteric nervous systems from widely divergent species  
104 (Furness and Stebbing, 2018; Gilbert, 2019). Specifically, these authors argued that the  
105 nerve net-like hydra nervous system displays features of the vertebrate enteric nervous  
106 system.

107         The self-contained and hypothetically primitive state of the *C. elegans* enteric nervous  
108 system, with all its unique features, encouraged us to use this system as a model to probe  
109 several concepts of neuronal identity specification that have emerged from the centralized,  
110 non-pharyngeal nervous system of *C. elegans*: (1) The first is the concept of terminal  
111 selectors, transcription factors that act in a master-regulatory manner to coordinately control  
112 the many identity features of a terminally differentiating neuron (Hobert, 2016). Are members  
113 of terminal gene batteries in each pharyngeal neuron also controlled in a coordinated  
114 manner, via terminal selectors? One study in the NSM neurons provided some limited  
115 evidence in this regard (Zhang et al., 2014), but how broadly this applies throughout the  
116 pharyngeal nervous system was less clear. (2) Second, homeodomain transcription factors  
117 have a predominant role as terminal selectors of neuronal identity in the non-pharyngeal  
118 nervous system (Hobert, 2021; Reilly et al., 2020). A recent cataloguing of the expression  
119 patterns of all homeodomain proteins in the *C. elegans* genome revealed that each one of the  
120 *C. elegans* 118 neuron classes, including the pharyngeal neurons, display a unique  
121 combinatorial signature of homeodomain protein expression (Reilly et al., 2020). Are all  
122 pharyngeal neurons indeed specified by homeodomain protein combinations? (3) Lastly,  
123 there is evidence from both *C. elegans* (Berghoff et al., 2021; Pereira et al., 2015) and other  
124 systems (Brunet and Pattyn, 2002), that synaptically connected neurons are often specified

125 by the same transcription factor, suggesting that such transcription factors may be involved in  
126 assembling neurons in functional circuitry. We have termed such transcription factors “circuit  
127 organizers” (Berghoff et al., 2021; Pereira et al., 2015) and sought to test whether the  
128 isolated pharyngeal circuitry is similarly specified by a circuit organizer transcription factor.

129 In this paper, we show that all three predictions are fulfilled in the context of the  
130 nematode’s pharyngeal/enteric nervous system. We show that a *C. elegans* ortholog of the  
131 Sine oculis/Six1/Six2 homeobox gene, *ceh-34*, is expressed in all pharyngeal neurons from  
132 their birth throughout their life time. Its expression is induced by the foregut organ selector  
133 gene *pha-4/FoxA*. We demonstrate that *ceh-34* initiates and maintains the terminally  
134 differentiated state of all synaptically connected pharyngeal neurons, that *ceh-34* is required  
135 to assemble pharyngeal neurons into proper circuitry and that in distinct pharyngeal neuron  
136 types, *ceh-34* cooperates with distinct homeobox genes to specify their respective identity.  
137 Taken together, our studies further substantiate overarching themes of nervous system  
138 development and potentially provide insights into the evolution of nervous systems.

139

140

## 141 RESULTS

142

### 143 Expression of paralogous genes *ceh-34* and *ceh-33*, the two *C. elegans* Sine 144 oculis/Six1/2 orthologs

145 Genome sequence mining revealed several *C. elegans* homologs of the Sine  
146 oculis/Six family of homeodomain proteins (Ruvkun and Hobert, 1998) whose founding  
147 member was first identified in *Drosophila* for its role in eye patterning (Cheyette et al., 1994).  
148 This specific homeodomain transcription factor family is characterized by the presence of a  
149 conserved domain, located N-terminally to the DNA binding homeodomain, the ~150 amino  
150 acid long SIX domain, involved in both protein-DNA, as well as protein-protein interactions  
151 (Kumar, 2009; Patrick et al., 2013). *C. elegans* Six-type homeodomain proteins fall into  
152 several, phylogenetically conserved families, the Sine oculis/Six1/2, the Six4/5 and the Six3/6  
153 subfamily (Dozier et al., 2001; Kumar, 2009). We focus here on the Sine oculis subfamily.

154 Through the analysis of multiple nematode genome sequences we found that  
155 nematodes generally contain a single ortholog of the Sine oculis/Six1/2 subfamily of SIX  
156 homeodomain proteins, but that this locus has duplicated in the *Caenorhabditis* genus into  
157 two immediately adjacent paralogs, *ceh-33* and *ceh-34* (**Fig.2A, Fig.2 – Supplement 1**).  
158 Using a fosmid-based reporter in which the *ceh-33* locus is tagged with *gfp*, we found that the  
159 CEH-33 protein shows no expression in the nervous system within or outside the pharynx at  
160 any developmental stage. The only observed expression was in a subset of head muscle  
161 cells (**Fig.2B**).

162 A previously described reporter construct that contains the coding region and 3.8kb of  
163 promoter region of the neighboring *ceh-34* gene showed expression in all pharyngeal  
164 neurons (Hirose et al., 2010). A fosmid-based reporter shows the same expression pattern  
165 (Reilly et al., 2020). To further confirm this strikingly selective pattern of neuronal expression  
166 and also to examine expression at different developmental stages with the best possible  
167 reagent, we used the CRISPR/Cas9 system to engineer a reporter allele of *ceh-34*. This  
168 reporter shows the same expression as the fosmid-based reporter in all pharyngeal neurons,  
169 but no other neurons (**Fig.2B**). The *ceh-34* reporter is turned on in the embryo at around the  
170 time of birth of pharyngeal neurons and is maintained in all pharyngeal neurons throughout all  
171 larval and adult stages (**Fig.2B**).

172 The remarkable restriction of *ceh-34* expression within the nervous system to all  
173 pharyngeal neurons prompted us to ask whether the Forkhead transcription factor *pha-4*, an  
174 organ selector gene involved in early patterning of the pharynx (Gaudet and Mango, 2002;  
175 Horner et al., 1998; Kalb et al., 1998; Mango et al., 1994), is required for *ceh-34* expression.  
176 Crossing a *ceh-34* reporter into *pha-4(q490)* mutant animals, we indeed observed a loss of  
177 *ceh-34* expression (**Fig.2C**). Conversely, *ceh-34* does not affect *pha-4* expression (**Fig.2 –**  
178 **Supplement 2A**). The regulation of *ceh-34* by *pha-4* mirrors the effects that *pha-4* has on the  
179 expression of other transcription factors that control terminal differentiation of other tissue  
180 types in the pharynx, for example the *ceh-22/NKX* homeobox gene that specifies pharyngeal  
181 muscle differentiation (Vilimas et al., 2004), or the *hlh-6* bHLH gene that specifies pharyngeal  
182 gland differentiation (Smit et al., 2008). We furthermore note that a *pha-4* reporter allele that  
183 we generated through CRISPR/Cas9 genome engineering is continuously expressed  
184 throughout the entire pharyngeal nervous system, at all postembryonic stages (**Fig.2 –**  
185 **Supplement 2B**), raising the possibility that *pha-4* may not only initiate, but also maintain  
186 *ceh-34* expression.

187

## 188 ***ceh-34* controls the expression of diverse neurotransmitter signaling pathways in** 189 **pharyngeal neurons**

190 To begin to assess the function of *ceh-34* in enteric nervous system differentiation, we  
191 used CRISPR/Cas9 engineering to generate a null allele of the *ceh-34* locus, *ot1014*, in  
192 which the entire *ceh-34* locus is deleted (**Fig.2A**). Previously isolated alleles include a  
193 hypomorphic splice site allele and a small deletion allele, *tm3733* (Amin et al., 2009; Hirose et  
194 al., 2010). In our ensuing mutant analysis, we found *ot1014* to be phenotypically  
195 indistinguishable from the *tm3733* deletion allele and we therefore used both alleles  
196 interchangeably. Both the *ot1014* and *tm3733* alleles result in a completely penetrant early  
197 larval arrest phenotype, as expected from loss of pharynx function and resulting inability to  
198 feed.

199 We first asked whether *ceh-34* is required for the generation of pharyngeal neurons.  
200 Using a *pha-4* reporter that labels all pharyngeal cells, we observed no obvious differences in  
201 the number of pharyngeal cells in *ceh-34* mutants (**Fig.2 – Supplement 2A**). Moreover, the  
202 expression of the panneuronal genes *ric-4/SNAP25*, *ric-19/ICA1*, *rab-3/RAB3* and *unc-*

203 11/AP180 is unaffected (**Fig.3A**), indicating that pharyngeal neurons are generated and  
204 properly execute a generic neuronal differentiation program.

205 We next assessed the effect of *ceh-34* on a large collection of neuron type-specific  
206 molecular identity features (illustrated in **Fig.1E**). To this end, we first focused on the  
207 signaling capacities of all pharyngeal neurons. In the vertebrate enteric nervous system, each  
208 individual neuron class is distinguished by its unique set of signaling molecules, from classic  
209 neurotransmitters to neuropeptides (Morarach et al., 2021). The same applies to all neuron  
210 classes in the pharyngeal/enteric nervous system of *C. elegans* (Horvitz et al., 1982; Pereira  
211 et al., 2015; Serrano-Saiz et al., 2013; Taylor et al., 2021). We first considered the three  
212 classic neurotransmitters ACh, Glu and serotonin which are employed in *C. elegans* much  
213 like in the enteric nervous system of other species: Seven of the 14 pharyngeal neuron  
214 classes use acetylcholine as neurotransmitter, four use glutamate and one uses serotonin  
215 (NSM) (Horvitz et al., 1982; Pereira et al., 2015; Serrano-Saiz et al., 2013; Taylor et al.,  
216 2021). Of those neurotransmitters, serotonin is perhaps the best studied neurotransmitter  
217 both in the vertebrate enteric nervous system (Gershon, 2013) as well as in the nematode  
218 pharyngeal nervous system (Horvitz et al., 1982; Ishita et al., 2020; Song and Avery, 2013).  
219 Acquisition of ACh, Glu and serotonin neurotransmitter identity features can be visualized  
220 through the expression of a number of enzymes and transporters: *unc-17/VACHT* for  
221 cholinergic identity, *eat-4/VGluT* for glutamatergic identity and *tph-1/TPH*, *cat-1/VMAT*, *bas-*  
222 *1/AAAD* and *cat-4/GCH* for serotonergic identity. We examined the expression of all these  
223 markers, using various reporter genes, in all pharyngeal neurons of *ceh-34* mutant animals  
224 and found that the seven cholinergic, four glutamatergic and single serotonergic neuron  
225 classes fail to acquire their respective neurotransmitter identity (**Fig.3B**). We schematize  
226 these results in the context of a pharyngeal circuit diagram to illustrate the breadth of effects  
227 of *ceh-34* on neurotransmitter identity acquisition (**Fig.3C**).

228 We note that while in most cases, the effect of *ceh-34* on expression of  
229 neurotransmitter systems (as well as other identity markers described in ensuing sections) is  
230 fully penetrant and fully expressive, in some cases reporter expression is diminished, but not  
231 completely eliminated. At the end of this paper, we describe cofactors for *ceh-34* which may  
232 be partially able to compensate for loss of *ceh-34* function.

233 As in vertebrate enteric nervous systems (Drokhlyansky et al., 2020), pharyngeal  
234 neurons also display highly patterned expression of various neurotransmitter receptors

(Taylor et al., 2021). We analyzed the *ceh-34*-dependence of three representative receptors, the serotonin receptor *ser-7*, the ortholog of vertebrate HTR7, as well as a metabotropic and an ionotropic Glu receptor, *mgl-1* and *glr-2*. Each of these receptors is expressed in specific subsets of pharyngeal neurons and *ser-7* is known to control feeding behavior (Hobson et al., 2006; Song and Avery, 2012; Song and Avery, 2013). Using a combination of reporter transgenes and CRISPR/Cas9-engineered reporter alleles, we found the expression of *mgl-1*, *glr-2* and *ser-7* is strongly affected in different pharyngeal neuron types, if not entirely abrogated upon removal of *ceh-34* (**Fig.4A-C**).

243

#### 244 ***ceh-34* controls diverse neuropeptidergic identities of pharyngeal neurons**

245 The function of vertebrate enteric nervous systems is modulated by a number of  
246 prominent neuropeptidergic signaling systems (Abot et al., 2018; Llewellyn-Smith, 1989). In  
247 some cases, both neuropeptide and receptor are expressed in the vertebrate enteric nervous  
248 system, while in others, the peptide is produced elsewhere but acts on neuropeptide  
249 receptors located in the enteric nervous system. Likewise, the *C. elegans* pharyngeal  
250 nervous system expresses a great diversity of neuropeptides and neuropeptide receptors,  
251 including homologs of neuropeptide signaling systems that function in the vertebrate enteric  
252 nervous system (Taylor et al., 2021). In fact, each pharyngeal neuron expresses a unique  
253 combination of neuropeptides and their receptor proteins (Taylor et al., 2021)(**Fig.5**). We  
254 tested whether *ceh-34* affects the neuron-type specific expression of various  
255 neuropeptidergic signaling systems.

256 We first examined the expression of the phylogenetically conserved Thyrotropin-  
257 releasing hormone (TRH) signaling axis that is important in stimulating gastrointestinal  
258 motility in vertebrates (Abot et al., 2018). *C. elegans* homologs of either the Thyrotropin-  
259 releasing hormone (TRH-1) or its receptor (TRHR-1) are expressed in the pharyngeal  
260 nervous system (Hunt-Newbury et al., 2007; Van Sinay et al., 2017), a notion we confirmed  
261 and extended with CRISPR/Cas9-engineered reporter alleles, showing that *trh-1* is  
262 expressed in the M1, M4 and M5 neurons and *trhr-1* in the M1, M2, M3 and I5 neurons  
263 (**Fig.4B, Fig.5A**). We found that the expression of the *trh-1* and *trhr-1* reporter alleles in these  
264 pharyngeal neurons is strongly affected in *ceh-34* mutants (**Fig.4B, Fig.5A**).

265 In addition to this deeply conserved neuropeptidergic system, we also tested the  
266 expression of a cohort of neuropeptides from the FMRFamide family (*flp-2*, *flp-4*, *flp-5*, *flp-15*,  
267 *flp-21*, *flp-28*) and other miscellaneous neuropeptides (*nlp-3*, *nlp-8*, *nlp-13*). The expression  
268 of these nine neuropeptides is neuron-type specific, but in aggregate they cover the entire  
269 pharyngeal nervous system, often with unique cell-type specific combinations (schematized  
270 in **Fig.5B**). We found that the expression of all of these nine neuropeptides, analyzed with  
271 either reporter transgenes or CRISPR/Cas9 genome-engineered reporter alleles, is affected  
272 in *ceh-34* mutants (**Fig.5A**). We schematize these results again in the context of a  
273 pharyngeal circuit diagram to illustrate the breadth of effects of *ceh-34* on neuropeptide  
274 expression (**Fig.5B**). Together with our analysis of classic neurotransmitters (ACh, Glu,  
275 serotonin) and receptors, we conclude that *ceh-34* is required to endow pharyngeal neurons  
276 with their neuron type-specific arsenal of signaling molecules and, hence, that *ceh-34* is a  
277 critical specifier of several key aspects of pharyngeal neuron identity.

278

#### 279 ***ceh-34* is required for sensory receptor expression in the pharyngeal nervous system**

280 We sought to extend our analysis of *ceh-34* mutants by examining the expression of  
281 other molecular features of pharyngeal neurons. Like neurons in the vertebrate enteric  
282 nervous system, many of the pharyngeal neurons are likely internal sensory neurons that  
283 perceive sensory information to modulate peristaltic movements of the alimentary tract (Cook  
284 et al., 2020). While the sensory apparatus of pharyngeal neurons is not well understood,  
285 there are several candidate sensory receptors expressed in pharyngeal neurons. A gustatory  
286 receptor family member, *gur-3*, a possible light receptor (Bhatla and Horvitz, 2015), is  
287 expressed in two pharyngeal neuron classes and its expression is lost in *ceh-34* mutants  
288 (**Fig.6A**). Pharyngeal neurons also express the two sole members of the ionotropic sensory  
289 receptor family (Croset et al., 2010), encoded by *glr-7* and *glr-8* in *C. elegans* (Brockie et al.,  
290 2001; Hobert, 2013). We examined expression of *glr-7* expression, normally observed in six  
291 pharyngeal neuron classes (I2, I3, I6, M2, M3 and NSM), in *ceh-34* mutants and found its  
292 expression to be completely lost (**Fig.6A**). Finally we analyzed the expression of *str-97*, a  
293 putative chemosensory receptor of the GPCR family which we found to be expressed in  
294 several pharyngeal neurons (Vidal et al., 2018) (**Fig.6A**). We found that *ceh-34* is required for  
295 proper *str-97* expression (**Fig.6A**).



296

297 ***ceh-34* is required for the expression of antimicrobial defense machinery**

298 One deeply conserved feature of the gut and its associated nervous system is its  
299 engagement in antimicrobial defense, either directly through the release of antimicrobial  
300 peptides or through the employment of signaling systems that activate the immune system  
301 (Klimovich and Bosch, 2018; Muniz et al., 2012). Similar defense strategies operate in *C.*  
302 *elegans* (Dierking et al., 2016). Aside from the epithelial cells of the intestine, the pharyngeal  
303 nervous system appears to play a direct role in these microbial control mechanisms, as  
304 inferred by the pharyngeal neuron expression of specific proteins implicated in antimicrobial  
305 defense. For example, pharyngeal neurons express a hormone, FLR-2, homologous to  
306 glycoprotein hormone alpha subunit, that signals to the intestine to orchestrate antimicrobial  
307 defense (Oishi et al., 2009). Pharyngeal neurons also secrete pore-forming polypeptides that  
308 directly kill bacteria, such as the SPP-12 protein (Hoeckendorf et al., 2012), as well as a  
309 defensin-type antimicrobial peptide, ABF-2 and fungal-induced peptides (FIPR proteins)(Kato  
310 et al., 2002; Taylor et al., 2021). Our scRNA transcriptome analysis (Taylor et al., 2021)  
311 revealed pharyngeal neuron expression of another saposin-related secreted protein, which  
312 we named *htrl-1* (see Methods). We visualized expression of these signaling molecules,  
313 using a promoter fusion for *spp-12* (Hoeckendorf et al., 2012) and CRISPR/Cas9-engineered  
314 reporter alleles for *flr-2* and *htrl-1* (**Fig.6B**). We found that the *spp-12* reporter is expressed in  
315 I4 and M4 neurons, the *flr-2::SL2::gfp::h2b* reporter allele is expressed 5 pharyngeal neuron  
316 classes (I4, I5, M1, M4 and M5) and the *htrl-1::SL2::gfp::h2b* reporter allele is expressed in all  
317 pharyngeal neurons (and in all other pharyngeal cells, but nowhere outside the pharynx at the  
318 L1 stage)(**Fig.6B**). A notable feature of the extrapharyngeal expression of the *flr-2* reporter  
319 allele is expression in the AVL and DVB neurons (**Fig.6B**), the only extrapharyngeal neurons  
320 of the *C. elegans* nervous system that innervate gut tissue (not the foregut, but the  
321 midgut)(White et al., 1986). Crossing these reporters into a *ceh-34* mutant background, we  
322 found that expression of all three genes (*spp-12*, *flr-2*, *htrl-1*) is severely reduced or  
323 eliminated in pharyngeal neurons (**Fig.6B**).

324

325 ***ceh-34* is required for the expression of pan-pharyngeal nervous system genes**

326 In addition to investigating the *ceh-34*-dependence of genes that fall into specific  
327 functional categories, we also sought to capitalize on the recently released single cell  
328 transcriptome profiling of the entire *C. elegans* nervous system that included the entire  
329 pharyngeal nervous system (Taylor et al., 2021). This analysis had shown that the molecular  
330 signatures of pharyngeal neurons are more similar to each other than to other neurons in the  
331 nervous system (Taylor et al., 2021)(**Fig.1D**). This pattern is driven, in part, by:  
332 (a) the pan-pharyngeal neuron, but pharynx-exclusive expression of *ceh-34*, as well as its  
333 transcriptional cofactor, Eyes absent/*eya-1* (described in more detail below),  
334 (b) pharynx-restricted expression of several neuropeptides (e.g. *tkr-1*).  
335 (c) a number of previously entirely uncharacterized genes with very broad, if not pan-  
336 pharyngeal nervous system expression (but no expression in non-pharyngeal neurons),  
337 including the above-mentioned saposin-related *htl-1* gene, small cell surface proteins (e.g.  
338 C54E4.4) and a novel receptor tyrosine kinase, which we named *kin-36* (**Fig.6 – Supplement**  
339 **1**). To confirm this expression pattern, we tagged the *kin-36* locus with a *gfp::H2B::SL2*  
340 cassette at its 5' end, using CRISPR/Cas9 genome engineering. We found that *gfp::kin-36*  
341 indeed displays pan-pharyngeal neuron expression; expression is also observed in all other  
342 pharyngeal cell types, but no cell types outside the pharynx, except some unidentified vulval  
343 cells (**Fig.6C**). Crossing *gfp::kin-36* into *ceh-34* mutants, we observed what appears to be  
344 selective loss of *kin-36* expression from many, albeit not all pharyngeal neurons, a similar  
345 effect to what we observed for *htl-1* (**Fig.6B,C**).

346 We conclude that *ceh-34* is required for the adoption of a broad palette of individual  
347 molecular features of all pharyngeal neurons (**Figure 12**), consistent with a role as a terminal  
348 selector of neuronal identity of all pharyngeal neurons. Like other terminal selectors, *ceh-34*  
349 only affects neuron-type specific features, but not features that are expressed by all neurons  
350 throughout the nervous system.

351

### 352 ***ceh-34* is continuously required to maintain the differentiated and functional state of**

### 353 **enteric neurons**

354 The effect of *ceh-34* on terminal marker expression and its continuous expression  
355 throughout the life of all pharyngeal neurons suggests that, like other terminal selectors in the  
356 non-pharyngeal nervous system, *ceh-34* may not only initiate but also maintain the terminally

357 differentiated state. To test this possibility, we generated a conditional *ceh-34* allele that  
358 allowed us to deplete CEH-34 protein postdevelopmentally. To this end, we inserted an  
359 auxin-inducible degron (Zhang et al., 2015) into the *ceh-34* locus using CRISPR/Cas9  
360 genome engineering. Together with a ubiquitously expressed *AtTIR1<sup>F79G</sup>* ubiquitin ligase that  
361 recognizes the degron (*rps-28* driver; *csh1s140*)(Hills-Muckey et al., 2022), this approach  
362 allows for temporal depletion of CEH-34 protein through addition of an auxin derivative (5-Ph-  
363 IAA) to the worm diet (**Fig.7A,B**). Postembryonic 5-Ph-IAA addition at either larval or adult  
364 stages resulted in downregulation of four tested markers for the differentiated state of  
365 different pharyngeal neuron classes, *eat-4/VGluT*, *unc-17/VACHT*, *ser-7* and *spp-12*  
366 (**Fig.7B,C**). These effects are not as strong as in null mutants, but this is likely due to  
367 incomplete CEH-34 protein depletion, since constitutive 5-Ph-IAA exposure from parental  
368 stages throughout all developmental stages also produces only limited defects in expression  
369 of these markers.

370 We also assessed the functional consequences of CEH-34 protein depletion in adult  
371 animals, as well as larval stage animals. Using again the auxin-inducible degron approach,  
372 we found that postembryonic CEH-34 depletion at either larval or adult stages results in  
373 substantial defects in pharyngeal pumping, as expected from a disruption of enteric nervous  
374 system function (**Fig.7D**). We conclude that *ceh-34* is required to maintain differentiated  
375 features of pharyngeal neurons and therefore fulfills another key criterion to classify as a  
376 terminal selector of pharyngeal neuron identity.

377

## 378 **Pharyngeal nervous system architecture is severely disorganized in *ceh-34* mutants**

379 We further extended our analysis of *ceh-34* function by analyzing the anatomy of  
380 pharyngeal neuron circuitry in *ceh-34* mutants. This analysis is particularly important in light  
381 of the observation that, both in *C. elegans* (Berghoff et al., 2021; Pereira et al., 2015) and in  
382 vertebrates (Brunet and Pattyn, 2002), several instances have been described in which  
383 synaptically interconnected, but otherwise distinct neurons express the same transcription  
384 factor. Such observation suggests that these transcription factors may have a role in  
385 assembling neurons into functional circuitry. *ceh-34* represents a particularly extreme version  
386 of this scenario, because all *ceh-34*(+) neurons are heavily synaptically interconnected and  
387 only make a single robust synaptic contact to the rest of the *C. elegans* nervous system

388 (Fig.1C)(Cook et al., 2020). To assess whether *ceh-34* not only specifies terminal molecular  
389 properties of pharyngeal neurons, but also organizes overall circuit architecture, we  
390 examined pharyngeal nervous system architecture using fluorescent reporter constructs.  
391 Such analysis is complicated by the fact that genes that are selectively expressed in *ceh-*  
392 *34(+)* neurons, and hence could serve as drivers for a fluorescent reporter, are turned off in  
393 *ceh-34* null mutant animals, thereby preventing an easy visualization of individual axonal  
394 tracts or synaptic contacts. However, we found that the *ceh-34* promoter itself is still  
395 expressed until the first larval stage in *ceh-34* null mutants, when these animals arrest  
396 development. This *ceh-34* promoter transgene (*otIs762*) reveals that although their identity is  
397 not properly specified, as described above, pharyngeal neurons retain the capability to grow  
398 neuronal projections in *ceh-34* mutants; however, axonal tracts are severely disorganized  
399 (Fig.8A).

400 We also expressed the cytoplasmically localized TagRFP reporter together with a  
401 synaptically localized, GFP-tagged CLA-1/Clarinet protein (a synaptic active zone  
402 marker)(Xuan et al., 2017) under control of the *ceh-34* promoter. In wild-type animals, this  
403 transgene (*otIs785*) reveals (a) the axonal tracts of the pharyngeal nervous system and (b)  
404 synaptic structures that are strongly enriched in the pharyngeal nerve ring (Fig.8B). In *ceh-34*  
405 null mutants, we observed not only a disruption of axonal tract anatomy, but a severe  
406 disorganization of synaptic clusters throughout the entire pharyngeal nervous system  
407 (Fig.8B).

408 Using the CLA-1 synaptic marker, we also asked whether CEH-34 is continuously  
409 required to maintain synaptic architecture postembryonically (i.e. after the time when synaptic  
410 connections initially form). To this end, we again made use of the auxin-inducible degron  
411 system and removed CEH-34::mNG::AID either throughout larval stages or in the adult stage.  
412 In both cases, we found that such depletion resulted in synaptic clusters becoming  
413 disorganized, such that ectopic presynaptic clusters form at ectopic locations in the isthmus  
414 of the pharynx (Fig.8 – Supplement 1).

415 Lastly, we made use of a mild *ceh-34* hypomorphic allele, *n4796* (Hirose et al., 2010).  
416 In *ceh-34(n4796)* animals, the expression of many molecular markers for individual  
417 pharyngeal neurons are not affected, allowing to visualize their morphology. Focusing on two  
418 neuron types, NSM and I5, we found that in both types, specific axons branches fail to form in  
419 *ceh-34(n4796)* animals (Fig.8C). We conclude that *ceh-34* is required to establish and

420 maintain proper pharyngeal nervous system architecture.

421

422 ***ceh-34* affects the expression of molecules involved in proper wiring of the pharyngeal**  
423 **nervous system**

424 To further explore how *ceh-34* may affect pharyngeal nervous system architecture, we  
425 considered the expression of molecules with potential or explicitly demonstrated roles in axon  
426 guidance, fasciculation and/or synapse formation. A genetic analysis of axon guidance and  
427 circuit formation has only been conducted in a small number of pharyngeal neurons, mainly  
428 the M2 and NSM neuron classes (Pilon, 2008). In both neuron classes, the SLT-1 axon  
429 guidance cue, the *C. elegans* orthologue of Slit, has been found to be required for proper  
430 axon guidance (Axang et al., 2008; Rauthan et al., 2007). We extended this phenotypic  
431 characterization, finding that other pharyngeal neurons also display axon pathfinding defects  
432 in *slt-1* mutants (**Fig.8 – Supplement 2**). To examine potential links between *slt-1* and *ceh-*  
433 *34*, we made use of a promoter::gfp fusion that captures the entire upstream intergenic region  
434 of the *slt-1* locus (Hao et al., 2001) and which shows selective expression in seven  
435 pharyngeal neuron classes (I2, I6, M1, M2, M4, M5 and MI) at the first larval stage. We found  
436 that *slt-1* expression is strongly affected in *ceh-34* mutants (**Fig.8D**).

437 Effects of *ceh-34* on molecules potentially involved in circuit formation are not  
438 restricted to *slt-1*. Two Ig superfamily members, *rig-3* and *rig-6* (the sole *C. elegans* ortholog  
439 of contactin) have previously been implicated in axon outgrowth and synapse function in the  
440 *C. elegans* nervous system (Babu et al., 2011; Bhardwaj et al., 2020; Katidou et al., 2013;  
441 Kim and Emmons, 2017) and promoter fusion transgenes have indicated their expression in  
442 pharyngeal neurons (Schwarz et al., 2009). We used CRISPR/Cas9 to tag both loci with *gfp*  
443 and found that both genes are broadly expressed in many pharyngeal neurons (**Fig.1E, 8E**).  
444 *ceh-34* affects the pharyngeal neuron expression of both *rig-3* and *rig-6* reporter alleles  
445 (**Fig.8E**).

446

447 **The Six homeodomain cofactor, Eyes absent/Eya, shows limited cooperation with *ceh-***  
448 ***34***

449 To gain further insights into how CEH-34 patterns the identity of a wide array of distinct  
450 pharyngeal neuron types, we considered the involvement of cell-type specific cofactors. As a

451 first step, we considered the EYes Absent/EYA protein, a phylogenetically conserved  
452 transcriptional co-activator of specific subsets of Six homeodomain proteins (Ohto et al.,  
453 1999; Patrick et al., 2013; Tadjuidje and Hegde, 2013). The *C. elegans* ortholog of Eyes  
454 absent, called *eya-1* (Furuya et al., 2005), also directly physically interacts with CEH-34  
455 protein (Amin et al., 2009; Hirose et al., 2010). We first examined *eya-1* expression in  
456 pharyngeal neurons using a genomic fragment that contains the entire, *gfp*-tagged *eya-1*  
457 locus (Furuya et al., 2005). We observed expression in all pharyngeal neurons throughout all  
458 larval and adult stages, a phenocopy of the *ceh-34* expression pattern (**Fig.9A**), an  
459 expression pattern also corroborated by our recent scRNA analysis (**Fig.6 – Supplement**  
460 **1**)(Taylor et al., 2021). Moreover, we found that *eya-1* expression requires *ceh-34* function,  
461 suggesting that *ceh-34* acts in a feedforward configuration to induce its own transcriptional  
462 cofactor (**Fig.9B**).

463 We analyzed the function of *eya-1* in the context of pharyngeal neuron specification.  
464 Animals that carry a deletion of a part of the *eya-1* locus, *ok654*, display pharyngeal neuron  
465 specification defects, albeit much milder than those observed in *ceh-34* null mutant animals  
466 (**Fig.9C**). The larval arrest phenotype of *ceh-34* null mutants is also more penetrant than that  
467 of *eya-1* mutants, which are very slow growing, but still homozygous viable (Furuya et al.,  
468 2005). To exclude the possibility that the *ok654* allele is not a null allele, we used  
469 CRISPR/Cas9 to generate a null allele in which the entire locus is deleted. Animals carrying  
470 this deletion allele (*ot1197*) display phenotypes that are indistinguishable from those of *ok654*  
471 animals. They are still homozygous viable, albeit as slowly growing as *ok654* animals, and  
472 they display very similar, limited neuronal cell fate marker defects (**Fig.9C**). Given the milder  
473 spectrum of *eya-1* defects compared to *ceh-34* null mutants, we conclude that *ceh-34* may be  
474 able to partly function without *eya-1*.

475 In other organisms, Dachshund proteins are components of Sine oculis/Eya  
476 complexes in several cellular contexts (Hanson, 2001). However, the sole *C. elegans*  
477 ortholog of Dachshund, is not expressed in pharyngeal neurons (Colosimo et al., 2004;  
478 Taylor et al., 2021) and, second, *dac-1* null mutants do not display the larval growth/arrest  
479 phenotype characteristic of *ceh-34* and *eya-1* mutants (Colosimo et al., 2004). While these  
480 observation do not entirely rule out a function for DAC-1 in pharyngeal neurons, it appears  
481 unlikely that DAC-1 is an essential cofactor of CEH-34.

482

483 ***ceh-34* cooperates with a multitude of other homeobox genes to specify distinct**  
484 **pharyngeal neuron types**

485         How does *ceh-34* activate distinct genes in different pharyngeal neuron types? One  
486 obvious possibility is that *ceh-34* cooperates with neuron type-specific cofactors in neuron-  
487 type specific terminal selector complexes to drive specific fates. As candidates for such  
488 cofactors, we considered homeobox genes, for two reasons: (1) like any other neuron in the  
489 *C. elegans* nervous system, each individual pharyngeal neuron expresses a unique  
490 combination of homeobox genes, in addition to pan-pharyngeal *ceh-34* (Reilly et al., 2020);  
491 (2) previous studies had already implicated a few homeobox genes in controlling some select  
492 functional or molecular aspects of individual pharyngeal neurons (Aspöck et al., 2003; Feng  
493 and Hope, 2013; Morck et al., 2004; Ramakrishnan and Okkema, 2014; Ray et al., 2008;  
494 Zhang et al., 2014). For example, the homeobox gene *ceh-2*, the *C. elegans* ortholog of  
495 vertebrate EMX and *Drosophila* Ems, is required for proper function of the M3 neuron, but  
496 effects of *ceh-2* on molecular aspects of M3 neuron differentiation had not been reported  
497 (Aspöck et al., 2003). We therefore set out to analyze homeobox gene function throughout  
498 the pharyngeal nervous system and to examine interaction of *ceh-34* with other homeobox  
499 genes.

500         *NSM neurons*: To ask whether distinct pharyngeal neuron type-specific homeobox  
501 genes cooperate with *ceh-34* in distinct neuronal cell types throughout the pharyngeal  
502 nervous system, we made use of a hypomorphic *ceh-34* allele, *n4796* (Hirose et al., 2010).  
503 Unlike the *ceh-34* null allele, which results in very strong expression defects of all NSM  
504 molecular markers (**Fig.3-6**), the *n4796* allele displays only subtle if any marker expression  
505 effects on its own (**Fig.10A**). However, when combined with a mutant allele of *unc-86*, a POU  
506 homeobox gene that affects many but not all NSM marker genes (Zhang et al., 2014), strong  
507 synergistic differentiation defects of NSM are observed (**Fig.10A**). This genetic interaction  
508 mirrors the synergistic effects of *unc-86* and the LIM homeobox gene *ttx-3*, another regulator  
509 of NSM differentiation (Zhang et al., 2014).

510         *I1 neurons*: A similar genetic interaction between *ceh-34* and *unc-86* is observed in  
511 the cholinergic I1 neuron pair, the only other pharyngeal neuron class that also co-expresses  
512 *ceh-34* and *unc-86* (Baumeister et al., 1996; Serrano-Saiz et al., 2018), but which does not  
513 express *ttx-3*. While cholinergic identity, visualized via *unc-17/VACHT* expression, is not

514 affected in *unc-86(n846)* single mutants, a combination of the *ceh-34(n4796)* hypomorphic  
515 allele with the *unc-86(n846)* mutation results in I1 losing its cholinergic identity (**Fig.10B**).

516 I2 neurons: Synergistic interactions are also observed in the glutamatergic I2 neuron  
517 pair. Like the I1 neurons, no identity regulators were previously known for this neuron class.  
518 Our homeobox gene mapping project (Reilly et al., 2020) showed that the I2 neuron  
519 expresses the LIM homeobox gene *ceh-14*, the *C. elegans* ortholog of vertebrate Lhx3/4. No  
520 other pharyngeal neuron expresses *ceh-14*. While *ceh-14* single null mutants show no effect  
521 on *eat-4/VGluT* expression (the marker of glutamatergic identity), in combination with the  
522 *ceh-34(n4796)* hypomorphic allele a strong synergistic effect on glutamatergic identity  
523 acquisition is observed in I2 (**Fig.10C**). Another molecular marker for I2 identity, the  
524 neuropeptide *nlp-8*, is also synergistically regulated by *ceh-34* and *ceh-14* (**Fig.10C**).

525 I3 neuron: The previously unstudied cholinergic I3 neuron class expresses, in addition  
526 to *ceh-34*, the *C. elegans* ortholog of Empty spiracles/EMX, *ceh-2* (Aspöck et al., 2003; Reilly  
527 et al., 2020), as well as the Prospero ortholog *pros-1*, whose function in the nervous system  
528 has not previously been examined. We find that in *pros-1* null mutant animals, cholinergic  
529 identity of I3, measured with an *unc-17/VACHT* reporter transgene, is not properly acquired  
530 (**Fig.10D**). The *ceh-2(ch4)* null allele, alone shows a reduction of *unc-17/VACHT* expression  
531 (**Fig.10F**), as well as a reduction of the serotonin receptor *ser-7* expression (**Fig.10E**). In  
532 combination with the *ceh-34(n4796)* hypomorphic allele, *unc-17/VACHT* expression and,  
533 hence, cholinergic identity of I3, is eliminated in *ceh-2* mutant animals (**Fig.10F**).

534 M3 neuron: Apart from expression in I3, the EMX ortholog *ceh-2* is also expressed in  
535 the glutamatergic M3 neurons and is required for proper M3 function (Aspöck et al., 2003),  
536 but molecular correlates for this functional defect have not previously been identified. We  
537 found that in *ceh-2* single mutants, expression of the *eat-4/VGluT* identity marker is affected  
538 in M3 (**Fig.11A**).

539 M4 neuron: In the cholinergic M4 neuron, the *ceh-28* and *zag-1* homeobox genes have  
540 previously been shown to each regulate subsets of M4 identity features (Ramakrishnan and  
541 Okkema, 2014). Both *zag-1* and *ceh-28* affected *flp-2* expression, but only *zag-1*, and not  
542 *ceh-28*, was found to affect *ser-7* expression (Ramakrishnan and Okkema, 2014). In contrast,  
543 *ceh-28* but not *zag-1* affected *flp-5* expression and neither *zag-1* nor *ceh-28* affected *unc-17*  
544 or *flp-21* expression (Ramakrishnan and Okkema, 2014). *ceh-34* null mutants show effects



545 on the expression of all the tested *ceh-28* or *zag-1*-dependent (*ser-7*, *flp-2* and *flp-5*) or  
546 independent markers (*unc-17*, *flp-21*)(**Fig.3-5**), indicating that *ceh-34* may collaborate with  
547 these homeobox genes to control distinct subsets of M4 differentiation markers. *ceh-34* also  
548 affects *ceh-28* expression (**Fig.6 – Supplement 2**)

549 *M5 neuron*: The cholinergic M5 neuron expresses, in addition to *ceh-34*, the Msh/Msx  
550 ortholog *vab-15* (Reilly et al., 2020). Since only a hypomorphic allele of *vab-15* was  
551 previously available (Du and Chalfie, 2001), we generated a molecular null allele, *ot1136*,  
552 through CRISPR/Cas9 genome engineering (**Fig.11 – Supplement 1A**). We found a  
553 complete loss of expression of the cholinergic marker *unc-17/VACHT*, as well as the  
554 neuropeptidergic marker, *trh-1*, in *vab-15(ot1136)* animals (**Fig.11B**). Complete loss of  
555 marker expression not an indicator of failure of this neuron to be generated, since crossing a  
556 *ceh-34* marker into *vab-15* null mutants revealed the presence and normal *ceh-34* expression  
557 of M5 (**Fig.11B**).

558 *MI neuron*: In our previous genome-wide analysis of homeobox gene expression  
559 (Reilly et al., 2020), we had shown that the glutamatergic MI neuron expresses the sole worm  
560 ortholog of the Goosecoid homeobox gene, *ceh-45*. Embryonically, *ceh-45* is expressed in  
561 multiple pharyngeal tissues (Ma et al., 2021), but its expression resolves to exclusive  
562 expression in the MI and I1 neurons (Reilly et al., 2020). *ceh-45* had not previously been  
563 functionally characterized. We examined *ceh-45* function by generating a null allele using  
564 CRISPR/Cas9 genome engineering, *ot1065* (**Fig.11 – Supplement 1A**). Mirroring the *ceh-34*  
565 defects, we found that glutamatergic identity specification of MI (as assessed by *eat-4/VGluT*  
566 expression) is strongly affected in *ceh-45* null mutant animals (**Fig.11C**). Similarly, expression  
567 of the neuropeptide *trh-1* is also affected in MI (**Fig.11C**).

568 In our search for potential *ceh-34* cofactors we also considered three divergent, non-  
569 conserved homeobox genes, *ceh-7*, *ceh-53* and *ceh-79* that display expression in subsets of  
570 pharyngeal neurons (Reilly et al., 2020). We generated null alleles for these three genes  
571 using CRISPR/Cas9 genome engineering (**Fig.11 – Supplement 1A**). However, we  
572 observed no *eat-4/VGluT* or *unc-17/VACHT* expression defects in either of these mutant  
573 strains, either alone or in combination with the *ceh-34* hypomorphic allele *n4796* (**Fig.11 –**  
574 **Supplement 1B**).

575           In conclusion, nine phylogenetically conserved homeobox genes appear to collaborate  
576 with *ceh-34* in eight of the 14 pharyngeal neuron classes to specify their proper identity  
577 (summarized in **Figure 12**). Since the remaining six classes also express specific  
578 combinations of homeobox genes (Reilly et al., 2020), we anticipate that future analysis will  
579 likely reveal homeobox codes throughout the entire pharyngeal nervous system.

580

## 581 DISCUSSION

582 We have identified here common, overarching themes in the differentiation of the  
583 pharyngeal nervous system, the enteric nervous system of the nematode *C. elegans*. A  
584 number of previous studies have identified transcription factors involved in regulating  
585 specific differentiation aspects of a small subset of pharyngeal neurons (Aspöck et al.,  
586 2003; Feng and Hope, 2013; Morck et al., 2004; Ramakrishnan and Okkema, 2014; Rauthan  
587 et al., 2007; Ray et al., 2008; Zhang et al., 2014), yet no common theme emerged from these  
588 studies. We have shown here that a *Sine oculis* ortholog, *ceh-34*, orchestrates the terminal  
589 differentiation program of all pharyngeal neurons. CEH-34 appears to act as a terminal  
590 selector of pharyngeal neuron identity, as inferred from its requirement to initiate terminal  
591 neuronal differentiation programs in all pharyngeal neurons (without affecting panneuronal  
592 identity, a unifying trait of all terminal selectors), as well as its continuous role in maintaining  
593 the differentiated state (another defining trait of terminal selectors). The aspects of the  
594 differentiation program that we consider here, and found to be under control of *ceh-34*,  
595 include anatomical (axon outgrowth and synapse formation), molecular and functional  
596 features. Molecular and functional features affected by *ceh-34* range from neuron-neuron  
597 communication to presumptive sensory functions to the intriguing function of enteric neurons  
598 as potential regulators of microbial colonization. There is good reason to believe that CEH-34  
599 controls these diverse phenotypic identity features in a direct manner, i.e. it may not act  
600 through intermediary factors. CEH-34 is among the many *C. elegans* transcription factors  
601 whose binding sites have been determined *in vitro* through protein binding microarrays  
602 (Narasimhan et al., 2015) and a phylogenetic footprinting pipeline reveals that these motifs  
603 are significantly enriched in the single cell transcriptome of most pharyngeal neuron classes  
604 (Glenwinkel et al., 2021). This is in accordance with CEH-34 being a shared terminal selector  
605 component of all pharyngeal neuron classes.

606 Within the nervous system, the selectivity of *ceh-34* expression in all pharyngeal  
607 neurons is remarkable – based on extensive gene expression pattern analysis, including  
608 recent scRNA data, there is no other transcription factor that so selectively and  
609 comprehensively defines all pharyngeal, but no non- pharyngeal neuronal cell types. We  
610 found that the key determinant of this expression is the organ selector PHA-4 (Gaudet and  
611 Mango, 2002; Horner et al., 1998; Kalb et al., 1998; Mango et al., 1994), which is expressed  
612 earlier in development to act both as a pioneer factor (Hsu et al., 2015) and to induce the

613 expression of a number of different terminal selectors for different tissue types within the  
614 foregut – the *ceh-34* gene for all neurons (this paper), the bHLH transcription factor *hlh-6* for  
615 pharyngeal gland cells (Smit et al., 2008) and the Nk-type homeobox gene *ceh-22* for  
616 pharyngeal muscle identity (Vilimas et al., 2004). Given the continuous PHA-4 pharyngeal  
617 expression that we observe throughout postembryonic life, it is conceivable that PHA-4 acts  
618 in a regulatory feedforward motif configuration, where it not only induces tissue-type terminal  
619 selectors (*ceh-34*, *hlh-6*, *ceh-22*), but then also collaborates with them to induce and maintain  
620 terminal differentiation batteries.

621 Our work indicates that CEH-34 is a shared component of neuron-type specific  
622 terminal selector complexes, such that CEH-34 interacts with a distinct set of at least eight  
623 homeodomain co-factors to impose unique features in distinct pharyngeal neuron types. As  
624 is the case for CEH-34 target sites, the *in vitro*-determined binding sites for these  
625 homeodomain co-factors display a phylogenetically conserved enrichment in the respective  
626 neuron type-specific gene batteries (Glenwinkel et al., 2021). For example, CEH-34 and  
627 UNC-86 binding sites are co-enriched in the I1 neuronal transcriptome, CEH-34 and CEH-14  
628 binding sites in the I2 neuronal transcriptome, CEH-34 and CEH-2 in the I3 transcriptome,  
629 CEH-34 and CEH-45 in the M1 transcriptome and VAB-15 and CEH-34 in the M5  
630 transcriptome (Glenwinkel et al., 2021). The interactions of CEH-34 with its various  
631 collaborating factors is likely highly dependent on the *cis*-regulatory architecture of individual  
632 target genes. We infer this from *ceh-34* mutant phenotypes, which, depending on target  
633 gene, can be fully or partially penetrant (i.e. not all animals affected), or fully or partially  
634 expressive (i.e. “dimming” of target gene expression), or a combination of both. Depending  
635 on the number, affinity and arrangement of binding sites for individual factors, CEH-34 and its  
636 individual cofactors may have a more or less pronounced role in the regulation of individual  
637 target genes.

638 We found that the ectopic expression of pharyngeal homeobox genes reveal a limited  
639 capacity to respecify identity features of pharyngeal neuron (**Fig.11 – Supplement 2**). This is  
640 a likely reflection of our incomplete knowledge of the entire set of collaborating factors and  
641 possibly also a reflection of the difficulties associated with overriding endogenous terminal  
642 differentiation programs by ectopic expression of drivers of alternative fates (Patel and  
643 Hobert, 2017).

644 Taken together, our findings not only reveal a common terminal selector-based  
645 regulatory logic for how a self-contained, enteric nervous system acquires its terminal  
646 differentiated state. They also corroborate two themes that have emerged from recent  
647 studies, primarily in *C. elegans* (and also emerging in other systems):

648 (1) homeobox genes – and more specifically, combinatorial codes of homeobox  
649 genes – are prominently employed in neuron identity specification throughout all neurons  
650 of the nervous system, as exemplified here in the context of the enteric nervous system,  
651 the so-called “second brain” of animals (Gershon, 1998).

652 (2) A number of identity-specifying terminal selectors, such as CEH-34, are  
653 expressed in synaptically connected neurons, suggesting they may specify the assembly of  
654 neurons into functional circuitry. It is presently unclear how prominent such a connectivity  
655 theme is. We observed a few cases of such putative “circuit organizer” transcription factors  
656 in the non-pharyngeal nervous system (Berghoff et al., 2021; Pereira et al., 2015) and there  
657 are some striking potential examples in vertebrates (Brunet and Pattyn, 2002; Dauger et al.,  
658 2003; Ha and Dougherty, 2018; Ruiz-Reig et al., 2019; Sokolowski et al., 2015). This present  
659 study provides an extreme example of this. An entire set of synaptically connected neurons  
660 (the worm’s enteric nervous system) is specified by a single transcription factor (CEH-34),  
661 which apparently helps these neurons to become assembled into functional circuitry. In  
662 each pharyngeal neuron type, CEH-34 pairs up with different homeodomain proteins to  
663 diversify pharyngeal neurons into distinct identities. Following Dobzhansky’s dictum that  
664 “nothing in biology makes sense except in the light of evolution” (Dobzhansky, 1964) we  
665 speculate that the pharyngeal nervous system may have derived from a homogenous set  
666 of interconnected, identical neurons, all specified by *ceh-34*, which may have regulated a  
667 homophilic adhesion molecule that functionally linked these ancestral neurons. The more  
668 complex, present day circuitry may have evolved through the eventual partnering of CEH-  
669 34 protein with distinct sets of homeodomain proteins that diversified neuronal identities,  
670 connectivity and function in the pharyngeal nervous system.

671 Arguing for a conserved function of Six homeodomain factors in enteric nervous  
672 system differentiation is the observation that in flies, the Sine oculis paralog Optix is indeed  
673 expressed in the frontal ganglion (Seo et al., 1999), which constitutes the nervous system  
674 of insect foreguts (Hartenstein, 1997). In the context of studying Sine oculis function in the  
675 *Drosophila* corpus cardiacum, it was also noted that the entire stomatogastric ganglion, i.e.

676 the entire enteric nervous system (of which the frontal ganglion is a part) does not form in  
677 Sine oculis mutants (De Velasco et al., 2004). In sea urchin, pharyngeal neurons also  
678 express, and require for their proper development, the Sine oculis paralog Six3 (Wei et al.,  
679 2011). Other than an early report of Six2 expression in the mouse foregut region (Ohto et  
680 al., 1998), the expression and function of Sine oculis orthologs in vertebrate enteric  
681 nervous systems has, to our knowledge, not yet been examined.

682         Notably, another homeobox gene appears to have a critical and very broad function  
683 in vertebrate enteric nervous system development that is akin to the broadness of *ceh-34*  
684 function in *C. elegans*. The Paired-type homeobox gene Phox2b is expressed in enteric  
685 nervous system precursors and required early in development for the generation of all  
686 enteric ganglia (Pattyn et al., 1999; Tiveron et al., 1996). While Phox2b is also  
687 continuously expressed throughout the adult enteric nervous system (Corpening et al.,  
688 2008; Drokhyansky et al., 2020; Morarach et al., 2021), its function in terminal  
689 differentiation and perhaps even maintenance of enteric neurons identity remains to be  
690 examined, for example, via temporally controlled, post-developmental knock-out in juvenile  
691 or adult stage animals. If the analogy to *ceh-34* holds, the enteric neurons of such animals  
692 may lose their differentiated state. Remarkably, additional homeobox genes have recently  
693 been noted to show highly selective expression patterns within the vertebrate enteric  
694 nervous system, effectively discriminating distinct neuronal subtypes (Memic et al., 2018).  
695 One of them, the Meis ortholog Pbx3 has been confirmed to play an important role in the  
696 postmitotic specification of distinct enteric neuron types (Morarach et al., 2021). Hence, it  
697 appears that the overall logic of a pan-enteric homeobox gene, cooperating with cell type  
698 specific homeobox genes, may be conserved from worms to vertebrates.

699         Another evolutionary perspective of our findings considers the origins of the enteric  
700 nervous system, and maybe nervous systems as a whole. Based on a number of  
701 anatomical and functional features, it has been proposed that enteric nervous systems  
702 preceded, and then paralleled the emergence of centralized nervous system of bilaterian  
703 animals (Furness and Stebbing, 2018; Gilbert, 2019; Klimovich and Bosch, 2018). This  
704 argument is bolstered by considering a number of features of the enteric, i.e. pharyngeal  
705 nervous system of *C. elegans*: (a) its polymodality (sensory + inter + motor neuron) of most  
706 pharyngeal neurons, (b) its innervation of what is essentially a single sheath of myoepithelial  
707 cells, a proposed feature of primitive nervous systems (Mackie, 1970), (c) its simple immune

708 functions (also thought to be a feature of primitive neurons, e.g. in hydra)(Klimovich et al.,  
709 2020; Klimovich and Bosch, 2018) and (d) the relatively indiscriminate synaptic cross-  
710 innervation patterns among pharyngeal neurons (Cook et al., 2020). If pharyngeal neurons  
711 indeed resemble a more primitive, ancestral state of neurons, our observation that CEH-34  
712 acts as a terminal selector in these neurons would point to the ancient nature of (a) a  
713 terminal selector-type logic of neuronal identity specification and (b) the deployment of a  
714 homeobox gene in such function. Sine oculis homologs appear to be employed broadly in  
715 sensory neuron specification across animal phylogeny, even in the most basal metazoan  
716 (Jacobs et al., 2007). CEH-34/Sine oculis may represent an ancestral determinant of  
717 neuronal cell types.

718

719

## 720 MATERIALS AND METHODS

721

### 722 Microscopy and image analysis

723 Worms were anesthetized using 100 mM sodium azide (NaN<sub>3</sub>) and mounted on 5%  
724 agarose pads on glass slides. Z-stack images (each ~0.7 micron thick) were acquired using a  
725 Zeiss confocal microscope (LSM880) or Zeiss compound microscope (Imager Z2) with the  
726 ZEN software. Maximum intensity projections of 2 to 30 slices were generated with the  
727 ImageJ software (Schindelin et al., 2012).

728 Reporter gene expression in different neurons was visualized in wild type and mutant  
729 animals and usually assigned to one of the following categories: “on” (fluorescence levels  
730 comparable to wild type animals), “dim” (fluorescence still detectable but much dimmer than  
731 wild type animals) or “off” (fluorescence not detectable). In cases where fluorescence levels  
732 were variable between animals and difference with wild type was not obvious mean  
733 fluorescence intensity in each neuron was measured with the ImageJ software.

734

### 735 *Caenorhabditis elegans* strains

736 Worms were grown at 20°C on nematode growth media (NGM) plates seeded with *E.*  
737 *coli* (OP50) bacteria as a food source. The wild-type strain used is Bristol N2. A complete list  
738 of strains used in this study can be found in **Supplemental File 1**.

### 739 Generation of deletion alleles

740 Mutant alleles for the *ceh-34*, *ceh-45*, *vab-15*, *ceh-7*, *ceh-53*, *ceh-79* and *eya-1* genes  
741 (schematized in **Fig.2A** and **Fig.11 – Supplement 1**) were generated by CRISPR/Cas9  
742 genome engineering as described (Dokshin et al., 2018). A deletion of the full locus was  
743 generated using two crRNAs and an ssODN donor. Sequences are as follows:

744 ***ceh-34(ot1014)***: crRNAs (cgacaagaggacgacgctct and ttattctaattggtcttgagg), ssODN  
745 (gcgacattcactgggggacgacaagaggacgacgcccaagaccattagaataacttttaactatattttg).

746 *ceh-34(ot1188)* and *ceh-34(ot1189)* were generated the same way as *ceh-34(ot1014)* and  
747 are molecularly identical. The difference is that *ot1188* was generated in the background of



748 *flr-2(syb4861)* and *ot1189* was generated in the background of *htrl-1(syb4895)* because  
749 these loci are very closely linked to *ceh-34*.

750 ***ceh-45(ot1065)***: crRNAs (taggccaccgatacaagcag and tccgccagagaccggctcggg), ssODN  
751 (aactgaaattcgaaattctagggccaccgatacaaggaccggctctcggcggattactgtagccgtttggg).

752 ***vab-15(ot1136)***: crRNAs (ggcacaacacatctgcttata and ttgtgaaaagcgtaatactt), ssODN  
753 (agcgcgtggtgttatattggtcaacacatctgctttattacgcttttcacaatatatttatggactaacca).

754 ***ceh-7(ot1138)***: crRNAs (cccctgtactgacaattga and tgatcaggaattgctctcg), ssODN  
755 (cgaaacgaaaacgggcgccccctgtactgacaatgagcaaattcctgatcatctgacactttccagac).

756 ***ceh-53(ot1066)***: crRNAs (gcggcgcttccgggactctg and gaaatcaggggcaaactgg ), ssODN  
757 (gctccatcagaaaaagggcgggcgcttccgggactagttgccccctgatttcgaatatattatgtgaaaaa).

758 ***ceh-79(ot1067)***: crRNAs (aagaagaaccgacgaaccca and cccccccaactgtgttcac), ssODN  
759 (aactcctgtctccttcgatgatctttccatggcactggacacatatcttaactttccgatgtgta).

760 ***eya-1(ot1197)***: crRNAs (tttgtacgagtgactcagt and acacctgtatctctgcgggg), ssODN  
761 (cggtcgtcagattggtagccctccaaaatcccactcgcagagatacaggtgttcaaaatcgggggtgaaga).

762 With the exception of *ceh-34(ot1014)* animals, all other null mutant alleles are homozygous  
763 viable. *ceh-45(ot1065)* and *vab-15(ot1136)* are slow growing and at least *ceh-45(ot1065)*  
764 animals also display a partially penetrant embryonic lethality.

765

## 766 Generation of reporter knock-ins

767 The *ceh-34* locus was tagged with *mNG::3xFLAG::AID* to generate *ceh-34(ot903)*. The  
768 Auxin-Inducible Degron (AID) sequence was amplified and inserted into the pDD268 vector  
769 (*mNG::SEC::3xFLAG*) (Dickinson et al., 2015) to generate the plasmid pUA77  
770 (*ccdB::mNG::SEC::3xFLAG::AID ccdB*)(Aghayeva et al., 2021). The construct contains a self-  
771 excising drug selection cassette (SEC) and was used for SEC-mediated CRISPR insertion of  
772 *mNG::3xFLAG::AID* right before the stop codon of *ceh-34* as described in (Dickinson et al.,  
773 2015). The guide RNA used targets the following sequence: ttattctaattggtcttgagg.

774 The *pha-4* locus was tagged with *gfp* at its 3'end to generate *pha-4(ot946)*, using Cas9  
775 protein, tracrRNA, and crRNA from IDT, as previously described (Dokshin et al., 2018). One

776 crRNA (attggagatttataggttg) and an asymmetric double stranded *gfp-loxP-3xFLAG* cassette,  
777 amplified from a plasmid, were used to insert the fluorescent tag at the C-terminal.

778 Reporter alleles for *flp-5(syb4513)*, *flp-28(syb3207)*, *flr-2(syb4861)*, *htl-1(syb4895)*,  
779 *ser-7(syb4502)*, *rig-3(syb4763)*, *rig-6(syb4729)*, *trh-1(syb4421)* and *trhr-1(syb4453)* were  
780 generated by CRISPR/Cas9 to insert an *SL2::GFP::H2B* cassette at the C-terminus of the  
781 respective gene. For the *unc-17(syb4491)* allele *T2A::GFP::H2B* was inserted at the C-  
782 terminus. For the *kin-36(syb4677)* locus, a *GFP::HIS::SL2* sequence was inserted at the N-  
783 terminus. These strains were generated by Sunybiotech and are listed in **Supplemental File**  
784 **1**.

#### 785 Generation of transgenic reporter strains

786 To generate *otIs762(ceh-34prom::TagRFP)* a 3720bp PCR fragment containing the  
787 whole *ceh-34* intergenic region plus the first 2 exons and 2 introns was amplified from N2  
788 genomic DNA and cloned into a TagRFP vector using Gibson Assembly (NEBuilder HiFi DNA  
789 Assembly Master Mix, Catalog # E2621L). The following primers were used:  
790 aatgaaataagcttgcacgctgcaTGTTTATTTTCTATGTAATTTCTAATAAAGTCCC and  
791 cccggggatcctctagagtcgacgctgcaCTGAAAGTTGAAATATAGAATTTTAAATTTTTTTTTTTTG. The resulting  
792 construct was injected as a simple extrachromosomal array (50ng/ul) into *pha-1(e2123)*  
793 animals, using a *pha-1* rescuing plasmid (pBX, 50ng/ul) as co-injection marker. A  
794 representative line was integrated into the genome with gamma irradiation and backcrossed  
795 4 times.

796 To generate *otIs785(ceh-34prom::GFP::CLA-1)* a 3720bp PCR fragment containing  
797 the whole *ceh-34* intergenic region plus the first 2 exons and 2 introns was amplified from N2  
798 genomic DNA and cloned into PK065 (kindly shared by Peri Kurshan) using Gibson  
799 Assembly (NEBuilder HiFi DNA Assembly Master Mix, Catalog # E2621L). The following  
800 primers were used: gattacgccaagcttgcacgctgcaTGTTTATTTTCTATGTAATTTCTAATAAAGTC and  
801 gttcttctccttactcatcccggtgCTGAAAGTTGAAATATAGAATTTTAAATTTTTTTTTTTTG. The resulting construct  
802 was injected at 7ng/ul together with *ceh-34prom::TagRFP* (50ng/ul) (see above) and *rol-*  
803 *6(su1006)* as a co-injection marker. A representative line was integrated into the genome with  
804 gamma irradiation and backcrossed 4 times.

805

#### 806 **Choice of pharyngeal fate markers**

807 Most fate markers used in this paper were previously described. For several of those,  
808 we used previous expression patterns (based on transgenic reporter fusions) as a guide to  
809 then generate reporter alleles by CRISPR/Cas9 genome engineering (e.g. *flp-5*, *ser-7*; all  
810 listed in previous sections). One case warrants specific emphasis: scRNA has shown that the  
811 T11F9.12 gene is expressed exclusively in most, if not all pharyngeal neurons, a notion we  
812 confirmed with a CRISPR/Cas9 genome engineered reporter allele. T11F9.12 encodes for a  
813 relatively large (736aa), secreted and nematode specific protein that contains a Pfam-  
814 annotated domain (HtrI domain; PF09612) that is, outside nematodes, only found in a bacterial  
815 protein HtrL. This bacterial protein currently has no assigned function but is found in a region  
816 of LPS core biosynthesis genes which are involved in bacterial immune defense (Bertani and  
817 Ruiz, 2018). Interestingly, hidden Markov model-based searches in the Panther database  
818 reveal a sequence pattern (PTHR21579) along the entire T11F9.12 protein that is otherwise  
819 only found in *C. elegans* saposin proteins, which are bona fide immune effector proteins  
820 (Banyai and Patthy, 1998; Hoeckendorf et al., 2012; Oishi et al., 2009). We named this  
821 protein HTRL-1.

822

### 823 **Temporally controlled CEH-34 protein degradation**

824 We used conditional protein depletion with a modified auxin-inducible degradation  
825 system (*C.e.AIDv2*)(Hills-Muckey et al., 2022). AID-tagged proteins are conditionally  
826 degraded when exposed to 5-Ph-IAA in the presence of  $_{At}TIR1^{F79G}$ . To generate the  
827 experimental strain, the conditional allele *ceh-34(ot903[ceh-34::mNG::AID])* was crossed with  
828 *cshIs140[rps-28p::TIR1(F79G)]*, which expresses  $_{At}TIR1^{F79G}$  ubiquitously. The synthetic auxin  
829 analog 5-Ph-IAA was purchased from BioAcademia (#30-003-10) and dissolved in ethanol  
830 (EtOH) to prepare 100 mM stock solutions. NGM agar plates with fully grown OP50 bacterial  
831 lawn were coated with the 5-Ph-IAA stock solution to a final concentration of 200  $\mu$ M and  
832 allowed to dry overnight at room temperature. To induce protein degradation, synchronized  
833 L1 or young adult worms were transferred onto 5-Ph-IAA -coated plates and kept at 20°C. As  
834 a control, worms were transferred onto EtOH-coated plates instead. 5-Ph-IAA solutions and  
835 experimental plates were shielded from light.

836

837

838 **ACKNOWLEDGEMENTS**

839 We thank Chi Chen for generating transgenic lines, Seth Taylor and Michael Gershon for  
840 discussion, Kelly Liu, Robert Horvitz, Peri Kurshan and Matthias Leippe for providing  
841 reagents, Steven Cook for providing illustrations and Michael Gershon and members of the  
842 Hobert lab for comments on the manuscript. This work was funded by NIH R21NS106843,  
843 NIH R01NS039996 and the Howard Hughes Medical Institute.

844

845

846

847

848

849 **FIGURE LEGENDS**

850

851 **Figure 1: The pharyngeal nervous system of *C. elegans*.**

852 **(A)** Overview of the *C. elegans* alimentary system from Wormbook (Hall and Altun, 2007),  
853 with neuronal cell bodies in the pharynx added in red.

854 **(B)** Projection patterns of pharyngeal neurons within the pharynx displayed in the format of a  
855 subway map (kindly provided by S.J. Cook).

856 **(C)** Full connectome of pharyngeal nervous system, adapted from (Cook et al., 2020). Square  
857 nodes are end-organs, including muscle (green), marginal cells (fuchsia), gland cells (blue),  
858 epithelial cells (grey), and basement membrane (orange). Neurons are red ellipses. Neurons  
859 with outlines have either apical (purple), unexposed (brown), or embedded (blue) sensory  
860 endings. Directed chemical edges and undirected gap junction edges are represented by  
861 black arrows and red lines, respectively. The line width is proportional to the anatomical  
862 strength of that connection (# serial sections). The pharyngeal nervous system is connected  
863 to the rest of the nervous system through a single neuron pair (RIP).

864 **(D)** Single cell transcriptome similarity between neuron types classes with widths of edges  
865 indicating strengths of similarity (Pearson correlation coefficients  $>0.7$ ), showing that  
866 pharyngeal neurons are more similar to each other than to other neurons in the *C. elegans*  
867 nervous system. Reproduced from (Taylor et al., 2021).

868 **(E)** Molecular markers used in this study for cell fate analysis. See **Supplemental File 1** for  
869 information on reporter constructs.

870

871

872 **Figure 2: *ceh-34* is expressed in all pharyngeal neurons.**

873 **(A)** *ceh-33* and *ceh-34* loci showing different alleles and fosmid reporters used in this study.

874 **(B)** Expression of the *ceh-34* CRISPR/Cas-9-engineered reporter allele *ot903* over the  
875 course of development. *ceh-33* fosmid reporter (*wgls575*) shows expression in a subset of  
876 head muscle cells.

877 **(C)** Pharynx organ selector *pha-4* controls *ceh-34* expression (as analyzed with the *wgls524*  
878 transgene). Animals were scored at the L1 stage. Presumptive “pharyngeal cells” in *pha-4*  
879 mutant are marked with a red *pha-4* promoter fusion (*stls10077*). Cells co-expressing *ceh-34*  
880 and *pha-4* were counted (yellow cells). *ceh-34* expression in head muscle cells, marked with  
881 red asterisk, is not affected since they do not express *pha-4*.

882

883 **Figure 2 – Supplement 1: Evolution of *Sine oculis* orthologs in nematodes.**

884 **(A)** Phylogeny of *ceh-33/34* gene duplication in nematodes. Phylogeny based on  
885 homeodomains.

886 **(B)** Synteny of the *ceh-33/ceh-34* locus across several *Caenorhabditis* species.

887

888 **Figure 2 – Supplement 2: Expression of the organ selector *pha-4*.**

889 **(A)** *pha-4* expression (*stls10077*) is not affected in *ceh-34* mutants. Animals were  
890 scored at the L1 stage. Statistical analysis was performed using unpaired t-test.

891 **(B)** *pha-4* is continuously expressed in pharyngeal neurons. Expression of a  
892 CRISPR/Cas9-engineered *pha-4* reporter allele (*ot946*) in green and a *rab-3<sup>prom</sup>* reporter  
893 (*otls355*) in red in L1 (left), L3 (middle) and adult (right) animals. High magnifications of  
894 the anterior bulb provided in the insets at the bottom left corner of the merged images.  
895 Arrows point to pharyngeal neurons expressing both *pha-4* and *rab-3*.

896

897

898 **Figure 3: Pharyngeal neurons are generated in *ceh-34* mutants but lose their**  
899 **neurotransmitter identity.**

900 **(A)** Pictures at the L1 stage showing expression of panneuronal reporter transgenes that  
901 monitor *ric-4* (*otIs350*) , *ric-19* (*otIs380*), *unc-11* (*otIs620*) and *rab-3* (*otIs291*) expression. A  
902 single plane with a subset of pharyngeal neurons marked with red arrows is shown for clarity.

903 **(B)** *ceh-34* affects the expression of neurotransmitter identity genes. Glutamatergic,  
904 cholinergic and serotonergic identity is lost. Reporter transgenes used are *eat-4* (*otIs487*,  
905 *otIs558*), *unc-17* (*otIs661*), *tph-1* (*otIs517*) , *cat-1* (*otIs221*), *cat-4* (*otIs225*) and *bas-1*  
906 (*otIs226*). Animals were scored at the L1 stage. Statistical analysis was performed using  
907 Fisher's exact test or Chi-Square test. N is indicated within each bar and represents number  
908 of neurons scored.

909 **(C)** Circuit diagram summarizing the effect of *ceh-34* on neurotransmitter identity. Nodes are  
910 colored to illustrate neurotransmitter identity gene expression. Nodes lose coloring when  
911 expression is affected in *ceh-34* mutants (grey indicates partial effect). Edges are colored if  
912 the source neuron expresses either *eat-4* (glutamatergic), *unc-17* (cholinergic) or *tph-1*  
913 (serotonergic). Edges lose coloring when expression of these genes is affected in the source  
914 neuron in *ceh-34* mutants (irrespective of whether the effect is partial or total). Note that in  
915 this and ensuing circuit diagrams, the existence of gray edges does not indicate whether  
916 those edges are generated properly in *ceh-34* mutants. Directed edges (arrows) represent  
917 chemical synapses. Undirected edges (dashed lines) represent electrical synapses. The  
918 width of the edge is proportional to the weight of the connection (the number of serial section  
919 electron micrographs where a synaptic specialization is observed).

920

921

922 **Figure 4: *ceh-34* affects the expression of receptors for neurotransmitters and**  
923 **neuropeptides.**

924 **(A)** Representative pictures and quantification showing neurotransmitter receptor expression  
925 loss in *ceh-34* mutants. Reporter genes used are transgenes *glr-2 (ivIs26)*, *mgl-1 (otIs341)*  
926 and a CRISPR/Cas9-engineered reporter allele for *ser-7 (syb4502)*. Animals were scored at  
927 the L1 stage. Statistical analysis was performed using Fisher's exact test or Chi-Square test.  
928 N is indicated within each bar and represents number of neurons scored.

929 **(B)** Representative pictures and quantification showing neuropeptide receptor expression  
930 loss in *ceh-34* mutants. Reporter gene used is the CRISPR/Cas9-engineered reporter allele  
931 *trhr-1 (syb4453)*. Animals were scored at the L1 stage. Statistical analysis was performed  
932 using unpaired t-test.

933 **(C)** Circuit diagram summarizing the effect of *ceh-34* on neurotransmitter and neuropeptide  
934 receptor expression. Nodes lose coloring when expression is affected in *ceh-34* mutants  
935 (gray indicates partial effect; *ser-7* and *trhr-1* are colored white in all neurons since identity of  
936 neurons with partial effect is not known). See legend to Figure 3 for more information on  
937 circuit diagram features.

938

939



940 **Figure 5: *ceh-34* affects neuropeptidergic identity of pharyngeal neurons.**

941 **(A)** Representative pictures and quantification showing expression of 10 different

942 neuropeptides is affected in *ceh-34* mutants. Reporter genes used are transgenic reporters

943 for *flp-2* (*ynIs57*), *flp-4* (*ynIs30*), *flp-15* (*ynIs45*), *flp-21* (*ynIs80*), *nlp-3* (*otIs695*), *nlp-8*

944 (*otIs711*) and *nlp-13* (*otIs742*) and CRISPR/Cas9-engineered reporter alleles for *flp-5*

945 (*syb4513*), *flp-28* (*syb3207*) and *trh-1* (*syb4421*). Animals were scored at the L1 stage.

946 Statistical analysis was performed using Fisher's exact test, Chi-Square test or unpaired t-

947 test. N is indicated within each bar and represents number of neurons scored.

948 **(B)** Circuit diagram summarizing the effect of *ceh-34* on neuropeptide expression. Nodes lose

949 coloring when neuropeptide expression is affected in *ceh-34* mutants (gray indicates partial

950 effect; *flp-5* and *nlp-3* are colored white in all neurons since identity of neurons with partial

951 effect is not known). See legend to Figure 3 for more information on circuit diagram features.

952

953

**Figure 6: *ceh-34* affects other identity features of pharyngeal neurons.**

**(A)** Representative pictures and quantification showing sensory receptor expression loss in *ceh-34* mutants. Reporter transgenes used are *glr-7* (*otIs809*), *gur-3* (*nIs780*) and *str-97* (*otIs716*). *str-97* (*otIs716*) is expressed in M1 in adult animals, but also in M4 in first larval stage animals. Expression in M4 is lost in *ceh-34* mutant, but expression in M1 could not be reliably scored. Animals were scored at the L1 stage. Statistical analysis was performed using Fisher's exact test. N is indicated within each bar and represents number of neurons scored.

**(B)** Representative pictures and quantification showing effect of *ceh-34* on antimicrobial defense genes. Reporter genes used are *spp-12* (*otIs868*) and CRISPR/Cas9-engineered reporter alleles for *flr-2* (*syb4861*) and *htrl-1* (*syb4895*). Animals were scored at the L1 stage. Statistical analysis was performed using Fisher's exact test, Chi-Square test or unpaired t-test. N is indicated within each bar and represents number of neurons scored.

**(C)** Representative pictures and quantification showing effect of *ceh-34* on pan-pharyngeal genes. Reporter gene is the CRISPR/Cas9-engineered reporter allele *kin-36* (*syb4677*). Animals were scored at the L1 stage. Statistical analysis was performed using unpaired t-test.

**Figure 6 – Supplement 1: Single cell transcriptomic analysis.**

scRNA data was extracted from the Cengen App and displayed in a heatmap format, as previously described (Taylor et al., 2021). The F13H10.6 gene was included here as well because of its striking expression outside the pharyngeal nervous system, in what appear to be exclusively sensory neurons, in line with most if not all pharyngeal neurons also having sensory function. Conversely, previously identified pan-sensory genes (e.g. cilium related genes) do not show expression in pharyngeal neurons.

**Figure 6 – Supplement 2: *ceh-34* affects *ceh-28* expression.**

Representative pictures and quantification are shown. Reporter gene used is *ceh-28* (*nIs175*). Twenty per cent of worms show a cell outside the pharynx ectopically expressing *ceh-28*. Animals were scored at the L1 stage. Statistical analysis was performed using Fisher's exact test. N is indicated within each bar and represents number of neurons scored.

987 **Figure 7: *ceh-34* is continuously required to maintain gene expression and function of**  
988 **pharyngeal neurons.**

989 **(A)** Schematic of the AIDv2 system (Hills-Muckey et al., 2022). Skp1, Cul1, Rbx1 and E2 are  
990 phylogenetically conserved components of the E3 ligase complex. TIR1<sup>F79G</sup> is a modified  
991 plant-specific substrate-recognizing subunit of the E3 ligase complex. In the presence of the  
992 auxin analog (5-Ph-IAA), the enzyme TIR1<sup>F79G</sup> binds to the AID fused to a protein of interest,  
993 leading to ubiquitination and proteasomal degradation of the targeted protein.

994 **(B)** Schematic depicting the 5-Ph-IAA treatment. Synchronized populations of worms at the  
995 L1 and young adult stage were transferred onto 5-Ph-IAA-coated plates and scored 48h later.  
996 Worms were expressing TIR1<sup>F79G</sup> ubiquitously under the *rps-28* promoter (*csHls140*). The  
997 *ceh-34* locus was tagged with *mNG::AID* (*ot903*).

998 **(C)** *ceh-34* is required for maintained expression of identity genes. Reporter genes used are  
999 *spp-12* (*otIs868*) and CRISPR/Cas-9-engineered reporter alleles for *eat-4* (*syb4257*), *unc-17*  
1000 (*syb4491*) and *ser-7* (*syb4502*). Since *ceh-34::mNG::AID* (*ot903*) and reporter genes scored  
1001 are all fluorescent green, and this was obscuring the scoring on ethanol conditions, the  
1002 control conditions are reporter genes on their own treated with 5-Ph-IAA. Representative  
1003 pictures of larval depletion are shown on the left and quantification for larval and adult  
1004 depletion is shown on the right. Quantification is only shown for neurons that were affected.  
1005 Some neurons were not affected and this may be explained by the fact that constitutive 5-Ph-  
1006 IAA treatment does not fully recapitulate the *ceh-34* null phenotype. Statistical analysis was  
1007 performed using unpaired t-test, Fisher's exact test or Chi-Square test. N is indicated within  
1008 each bar and represents number of neurons scored.

1009 **(D)** *ceh-34* is required for maintained pharyngeal function. Larval and adult *ceh-34* depletion  
1010 results in decreased pharyngeal pumping. Statistical analysis was performed using two-way  
1011 ANOVA.

1012

1013

1014

**Figure 8: *ceh-34* affects the assembly of pharyngeal circuitry**

**(A)** *ceh-34* null mutants have very disorganized axonal projections. Axonal projections were scored as a whole rather than by individual neuron because with all the pharyngeal neurons being labeled it was difficult to assign specific projections to individual neurons. Neurites were classified as defective when obviously deviating from the wild type path. Representative pictures and quantification are shown. Reporter gene is *ceh-34 (otIs762)*. Animals were scored at the L1 stage. Statistical analysis was performed using Fisher's exact test. N is indicated within each bar and represents number of worms.

**(B)** *ceh-34* null mutants show disorganized pharyngeal nerve ring presynaptic specializations as visualized with CLA-1 puncta. Representative pictures are shown. Quantification (right panels) shows gfp intensity profiles along the anterior posterior axis. Reporter gene is *otIs785*. Animals were scored at the L1 stage.

**(C)** *ceh-34(n4796)* hypomorph mutants show axonal defects in NSM (top panel) and I5 (bottom panel). Representative pictures and quantification are shown. For NSM the ventral, dorsal and thin projection (not visible in picture) were scored separately (graph on the left) and then data was pulled together to indicate the percentage of worms showing any defect (graph on the right). Reporter genes used are *tph-1 (zdIs13)* and *unc-4 (otEx7503)*. Animals were scored at the L4 stage. Statistical analysis was performed using Fisher's exact test. N is indicated within each bar and represents number of neurons or number of worms.

**(D)** *ceh-34* affects expression of the axon guidance cue *sIt-1 (kyls174)*. Representative pictures and quantification are shown. Animals were scored at the L1 stage. Statistical analysis was performed using Fisher's exact test. N is indicated within each bar and represents number of neurons scored.

**(E)** *ceh-34* affects expression of CRISPR/Cas9-engineered reporter alleles for *rig-3 (syb4763)* and *rig-6 (syb4729)*, two Ig superfamily members. *rig-3* and *rig-6* are expressed in almost all pharyngeal neurons plus many other cells within and outside the pharynx. Worms were scored with a red panneuronal marker (*otIs355*) or a red *ceh-34promoter* fusion (*stIs10447*) in the background to facilitate scoring. Number of yellow cells were counted within the pharynx. Animals were scored at the L1 stage. Statistical analysis was performed using unpaired t-test.

1045

**Figure 8 – Supplement 1: *ceh-34* is required to maintain synapse organization in the pharyngeal nervous system.**

1047

Synchronized population of worms at the L1 or young adult stage were transferred onto Ethanol or 5-Ph-IAA-coated plates and scored 48h later. Worms were expressing TIR1<sup>F79G</sup> ubiquitously under the *rps-28* promoter (*csH/s140*). Reporter gene scored is *cla-1* (*otIs785*). Representative pictures and quantification are shown. Orange bar indicates the region that was quantified. Statistical analysis was performed using unpaired t-test.

**Figure 8 – Supplement 2: Axonal defects in *slt-1* mutants.**

**(A)** Effects of *slt-1* on the I2/I4 neurons. Orange arrows indicate position of pharyngeal nerve ring. Blue arrow indicates ectopic projection. Reporter gene is *gur-3* (*nIs780*).

**(B)** Effects of *slt-1* on the M1 neuron. Orange arrow indicate shortened M1 process, which normally extends to the anterior end of the pharynx. Reporter gene is *str-97* (*otIs716*).

Representative images and quantification are shown. Animals were scored at the L4 stage. Statistical analysis was performed using Chi-Square test. N is indicated within each bar and represents number of neurons scored.

1066 **Figure 9: Limited involvement of *eya-1* in pharyngeal neuron identity specification.**

1067 **(A)** *eya-1* is expressed in all pharyngeal neurons throughout the life of the worm. Images of

1068 L1 and adult worms showing co-localization of *eya-1* expression (*nls352*) with the

1069 panneuronal gene *rab-3* (*otls355*) in pharyngeal neurons.

1070 **(B)** *eya-1* expression is regulated by *ceh-34*. Representative pictures and quantification are

1071 shown. Reporter gene is *eya-1* (*nls352*). Animals were scored at the L1 stage. Statistical

1072 analysis was performed using Fisher's exact test. N is indicated within each bar and

1073 represents number of worms scored.

1074 **(C)** *eya-1* mutant shows defects in pharyngeal neuron neurotransmitter identity.

1075 Representative images and quantification are shown for *unc-17* (*otls661*), *eat-4* (*otls487*) and

1076 *tph-1* (*otls517*). Animals were scored at the L4 stage. Statistical analysis was performed

1077 using Fisher's exact test. N is indicated within each bar and represents number of neurons

1078 scored.

1079

1080

1081 **Figure 10: *ceh-34* cooperates with homeobox genes to specify distinct pharyngeal**  
1082 **neuron types.**

1083 **(A)** *unc-86* and *ceh-34* show synergistic effects in NSM differentiation. Representative  
1084 images and quantification are shown. Reporter gene used is *cat-1 (otIs224)*. Animals were  
1085 scored at the L4 stage. Statistical analysis was performed using Fisher's exact test. P-values  
1086 were adjusted with the Holm-Sidak correction for multiple comparisons. N is indicated within  
1087 each bar and represents number of neurons scored.

1088 **(B)** *unc-86* and *ceh-34* show synergistic effects in I1 neuron differentiation. Representative  
1089 images and quantification are shown. Reporter gene used is *unc-17 (otIs661)*. Animals were  
1090 scored at the L4 stage. Statistical analysis was performed using Fisher's exact test. P-values  
1091 were adjusted with the Holm-Sidak correction for multiple comparisons. N is indicated within  
1092 each bar and represents number of neurons scored.

1093 **(C)** *ceh-14* and *ceh-34* show synergistic effects in I2 neuron differentiation. Representative  
1094 images and quantification are shown for *eat-4 (otIs518)*. Bottom graph shows quantification  
1095 for *nlp-8 (otIs711)*. Animals were scored at the L4 stage. Statistical analysis was performed  
1096 using Fisher's exact test or Chi-Square test . P-values were adjusted with the Holm-Sidak  
1097 correction for multiple comparisons. N is indicated within each bar and represents number of  
1098 neurons scored.

1099 **(D)** *pros-1* affects I3 neuron differentiation. Representative images and quantification are  
1100 shown. Reporter gene is *unc-17 (otIs576)*. Animals were scored at the L1 stage. Statistical  
1101 analysis was performed using Fisher's exact test. N is indicated within each bar and  
1102 represents number of neurons scored.

1103 **(E)** *ceh-2* affects I3 neuron differentiation. Representative images and quantification are  
1104 shown. Reporter gene used is a CRISPR/Cas9-engineered allele for *ser-7 (syb4502)*.  
1105 Animals were scored at the L4 stage. Statistical analysis was performed using Fisher's exact  
1106 test. N is indicated within each bar and represents number of neurons scored.

1107 **(F)** *ceh-2* and *ceh-34* show synergistic effects in I3 neuron differentiation. Representative  
1108 images and quantification are shown. Reporter gene used is CRISPR/Cas9-engineered allele  
1109 for *unc-17 (syb4491)*. Animals were scored at the L4 stage. Statistical analysis was  
1110 performed using Fisher's exact test. P-values were adjusted with the Holm-Sidak correction  
1111 for multiple comparisons. N is indicated within each bar and represents number of neurons  
1112 scored.

1113

1114 **Figure 11: Other homeobox genes involved in specifying distinct pharyngeal neuron**  
1115 **types.**

1116 **(A)** *ceh-2* affects M3 neuron differentiation. Representative images and quantification are  
1117 shown. Reporter gene is *eat-4* (*otIs388*). Animals scored at the L4 stage. Statistical analysis  
1118 was performed using Chi-Square test. N is indicated within each bar and represents number  
1119 of neurons scored.

1120 **(B)** *vab-15* affects M5 neuron differentiation. Representative images and quantification are  
1121 shown. Reporter genes used are *ceh-34* (*stIs10447*) and CRISPR/Cas9-engineered alleles  
1122 for *unc-17* (*ot907*) and *trh-1* (*syb4421*). Animals were scored at the L4 stage. Statistical  
1123 analysis was performed using Fisher's exact test. N is indicated within each bar and  
1124 represents number of neurons scored.

1125 **(C)** *ceh-45* affects M1 neuron differentiation. Representative images and quantification are  
1126 shown. Reporter genes used are *eat-4* (*otIs388*) and CRISPR/Cas9-engineered allele for *trh-*  
1127 *1* (*syb4421*). Animals were scored at the L4 stage. Statistical analysis was performed using  
1128 Fisher's exact test. N is indicated within each bar and represents number of neurons scored.

1129

1130 **Figure 11 – Supplement 1. Homeobox mutant alleles.**

1131 **(A)** Homeobox mutant alleles generated in this study. Numbers indicating beginning and  
1132 end of deletion are relative to the start codon of the gene of interest. See Methods for  
1133 detail.

1134 **(B)** *ceh-79*, *ceh-7* and *ceh-53* do not show defects in pharyngeal neuron differentiation  
1135 or synergistic effects with *ceh-34*. Reporter genes used are *eat-4* (*otIs388* and *otIs518*)  
1136 and a CRISPR/Cas9-engineered allele for *unc-17* (*syb4491*). Animals were scored at  
1137 the L4 stage. Statistical analysis was performed using Fisher's exact test or Chi-Square  
1138 test . P-values were adjusted with the Holm-Sidak correction for multiple comparisons. N  
1139 is indicated within each bar and represents number of neurons scored.

1140

1141 **Figure 11 – Supplement 2. Misexpression experiments**

1142 We misexpressed genomic copies of the *unc-86* and *ttx-3* locus, driven by the pan-  
1143 pharyngeal neuron promoter *ehs-1* in several independent transgenic lines to generate  
1144 the normally NSM-specific CEH-34/UNC-86/TTX-3 combination in all pharyngeal  
1145 neurons to then ask whether the NSM marker *tph-1* becomes expressed in other



pharyngeal neurons. Ectopic expression of *tph-1* was indeed observed, albeit at limited penetrance and in only some select neuron classes.

**Supplemental Data File 1. Strain list.** This file provides a list of all *C. elegans* strains used in this study.

**Source Data File.** This file provides all the primary animal scoring data.

1156 **Figure 12: Summary of homeobox gene codes involved in pharyngeal neuron identity**  
1157 **specification.** Shown here are homeobox genes for which an involvement in pharyngeal  
1158 neuron differentiation has been shown, as well as the 8 (of a total of 14) pharyngeal neuron  
1159 classes for which a homeobox regulator *besides ceh-34* has been identified to date. Each  
1160 neuron expresses additional homeobox genes (resulting in neuron-type specific combination  
1161 of homeobox genes)(Reilly et al., 2020) but the function of these additional genes remains to  
1162 be characterized.

1163

1164

1165

## 1166 REFERENCES

- 1167 Abot, A., Cani, P.D., and Knauf, C. (2018). Impact of Intestinal Peptides on the Enteric  
1168 Nervous System: Novel Approaches to Control Glucose Metabolism and Food Intake. *Front*  
1169 *Endocrinol (Lausanne)* 9, 328.
- 1170 Aghayeva, U., Bhattacharya, A., Sural, S., Jaeger, E., Churgin, M., Fang-Yen, C., and  
1171 Hobert, O. (2021). DAF-16/FoxO and DAF-12/VDR control cellular plasticity both cell-  
1172 autonomously and via interorgan signaling. *BioRxiv*.
- 1173 Albertson, D.G., and Thomson, J.N. (1976). The pharynx of *Caenorhabditis elegans*. *Philos*  
1174 *Trans R Soc Lond B Biol Sci* 275, 299-325.
- 1175 Amin, N.M., Lim, S.E., Shi, H., Chan, T.L., and Liu, J. (2009). A conserved Six-Eya cassette  
1176 acts downstream of Wnt signaling to direct non-myogenic versus myogenic fates in the *C.*  
1177 *elegans* postembryonic mesoderm. *Dev Biol* 331, 350-360.
- 1178 Arendt, D. (2008). The evolution of cell types in animals: emerging principles from molecular  
1179 studies. *Nature Reviews Genetics* 9, 868-882.
- 1180 Aspöck, G., Ruvkun, G., and Burglin, T.R. (2003). The *Caenorhabditis elegans* *ems* class  
1181 homeobox gene *ceh-2* is required for M3 pharynx motoneuron function. *Development* 130,  
1182 3369-3378.
- 1183 Avery, L. (2012). *C. elegans* feeding. *WormBook*, 1-23.
- 1184 Avery, L., and Horvitz, H.R. (1989). Pharyngeal pumping continues after laser killing of the  
1185 pharyngeal nervous system of *C. elegans*. *Neuron* 3, 473-485.
- 1186 Axang, C., Rauthan, M., Hall, D.H., and Pilon, M. (2008). Developmental genetics of the *C.*  
1187 *elegans* pharyngeal neurons NSML and NSMR. *BMC Dev Biol* 8, 38.
- 1188 Ayali, A. (2004). The insect frontal ganglion and stomatogastric pattern generator networks.  
1189 *Neurosignals* 13, 20-36.
- 1190 Babu, K., Hu, Z., Chien, S.C., Garriga, G., and Kaplan, J.M. (2011). The immunoglobulin  
1191 super family protein RIG-3 prevents synaptic potentiation and regulates Wnt signaling.  
1192 *Neuron* 71, 103-116.
- 1193 Banyai, L., and Patthy, L. (1998). Amoebapore homologs of *Caenorhabditis elegans*. *Biochim*  
1194 *Biophys Acta* 1429, 259-264.
- 1195 Baumeister, R., Liu, Y., and Ruvkun, G. (1996). Lineage-specific regulators couple cell  
1196 lineage asymmetry to the transcription of the *Caenorhabditis elegans* POU gene *unc-86*  
1197 during neurogenesis. *Genes Dev* 10, 1395-1410.
- 1198 Berghoff, E.G., Glenwinkel, L., Bhattacharya, A., Sun, H., Varol, E., Mohammadi, N., Antone,  
1199 A., Feng, Y., Nguyen, K., Cook, S.J., *et al.* (2021). The Prop1-like homeobox gene *unc-42*  
1200 specifies the identity of synaptically connected neurons. *eLife* 10.
- 1201 Bertani, B., and Ruiz, N. (2018). Function and Biogenesis of Lipopolysaccharides. *EcoSal*  
1202 *Plus* 8.
- 1203 Bhardwaj, A., Pandey, P., and Babu, K. (2020). Control of Locomotory Behavior of  
1204 *Caenorhabditis elegans* by the Immunoglobulin Superfamily Protein RIG-3. *Genetics* 214,  
1205 135-145.

1206 Bhatla, N., and Horvitz, H.R. (2015). Light and hydrogen peroxide inhibit *C. elegans* Feeding  
1207 through gustatory receptor orthologs and pharyngeal neurons. *Neuron* 85, 804-818.

1208 Brockie, P.J., Madsen, D.M., Zheng, Y., Mellem, J., and Maricq, A.V. (2001). Differential  
1209 expression of glutamate receptor subunits in the nervous system of *Caenorhabditis elegans*  
1210 and their regulation by the homeodomain protein UNC-42. *J Neurosci* 21, 1510-1522.

1211 Brunet, J.F., and Pattyn, A. (2002). Phox2 genes - from patterning to connectivity. *Curr Opin*  
1212 *Genet Dev* 12, 435-440.

1213 Cheyette, B.N., Green, P.J., Martin, K., Garren, H., Hartenstein, V., and Zipursky, S.L.  
1214 (1994). The *Drosophila* sine oculis locus encodes a homeodomain-containing protein  
1215 required for the development of the entire visual system. *Neuron* 12, 977-996.

1216 Colosimo, M.E., Brown, A., Mukhopadhyay, S., Gabel, C., Lanjuin, A.E., Samuel, A.D., and  
1217 Sengupta, P. (2004). Identification of thermosensory and olfactory neuron-specific genes via  
1218 expression profiling of single neuron types. *Curr Biol* 14, 2245-2251.

1219 Cook, S.J., Crouse, C.M., Yemini, E., Hall, D.H., Emmons, S.W., and Hobert, O. (2020). The  
1220 connectome of the *Caenorhabditis elegans* pharynx. *The Journal of comparative neurology*.

1221 Cook, S.J., Jarrell, T.A., Brittin, C.A., Wang, Y., Bloniarz, A.E., Yakovlev, M.A., Nguyen,  
1222 K.C.Q., Tang, L.T., Bayer, E.A., Duerr, J.S., *et al.* (2019). Whole-animal connectomes of both  
1223 *Caenorhabditis elegans* sexes. *Nature* 571, 63-71.

1224 Copenhaver, P.F. (2007). How to innervate a simple gut: familiar themes and unique aspects  
1225 in the formation of the insect enteric nervous system. *Dev Dyn* 236, 1841-1864.

1226 Corpening, J.C., Cantrell, V.A., Deal, K.K., and Southard-Smith, E.M. (2008). A  
1227 Histone2BCerulean BAC transgene identifies differential expression of Phox2b in migrating  
1228 enteric neural crest derivatives and enteric glia. *Dev Dyn* 237, 1119-1132.

1229 Croset, V., Rytz, R., Cummins, S.F., Budd, A., Brawand, D., Kaessmann, H., Gibson, T.J.,  
1230 and Benton, R. (2010). Ancient protostome origin of chemosensory ionotropic glutamate  
1231 receptors and the evolution of insect taste and olfaction. *PLoS Genet* 6, e1001064.

1232 Dager, S., Pattyn, A., Lofaso, F., Gaultier, C., Goridis, C., Gallego, J., and Brunet, J.F.  
1233 (2003). Phox2b controls the development of peripheral chemoreceptors and afferent visceral  
1234 pathways. *Development* 130, 6635-6642.

1235 De Velasco, B., Shen, J., Go, S., and Hartenstein, V. (2004). Embryonic development of the  
1236 *Drosophila* corpus cardiacum, a neuroendocrine gland with similarity to the vertebrate  
1237 pituitary, is controlled by sine oculis and glass. *Dev Biol* 274, 280-294.

1238 Dickinson, D.J., Pani, A.M., Heppert, J.K., Higgins, C.D., and Goldstein, B. (2015).  
1239 Streamlined Genome Engineering with a Self-Excising Drug Selection Cassette. *Genetics*  
1240 200, 1035-1049.

1241 Dierking, K., Yang, W., and Schulenburg, H. (2016). Antimicrobial effectors in the nematode  
1242 *Caenorhabditis elegans*: an outgroup to the Arthropoda. *Philos Trans R Soc Lond B Biol Sci*  
1243 371.

1244 Dobzhansky, T. (1964). Biology, Molecular and Organismic. *American Zoologist* 4, 443-452.

1245 Dokshin, G.A., Ghanta, K.S., Piscopo, K.M., and Mello, C.C. (2018). Robust Genome Editing  
1246 with Short Single-Stranded and Long, Partially Single-Stranded DNA Donors in  
1247 *Caenorhabditis elegans*. *Genetics* 210, 781-787.

1248 Dozier, C., Kagoshima, H., Niklaus, G., Cassata, G., and Burglin, T.R. (2001). The  
1249 *Caenorhabditis elegans* Six/sine oculis class homeobox gene *ceh-32* is required for head  
1250 morphogenesis. *Dev Biol* 236, 289-303.

1251 Drokhlyansky, E., Smillie, C.S., Van Wittenberghe, N., Ericsson, M., Griffin, G.K., Eraslan, G.,  
1252 Dionne, D., Cuoco, M.S., Goder-Reiser, M.N., Sharova, T., *et al.* (2020). The Human and  
1253 Mouse Enteric Nervous System at Single-Cell Resolution. *Cell* 182, 1606-1622 e1623.

1254 Du, H., and Chalfie, M. (2001). Genes Regulating Touch Cell Development in *Caenorhabditis*  
1255 *elegans*. *Genetics* 158, 197-207.

1256 Feng, H., and Hope, I.A. (2013). The *Caenorhabditis elegans* homeobox gene *ceh-19* is  
1257 required for MC motoneuron function. *Genesis* 51, 163-178.

1258 Fung, C., and Vanden Berghe, P. (2020). Functional circuits and signal processing in the  
1259 enteric nervous system. *Cell Mol Life Sci* 77, 4505-4522.

1260 Furness, J.B. (2000). Types of neurons in the enteric nervous system. *J Auton Nerv Syst* 81,  
1261 87-96.

1262 Furness, J.B., and Stebbing, M.J. (2018). The first brain: Species comparisons and  
1263 evolutionary implications for the enteric and central nervous systems. *Neurogastroenterol*  
1264 *Motil* 30.

1265 Furuya, M., Qadota, H., Chisholm, A.D., and Sugimoto, A. (2005). The *C. elegans* eyes  
1266 absent ortholog EYA-1 is required for tissue differentiation and plays partially redundant roles  
1267 with PAX-6. *Dev Biol* 286, 452-463.

1268 Ganz, J. (2018). Gut feelings: Studying enteric nervous system development, function, and  
1269 disease in the zebrafish model system. *Dev Dyn* 247, 268-278.

1270 Gaudet, J., and Mango, S.E. (2002). Regulation of organogenesis by the *Caenorhabditis*  
1271 *elegans* FoxA protein PHA-4. *Science* 295, 821-825.

1272 Gershon, M.D. (1998). *The Second Brain* (HarperCollins).

1273 Gershon, M.D. (2013). 5-Hydroxytryptamine (serotonin) in the gastrointestinal tract. *Curr Opin*  
1274 *Endocrinol Diabetes Obes* 20, 14-21.

1275 Gilbert, S.F. (2019). Evolutionary transitions revisited: Holobiont evo-devo. *J Exp Zool B Mol*  
1276 *Dev Evol* 332, 307-314.

1277 Glenwinkel, L., Taylor, S.R., Langebeck-Jensen, K., Pereira, L., Reilly, M.B., Basavaraju, M.,  
1278 Rafi, I., Yemini, E., Pocock, R., Sestan, N., *et al.* (2021). In silico analysis of the  
1279 transcriptional regulatory logic of neuronal identity specification throughout the *C. elegans*  
1280 nervous system. *eLife* 10.

1281 Ha, N.T., and Dougherty, K.J. (2018). Spinal Shox2 interneuron interconnectivity related to  
1282 function and development. *eLife* 7.

1283 Hall, D.H., and Altun, Z. (2007). *C. Elegans Atlas* (Cold Spring Harbor Laboratory Press).

1284 Hanson, I.M. (2001). Mammalian homologues of the *Drosophila* eye specification genes.  
1285 *Semin Cell Dev Biol* 12, 475-484.

1286 Hao, J.C., Yu, T.W., Fujisawa, K., Culotti, J.G., Gengyo-Ando, K., Mitani, S., Moulder, G.,  
1287 Barstead, R., Tessier-Lavigne, M., and Bargmann, C.I. (2001). *C. elegans* Slit Acts in Midline,

1288 Dorsal-Ventral, and Anterior-Posterior Guidance via the SAX-3/Robo Receptor. *Neuron* 32,  
1289 25-38.

1290 Hao, M.M., and Young, H.M. (2009). Development of enteric neuron diversity. *J Cell Mol Med*  
1291 13, 1193-1210.

1292 Hartenstein, V. (1997). Development of the insect stomatogastric nervous system. *Trends in*  
1293 *neurosciences* 20, 421-427.

1294 Hills-Muckey, K., Martinez, M.A.Q., Stec, N., Hebbar, S., Saldanha, J., Medwig-Kinney, T.N.,  
1295 Moore, F.E.Q., Ivanova, M., Morao, A., Ward, J.D., *et al.* (2022). An engineered, orthogonal  
1296 auxin analog/AtTIR1(F79G) pairing improves both specificity and efficacy of the auxin  
1297 degradation system in *Caenorhabditis elegans*. *Genetics* 220.

1298 Hirose, T., Galvin, B.D., and Horvitz, H.R. (2010). Six and Eya promote apoptosis through  
1299 direct transcriptional activation of the proapoptotic BH3-only gene *egl-1* in *Caenorhabditis*  
1300 *elegans*. *Proc Natl Acad Sci U S A* 107, 15479-15484.

1301 Hobert, O. (2013). The neuronal genome of *Caenorhabditis elegans*. *WormBook*, 1-106.

1302 Hobert, O. (2016). Terminal Selectors of Neuronal Identity. *Curr Top Dev Biol* 116, 455-475.

1303 Hobert, O. (2021). Homeobox genes and the specification of neuronal identity. *Nat Rev*  
1304 *Neurosci* 22, 627-636.

1305 Hobson, R.J., Hapiak, V.M., Xiao, H., Buehrer, K.L., Komuniecki, P.R., and Komuniecki, R.W.  
1306 (2006). SER-7, a *Caenorhabditis elegans* 5-HT7-like receptor, is essential for the 5-HT  
1307 stimulation of pharyngeal pumping and egg laying. *Genetics* 172, 159-169.

1308 Hoeckendorf, A., Stanisak, M., and Leippe, M. (2012). The saposin-like protein SPP-12 is an  
1309 antimicrobial polypeptide in the pharyngeal neurons of *Caenorhabditis elegans* and  
1310 participates in defence against a natural bacterial pathogen. *Biochem J* 445, 205-212.

1311 Horner, M.A., Quintin, S., Domeier, M.E., Kimble, J., Labouesse, M., and Mango, S.E. (1998).  
1312 *pha-4*, an HNF-3 homolog, specifies pharyngeal organ identity in *Caenorhabditis elegans*.  
1313 *Genes Dev* 12, 1947-1952.

1314 Horvitz, H.R., Chalfie, M., Trent, C., Sulston, J.E., and Evans, P.D. (1982). Serotonin and  
1315 octopamine in the nematode *Caenorhabditis elegans*. *Science* 216, 1012-1014.

1316 Hsu, H.T., Chen, H.M., Yang, Z., Wang, J., Lee, N.K., Burger, A., Zaret, K., Liu, T., Levine,  
1317 E., and Mango, S.E. (2015). TRANSCRIPTION. Recruitment of RNA polymerase II by the  
1318 pioneer transcription factor PHA-4. *Science* 348, 1372-1376.

1319 Hunt-Newbury, R., Viveiros, R., Johnsen, R., Mah, A., Anastas, D., Fang, L., Halfnight, E.,  
1320 Lee, D., Lin, J., Lorch, A., *et al.* (2007). High-throughput in vivo analysis of gene expression  
1321 in *Caenorhabditis elegans*. *PLoS Biol* 5, e237.

1322 Ishita, Y., Chihara, T., and Okumura, M. (2020). Serotonergic modulation of feeding behavior  
1323 in *Caenorhabditis elegans* and other related nematodes. *Neurosci Res* 154, 9-19.

1324 Jacobs, D.K., Nakanishi, N., Yuan, D., Camara, A., Nichols, S.A., and Hartenstein, V. (2007).  
1325 Evolution of sensory structures in basal metazoa. *Integr Comp Biol* 47, 712-723.

1326 Kalb, J.M., Lau, K.K., Goszczynski, B., Fukushige, T., Moons, D., Okkema, P.G., and  
1327 McGhee, J.D. (1998). *pha-4* is Ce-fkh-1, a fork head/HNF-3alpha,beta,gamma homolog that  
1328 functions in organogenesis of the *C. elegans* pharynx. *Development* 125, 2171-2180.

1329 Katidou, M., Tavernarakis, N., and Karagogeos, D. (2013). The contactin RIG-6 mediates  
1330 neuronal and non-neuronal cell migration in *Caenorhabditis elegans*. *Dev Biol* 373, 184-195.

1331 Kato, Y., Aizawa, T., Hoshino, H., Kawano, K., Nitta, K., and Zhang, H. (2002). *abf-1* and *abf-*  
1332 *2*, ASABF-type antimicrobial peptide genes in *Caenorhabditis elegans*. *Biochem J* 361, 221-  
1333 230.

1334 Kim, B., and Emmons, S.W. (2017). Multiple conserved cell adhesion protein interactions  
1335 mediate neural wiring of a sensory circuit in *C. elegans*. *eLife* 6.

1336 Klimovich, A., Giacomello, S., Bjorklund, A., Faure, L., Kaucka, M., Giez, C., Murillo-Rincon,  
1337 A.P., Matt, A.S., Willoweit-Ohl, D., Crupi, G., *et al.* (2020). Prototypical pacemaker neurons  
1338 interact with the resident microbiota. *Proc Natl Acad Sci U S A* 117, 17854-17863.

1339 Klimovich, A.V., and Bosch, T.C.G. (2018). Rethinking the Role of the Nervous System:  
1340 Lessons From the Hydra Holobiont. *Bioessays* 40, e1800060.

1341 Koizumi, O. (2007). Nerve ring of the hypostome in hydra: is it an origin of the central nervous  
1342 system of bilaterian animals? *Brain Behav Evol* 69, 151-159.

1343 Kumar, J.P. (2009). The sine oculis homeobox (SIX) family of transcription factors as  
1344 regulators of development and disease. *Cell Mol Life Sci* 66, 565-583.

1345 Laranjeira, C., and Pachnis, V. (2009). Enteric nervous system development: Recent  
1346 progress and future challenges. *Auton Neurosci* 151, 61-69.

1347 Llewellyn-Smith, I.J. (1989). Neuropeptides and the microcircuitry of the enteric nervous  
1348 system. In *Regulatory Peptides*, J.M. Polak, ed. (Basel: Birkhäuser Basel), pp. 247-265.

1349 Ma, X., Zhao, Z., Xiao, L., Xu, W., Kou, Y., Zhang, Y., Wu, G., Wang, Y., and Du, Z. (2021). A  
1350 4D single-cell protein atlas of transcription factors delineates spatiotemporal patterning during  
1351 embryogenesis. *Nat Methods* 18, 893-902.

1352 Mackie, G.O. (1970). Neuroid conduction and the evolution of conducting tissues. *Q Rev Biol*  
1353 45, 319-332.

1354 Mango, S.E. (2007). The *C. elegans* pharynx : a model for organogenesis. *Wormbook*.

1355 Mango, S.E., Lambie, E.J., and Kimble, J. (1994). The *pha-4* gene is required to generate the  
1356 pharyngeal primordium of *Caenorhabditis elegans*. *Development* 120, 3019-3031.

1357 Memic, F., Knoflach, V., Morarach, K., Sadler, R., Laranjeira, C., Hjerling-Leffler, J.,  
1358 Sundstrom, E., Pachnis, V., and Marklund, U. (2018). Transcription and Signaling Regulators  
1359 in Developing Neuronal Subtypes of Mouse and Human Enteric Nervous System.  
1360 *Gastroenterology* 154, 624-636.

1361 Morarach, K., Mikhailova, A., Knoflach, V., Memic, F., Kumar, R., Li, W., Ernfors, P., and  
1362 Marklund, U. (2021). Diversification of molecularly defined myenteric neuron classes revealed  
1363 by single-cell RNA sequencing. *Nat Neurosci* 24, 34-46.

1364 Morck, C., Rauthan, M., Wagberg, F., and Pilon, M. (2004). *pha-2* encodes the *C. elegans*  
1365 ortholog of the homeodomain protein HEX and is required for the formation of the pharyngeal  
1366 isthmus. *Dev Biol* 272, 403-418.

1367 Muniz, L.R., Knosp, C., and Yeretssian, G. (2012). Intestinal antimicrobial peptides during  
1368 homeostasis, infection, and disease. *Front Immunol* 3, 310.

1369 Myers, L., Perera, H., Alvarado, M.G., and Kidd, T. (2018). The *Drosophila* Ret gene  
1370 functions in the stomatogastric nervous system with the Maverick TGFbeta ligand and the  
1371 Gfrl co-receptor. *Development* 145.

1372 Nagy, N., and Goldstein, A.M. (2017). Enteric nervous system development: A crest cell's  
1373 journey from neural tube to colon. *Semin Cell Dev Biol* 66, 94-106.

1374 Narasimhan, K., Lambert, S.A., Yang, A.W., Riddell, J., Mnaimneh, S., Zheng, H., Albu, M.,  
1375 Najafabadi, H.S., Reece-Hoyes, J.S., Fuxman Bass, J.I., *et al.* (2015). Mapping and analysis  
1376 of *Caenorhabditis elegans* transcription factor sequence specificities. *eLife* 4.

1377 Ohto, H., Kamada, S., Tago, K., Tominaga, S.I., Ozaki, H., Sato, S., and Kawakami, K.  
1378 (1999). Cooperation of six and eya in activation of their target genes through nuclear  
1379 translocation of Eya. *Mol Cell Biol* 19, 6815-6824.

1380 Ohto, H., Takizawa, T., Saito, T., Kobayashi, M., Ikeda, K., and Kawakami, K. (1998). Tissue  
1381 and developmental distribution of Six family gene products. *Int J Dev Biol* 42, 141-148.

1382 Oishi, A., Gengyo-Ando, K., Mitani, S., Mohri-Shiomi, A., Kimura, K.D., Ishihara, T., and  
1383 Katsura, I. (2009). FLR-2, the glycoprotein hormone alpha subunit, is involved in the neural  
1384 control of intestinal functions in *Caenorhabditis elegans*. *Genes Cells* 14, 1141-1154.

1385 Patel, T., and Hobert, O. (2017). Coordinated control of terminal differentiation and restriction  
1386 of cellular plasticity. *eLife* 6.

1387 Patrick, A.N., Cabrera, J.H., Smith, A.L., Chen, X.S., Ford, H.L., and Zhao, R. (2013).  
1388 Structure-function analyses of the human SIX1-EYA2 complex reveal insights into metastasis  
1389 and BOR syndrome. *Nat Struct Mol Biol* 20, 447-453.

1390 Pattyn, A., Morin, X., Cremer, H., Goridis, C., and Brunet, J.F. (1999). The homeobox gene  
1391 Phox2b is essential for the development of autonomic neural crest derivatives. *Nature* 399,  
1392 366-370.

1393 Pereira, L., Kratsios, P., Serrano-Saiz, E., Sheftel, H., Mayo, A.E., Hall, D.H., White, J.G.,  
1394 LeBoeuf, B., Garcia, L.R., Alon, U., *et al.* (2015). A cellular and regulatory map of the  
1395 cholinergic nervous system of *C. elegans*. *eLife* 4.

1396 Pilon, M. (2008). Fishing lines, time-delayed guideposts, and other tricks used by developing  
1397 pharyngeal neurons in *Caenorhabditis elegans*. *Dev Dyn* 237, 2073-2080.

1398 Portereiko, M.F., and Mango, S.E. (2001). Early morphogenesis of the *Caenorhabditis*  
1399 *elegans* pharynx. *Dev Biol* 233, 482-494.

1400 Ramakrishnan, K., and Okkema, P.G. (2014). Regulation of *C. elegans* neuronal  
1401 differentiation by the ZEB-family factor ZAG-1 and the NK-2 homeodomain factor CEH-28.  
1402 *PLoS One* 9, e113893.

1403 Rao, M., and Gershon, M.D. (2018). Enteric nervous system development: what could  
1404 possibly go wrong? *Nat Rev Neurosci* 19, 552-565.

1405 Rauthan, M., Morck, C., and Pilon, M. (2007). The *C. elegans* M3 neuron guides the growth  
1406 cone of its sister cell M2 via the Kruppel-like zinc finger protein MNM-2. *Dev Biol* 311, 185-  
1407 199.

1408 Ray, P., Schnabel, R., and Okkema, P.G. (2008). Behavioral and synaptic defects in *C.*  
1409 *elegans* lacking the NK-2 homeobox gene *ceh-28*. *Dev Neurobiol* 68, 421-433.



1410 Reilly, M.B., Cros, C., Varol, E., Yemini, E., and Hobert, O. (2020). Unique homeobox codes  
1411 delineate all the neuron classes of *C. elegans*. *Nature* 584, 595-601.

1412 Ruiz-Reig, N., Rakotobe, M., Bethus, I., Le Menn, G., Huditz, H.I., Marie, H., Lamonerie, T.,  
1413 and D'Autreaux, F. (2019). Developmental Requirement of Homeoprotein Otx2 for Specific  
1414 Habenulo-Interpeduncular Subcircuits. *J Neurosci* 39, 1005-1019.

1415 Ruvkun, G., and Hobert, O. (1998). The Taxonomy of Developmental Control in  
1416 *Caenorhabditis elegans*. *Science* 282, 2033-2041.

1417 Sasselli, V., Pachnis, V., and Burns, A.J. (2012). The enteric nervous system. *Dev Biol* 366,  
1418 64-73.

1419 Schindelin, J., Arganda-Carreras, I., Frise, E., Kaynig, V., Longair, M., Pietzsch, T., Preibisch,  
1420 S., Rueden, C., Saalfeld, S., Schmid, B., *et al.* (2012). Fiji: an open-source platform for  
1421 biological-image analysis. *Nat Methods* 9, 676-682.

1422 Schwarz, V., Pan, J., Voltmer-Irsch, S., and Hutter, H. (2009). IgCAMs redundantly control  
1423 axon navigation in *Caenorhabditis elegans*. *Neural Dev* 4, 13.

1424 Seo, H.C., Curtiss, J., Mlodzik, M., and Fjose, A. (1999). Six class homeobox genes in  
1425 *drosophila* belong to three distinct families and are involved in head development. *Mech Dev*  
1426 83, 127-139.

1427 Serrano-Saiz, E., Leyva-Diaz, E., De La Cruz, E., and Hobert, O. (2018). BRN3-type POU  
1428 Homeobox Genes Maintain the Identity of Mature Postmitotic Neurons in Nematodes and  
1429 Mice. *Curr Biol* 28, 2813-2823 e2812.

1430 Serrano-Saiz, E., Poole, Richard J., Felton, T., Zhang, F., De La Cruz, Estanislao D., and  
1431 Hobert, O. (2013). Modular Control of Glutamatergic Neuronal Identity in *C. elegans* by  
1432 Distinct Homeodomain Proteins. *Cell* 155, 659-673.

1433 Smit, R.B., Schnabel, R., and Gaudet, J. (2008). The HLH-6 transcription factor regulates *C.*  
1434 *elegans* pharyngeal gland development and function. *PLoS Genet* 4, e1000222.

1435 Sokolowski, K., Esumi, S., Hirata, T., Kamal, Y., Tran, T., Lam, A., Oboti, L., Brighthaupt,  
1436 S.C., Zaghlula, M., Martinez, J., *et al.* (2015). Specification of select hypothalamic circuits and  
1437 innate behaviors by the embryonic patterning gene *dbx1*. *Neuron* 86, 403-416.

1438 Song, B.m., and Avery, L. (2012). Serotonin Activates Overall Feeding by Activating Two  
1439 Separate Neural Pathways in *Caenorhabditis elegans*. *Journal of Neuroscience* 32, 1920-  
1440 1931.

1441 Song, B.M., and Avery, L. (2013). The pharynx of the nematode *C. elegans*: A model system  
1442 for the study of motor control. *Worm* 2, e21833.

1443 Sulston, J.E., Schierenberg, E., White, J.G., and Thomson, J.N. (1983). The embryonic cell  
1444 lineage of the nematode *Caenorhabditis elegans*. *Dev Biol* 100, 64-119.

1445 Tadjuidje, E., and Hegde, R.S. (2013). The Eyes Absent proteins in development and  
1446 disease. *Cell Mol Life Sci* 70, 1897-1913.

1447 Taylor, S.R., Santpere, G., Weinreb, A., Barrett, A., Reilly, M.B., Xu, C., Varol, E.,  
1448 Oikonomou, P., Glenwinkel, L., McWhirter, R., *et al.* (2021). Molecular topography of an  
1449 entire nervous system. *Cell*.

1450 Tiveron, M.C., Hirsch, M.R., and Brunet, J.F. (1996). The expression pattern of the  
1451 transcription factor Phox2 delineates synaptic pathways of the autonomic nervous system. *J*  
1452 *Neurosci* *16*, 7649-7660.

1453 Trojanowski, N.F., Padovan-Merhar, O., Raizen, D.M., and Fang-Yen, C. (2014). Neural and  
1454 genetic degeneracy underlies *Caenorhabditis elegans* feeding behavior. *Journal of*  
1455 *neurophysiology* *112*, 951-961.

1456 Van Sinay, E., Mirabeau, O., Depuydt, G., Van Hiel, M.B., Peymen, K., Watteyne, J., Zels, S.,  
1457 Schoofs, L., and Beets, I. (2017). Evolutionarily conserved TRH neuropeptide pathway  
1458 regulates growth in *Caenorhabditis elegans*. *Proc Natl Acad Sci U S A* *114*, E4065-E4074.

1459 Varoqueaux, F., and Fashauer, D. (2017). Getting Nervous: An Evolutionary Overhaul for  
1460 Communication. *Annu Rev Genet* *51*, 455-476.

1461 Vidal, B., Aghayeva, U., Sun, H., Wang, C., Glenwinkel, L., Bayer, E.A., and Hobert, O.  
1462 (2018). An atlas of *Caenorhabditis elegans* chemoreceptor expression. *PLoS Biol* *16*,  
1463 e2004218.

1464 Vilimas, T., Abraham, A., and Okkema, P.G. (2004). An early pharyngeal muscle enhancer  
1465 from the *Caenorhabditis elegans* *ceh-22* gene is targeted by the Forkhead factor PHA-4. *Dev*  
1466 *Biol* *266*, 388-398.

1467 Watanabe, H., Fujisawa, T., and Holstein, T.W. (2009). Cnidarians and the evolutionary origin  
1468 of the nervous system. *Dev Growth Differ* *51*, 167-183.

1469 Wei, Z., Angerer, R.C., and Angerer, L.M. (2011). Direct development of neurons within  
1470 foregut endoderm of sea urchin embryos. *Proc Natl Acad Sci U S A* *108*, 9143-9147.

1471 White, J.G., Southgate, E., Thomson, J.N., and Brenner, S. (1986). The structure of the  
1472 nervous system of the nematode *Caenorhabditis elegans*. *Philosophical Transactions of the*  
1473 *Royal Society of London B Biological Sciences* *314*, 1-340.

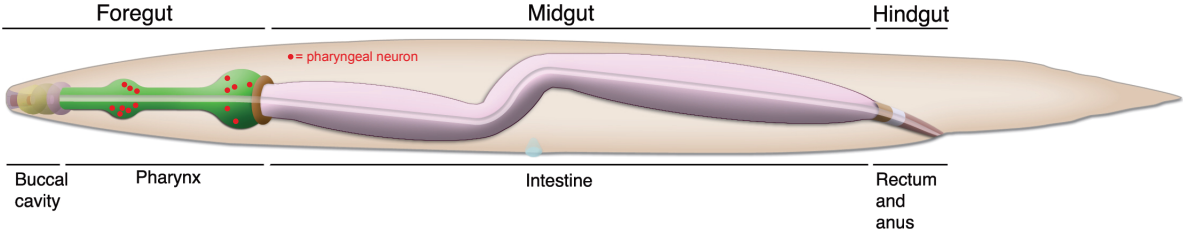
1474 Xuan, Z., Manning, L., Nelson, J., Richmond, J.E., Colon-Ramos, D.A., Shen, K., and  
1475 Kurshan, P.T. (2017). Clarinet (CLA-1), a novel active zone protein required for synaptic  
1476 vesicle clustering and release. *eLife* *6*.

1477 Zhang, F., Bhattacharya, A., Nelson, J.C., Abe, N., Gordon, P., Lloret-Fernandez, C., Maicas,  
1478 M., Flames, N., Mann, R.S., Colon-Ramos, D.A., *et al.* (2014). The LIM and POU homeobox  
1479 genes *ttx-3* and *unc-86* act as terminal selectors in distinct cholinergic and serotonergic  
1480 neuron types. *Development* *141*, 422-435.

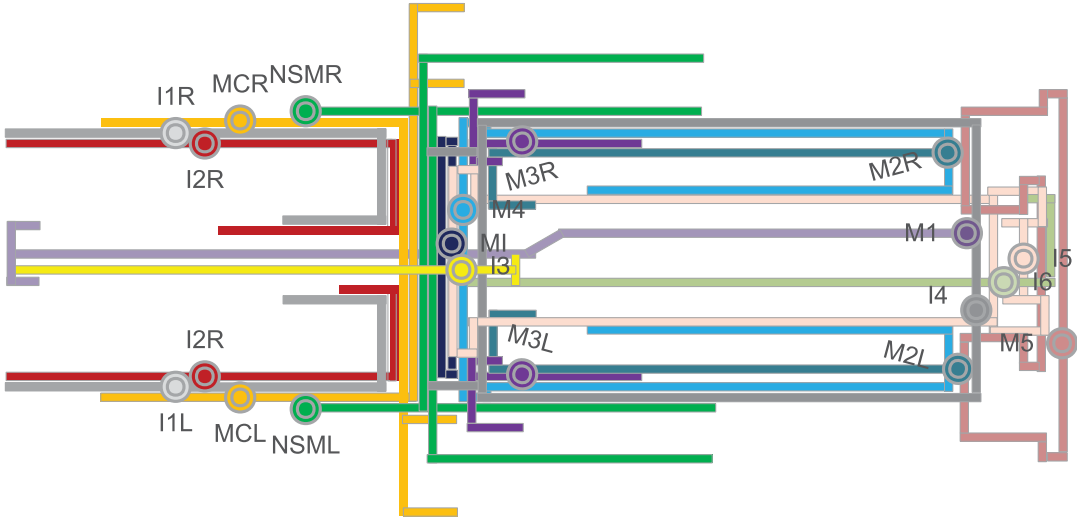
1481 Zhang, L., Ward, J.D., Cheng, Z., and Dernburg, A.F. (2015). The auxin-inducible  
1482 degradation (AID) system enables versatile conditional protein depletion in *C. elegans*.  
1483 *Development* *142*, 4374-4384.

1484

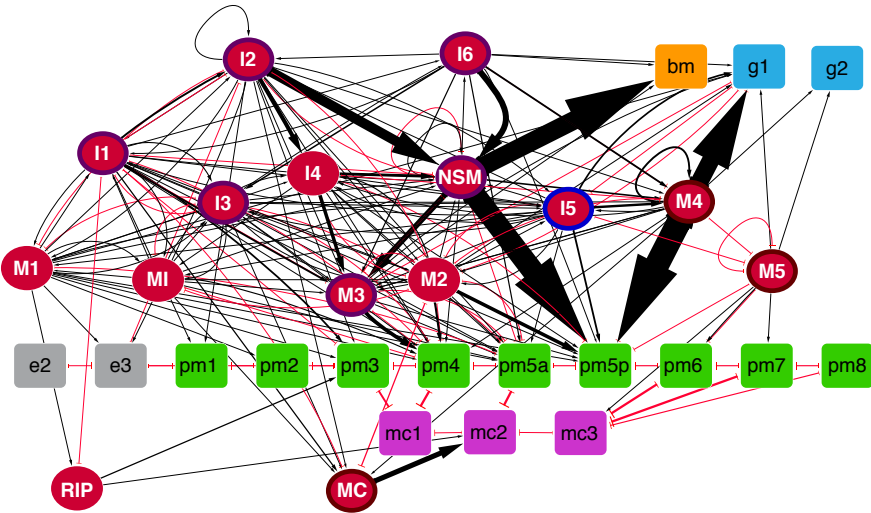
A



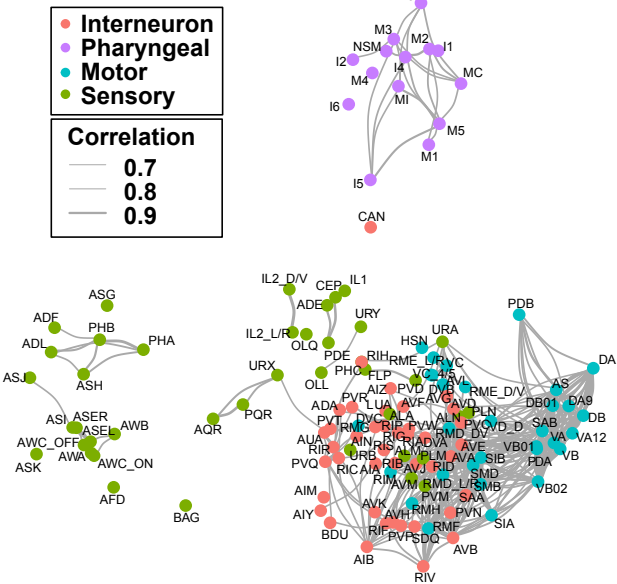
B



C



D



E

Pharyngeal neuron classes

	I1	I2	I3	I4	I5	I6	M1	M2	M3	M4	M5	MC	MI	NSM
Neuro-transmitter	<i>unc-17</i>	<i>eat-4</i>	<i>tph-1</i>	<i>cat-1</i>	<i>cat-4</i>	<i>bas-1</i>								
Neuropeptide	<i>flp-2</i>	<i>flp-4</i>	<i>flp-5</i>	<i>flp-15</i>	<i>flp-21</i>	<i>flp-28</i>	<i>nlp-3</i>	<i>nlp-8</i>	<i>nlp-13</i>	<i>trh-1</i>				
Receptor	<i>glr-2</i>	<i>mg1-1</i>	<i>ser-7</i>	<i>thr-1</i>	<i>glr-7</i>	<i>gur-3</i>	<i>str-97</i>	<i>spp-12</i>	<i>flr-2</i>					
Other	<i>kin-36</i>	<i>htr1-1</i>	<i>slt-1</i>	<i>rig-3</i>	<i>rig-6</i>									

Figure 1

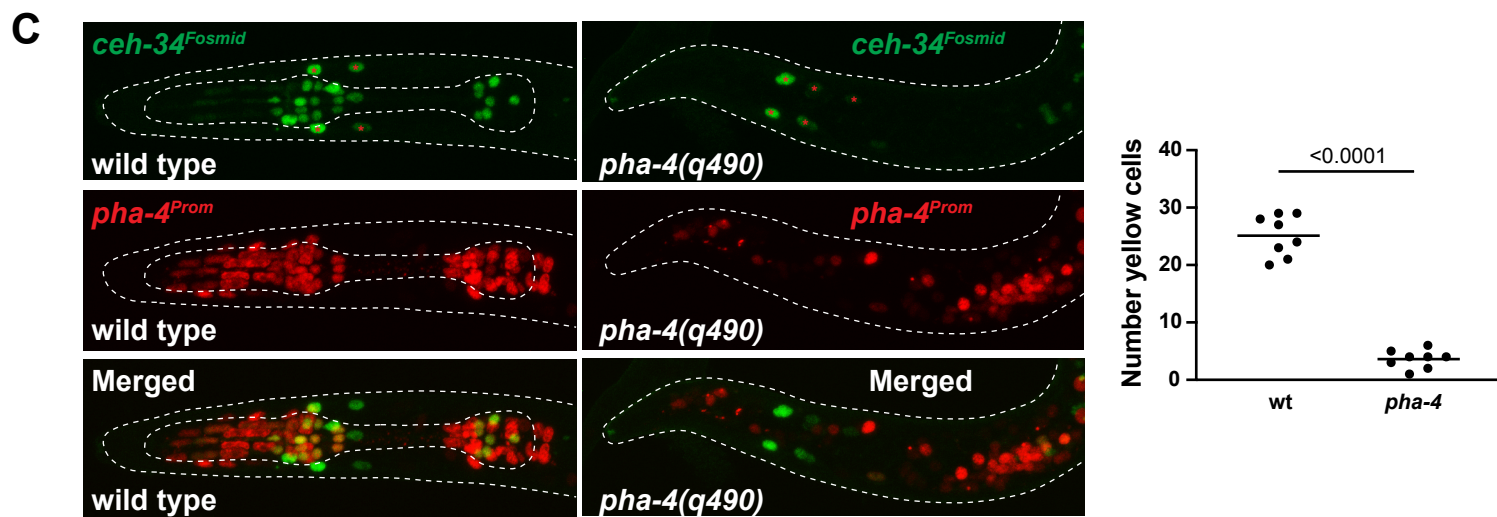
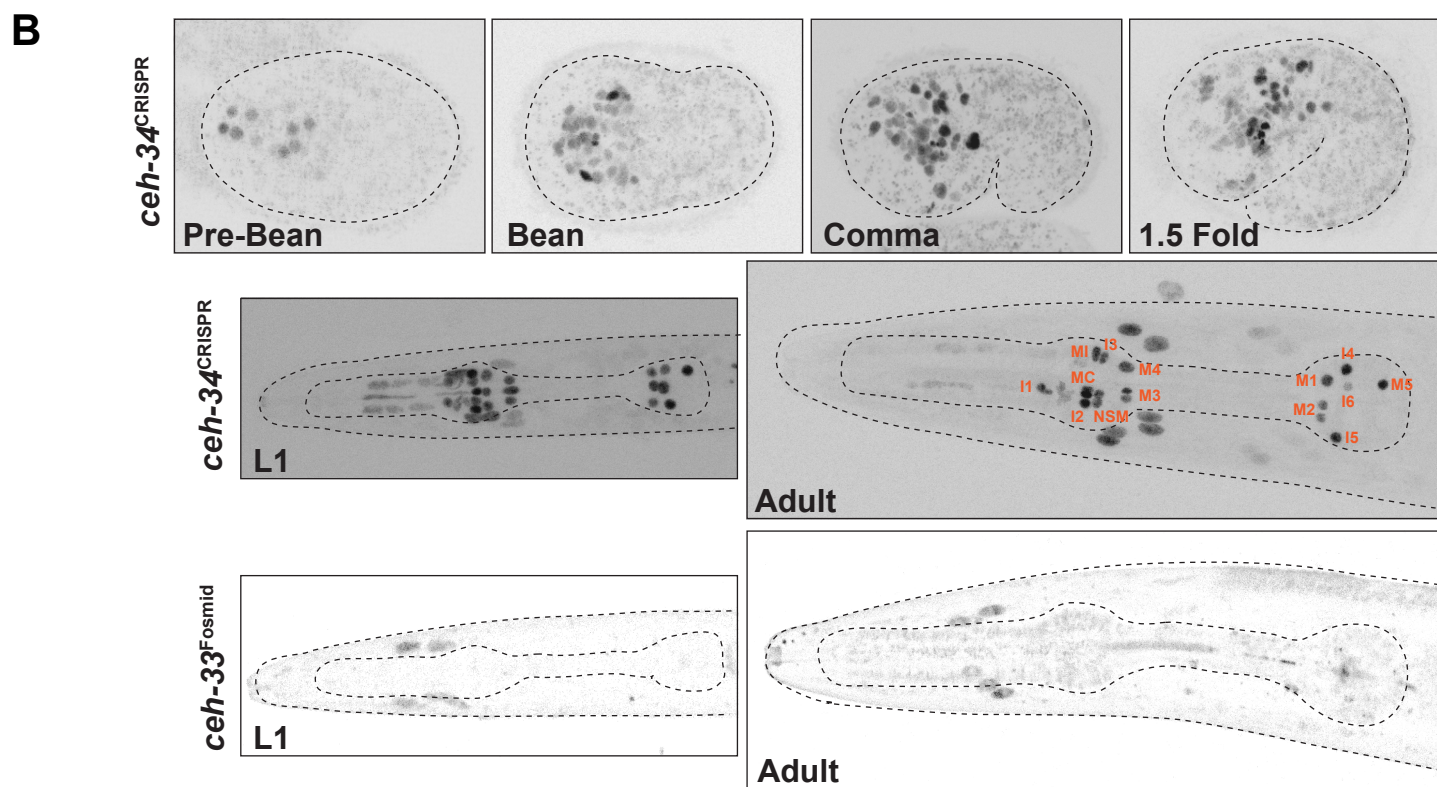
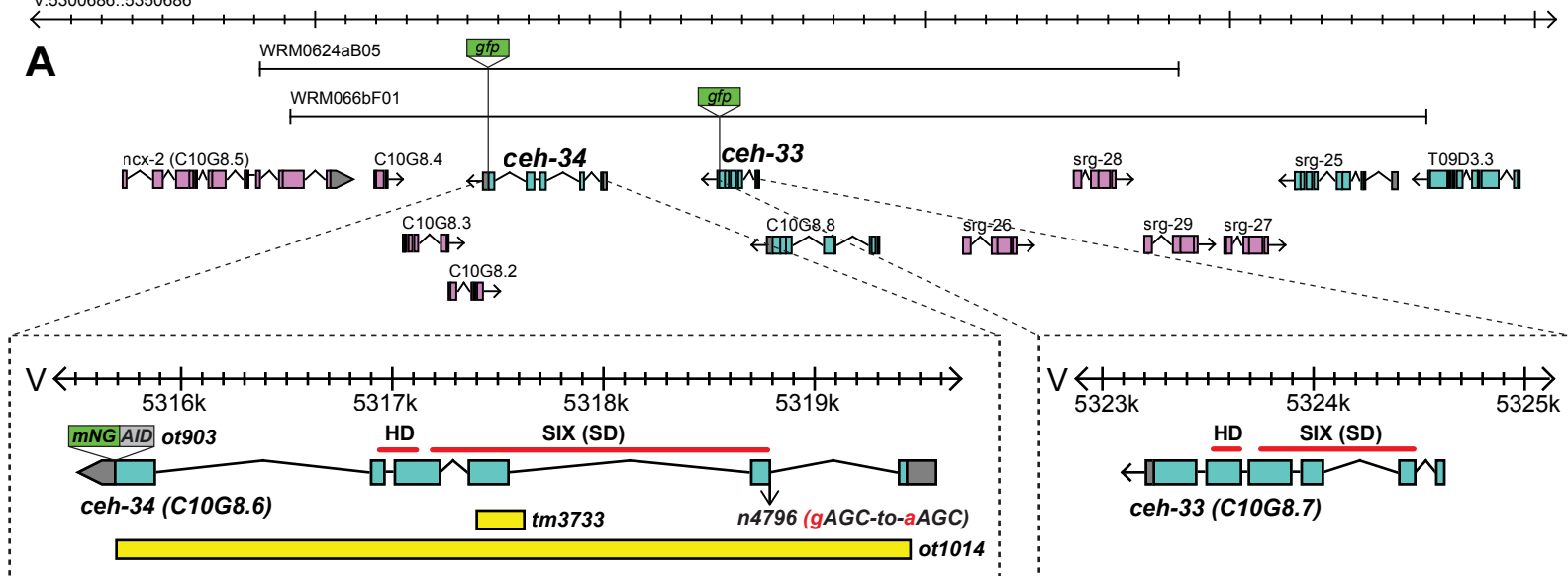


Figure 2

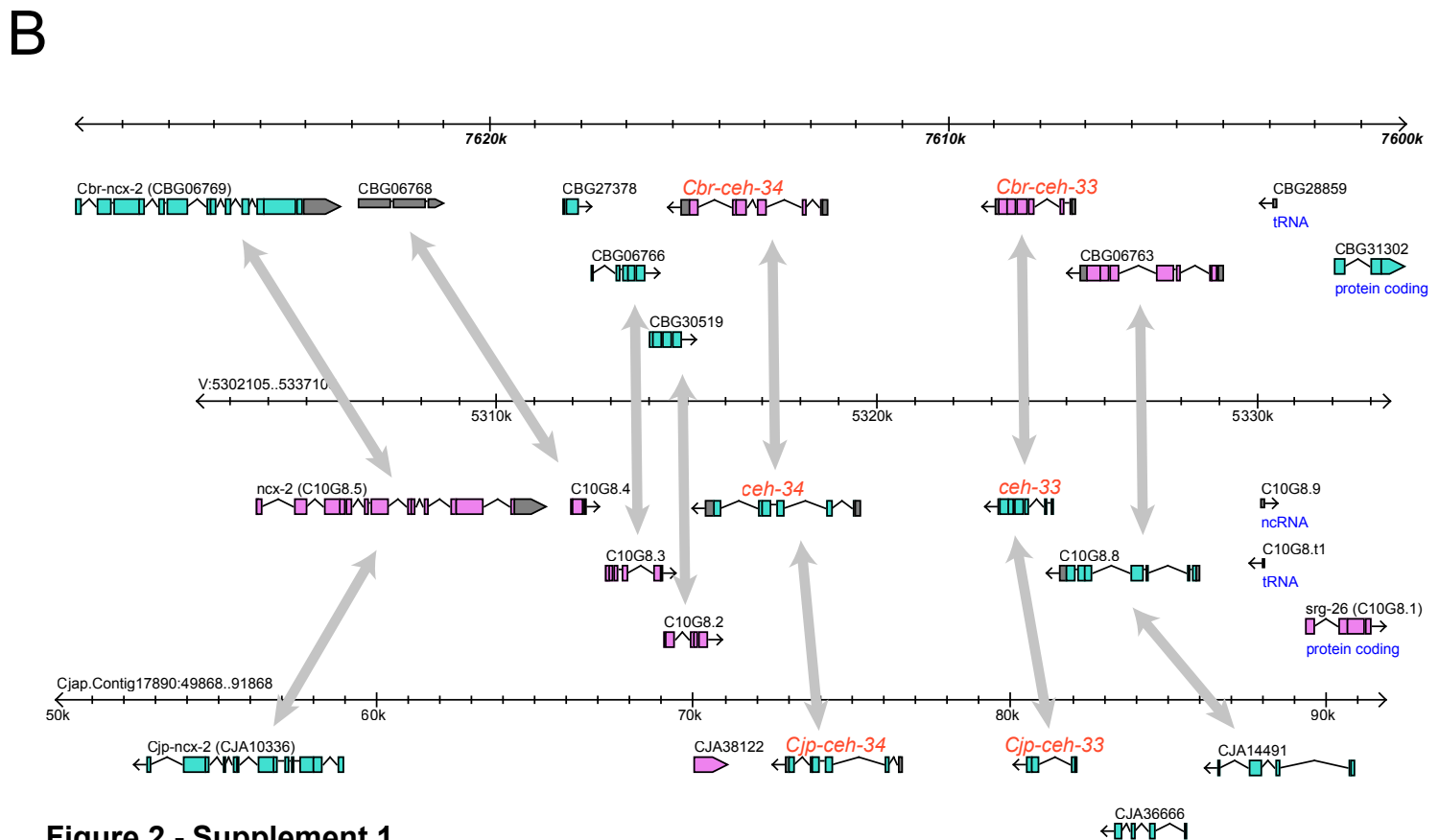
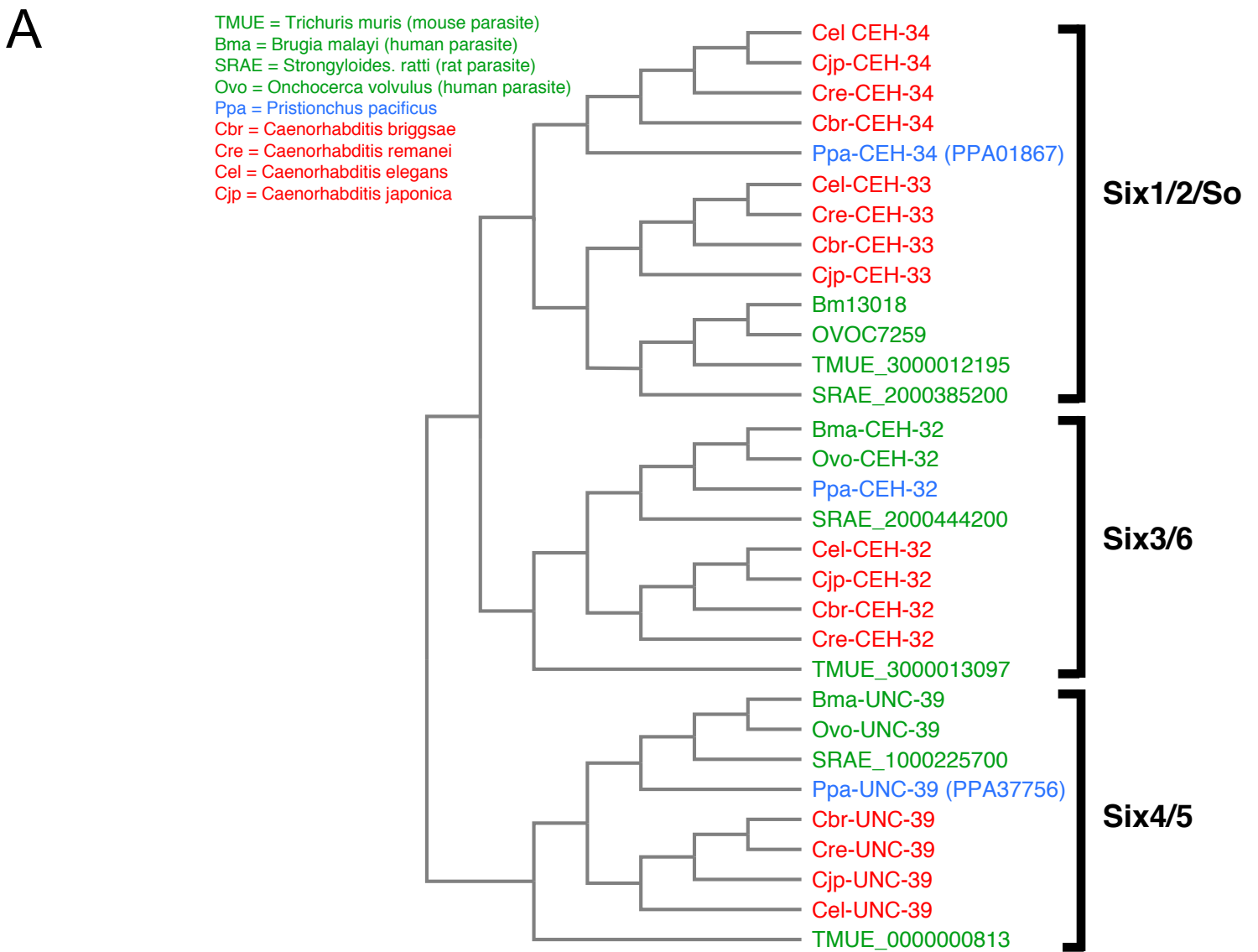
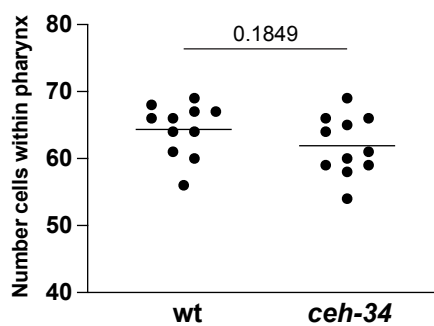
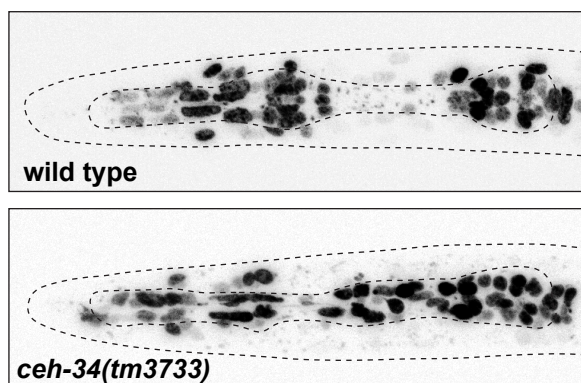


Figure 2 - Supplement 1



**A**

*pha-4<sup>Prom</sup>*



**B**

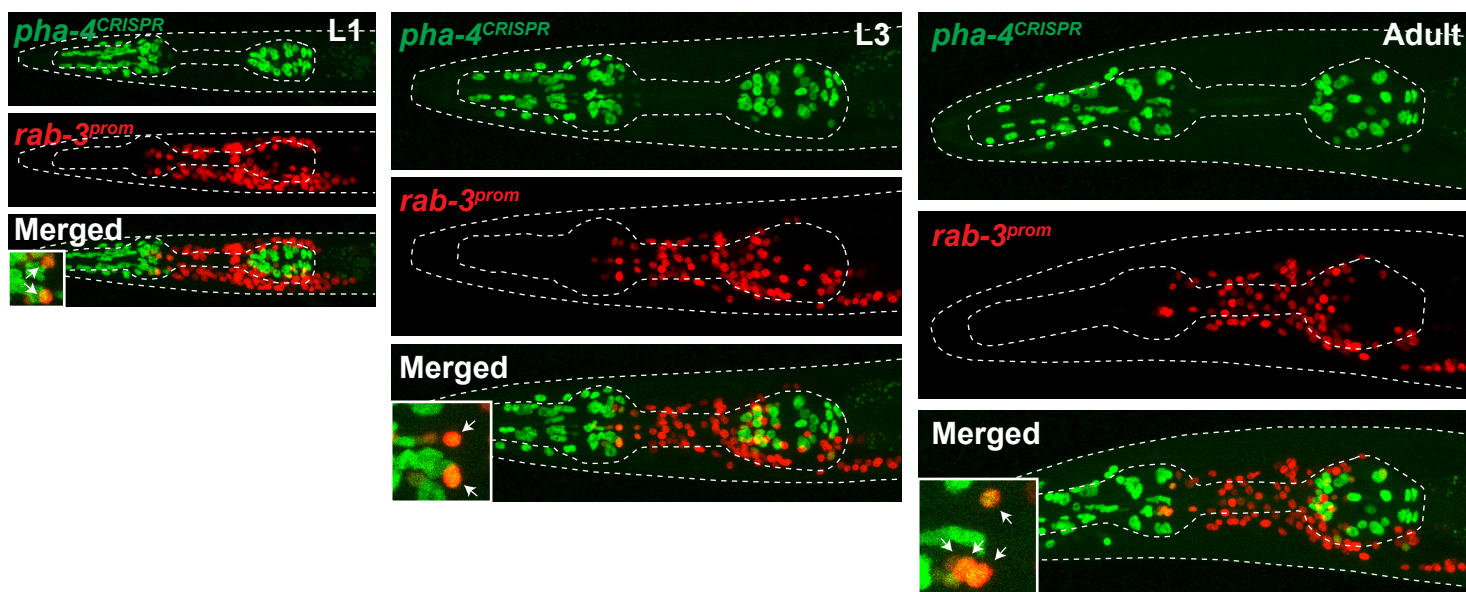
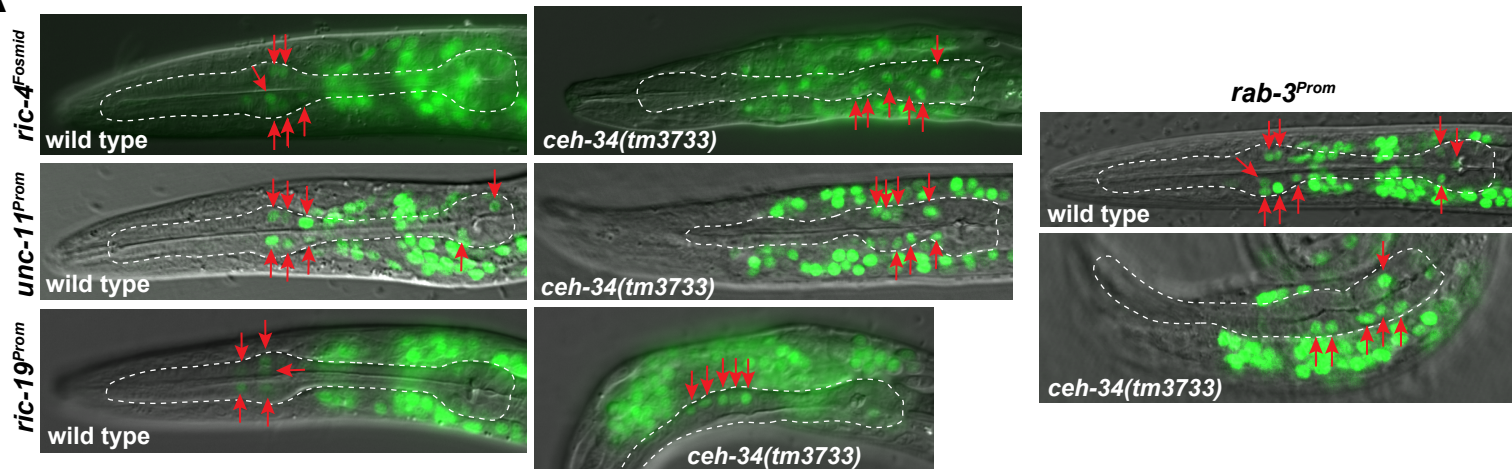
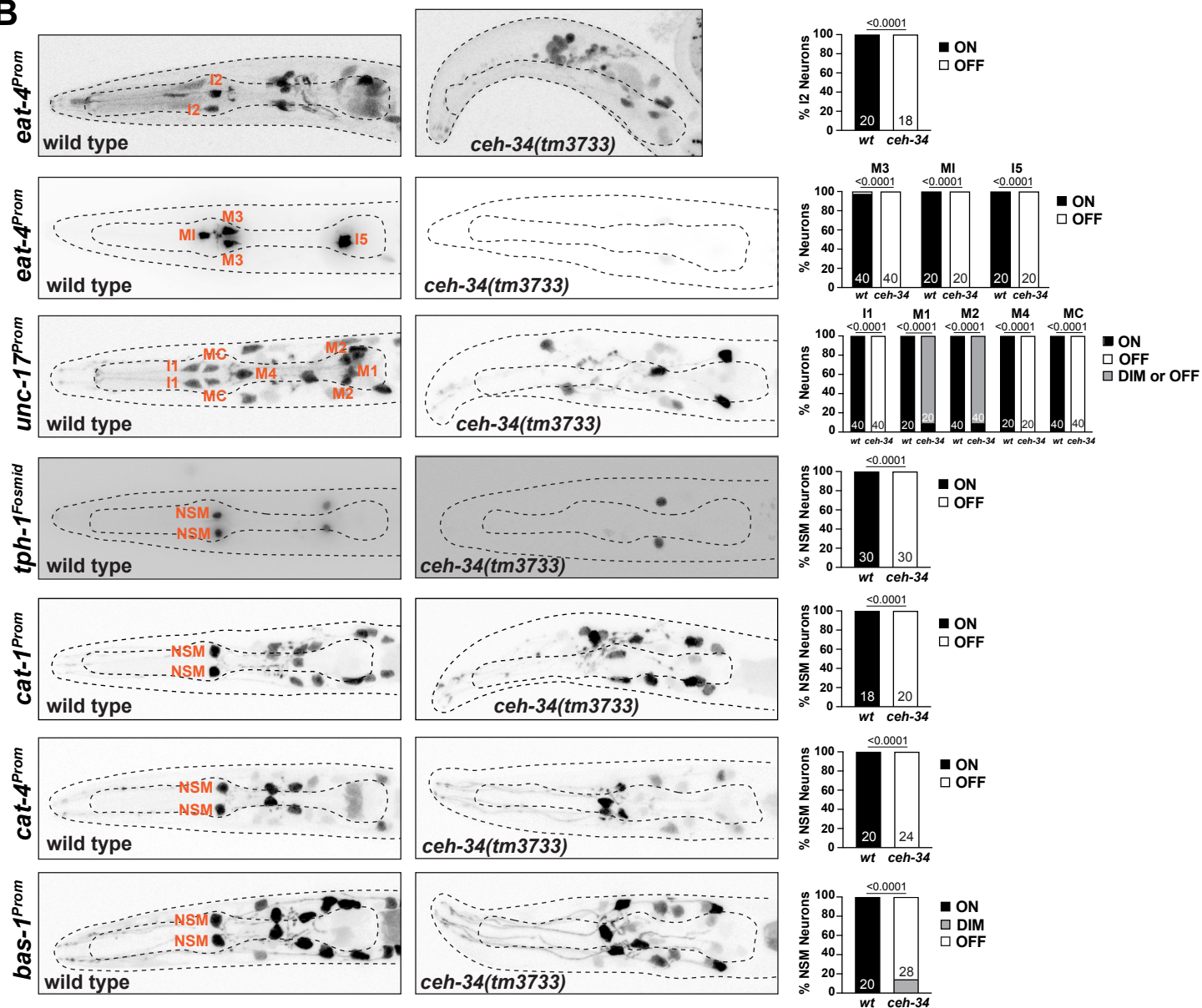
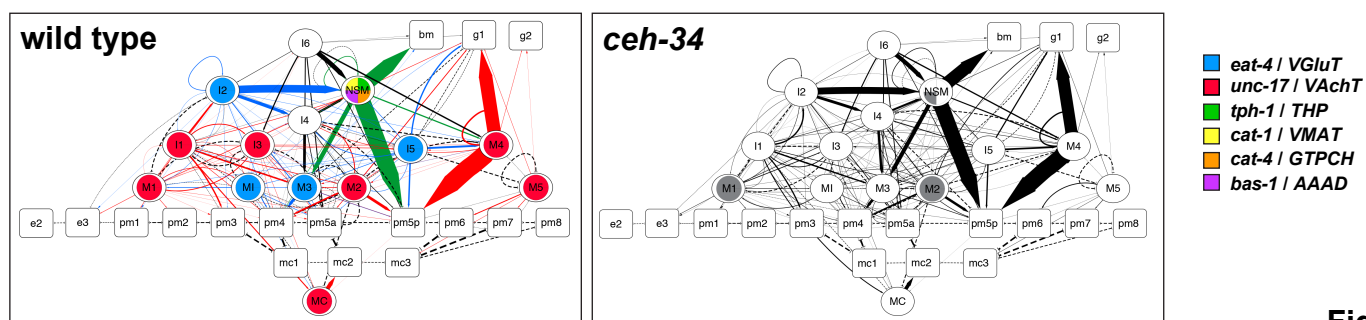


Figure 2 - Supplement 2

**A****B****C****Figure 3**

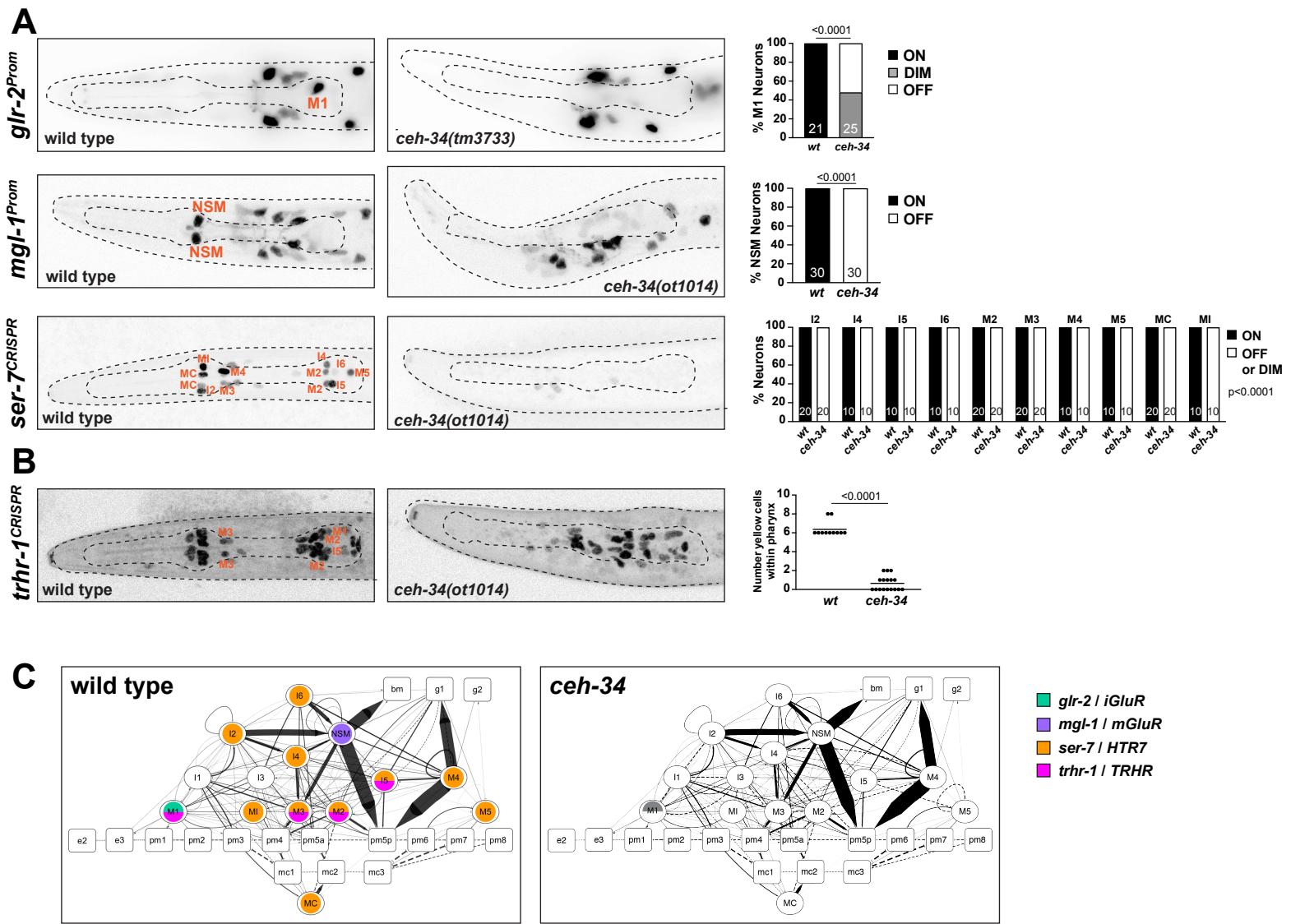
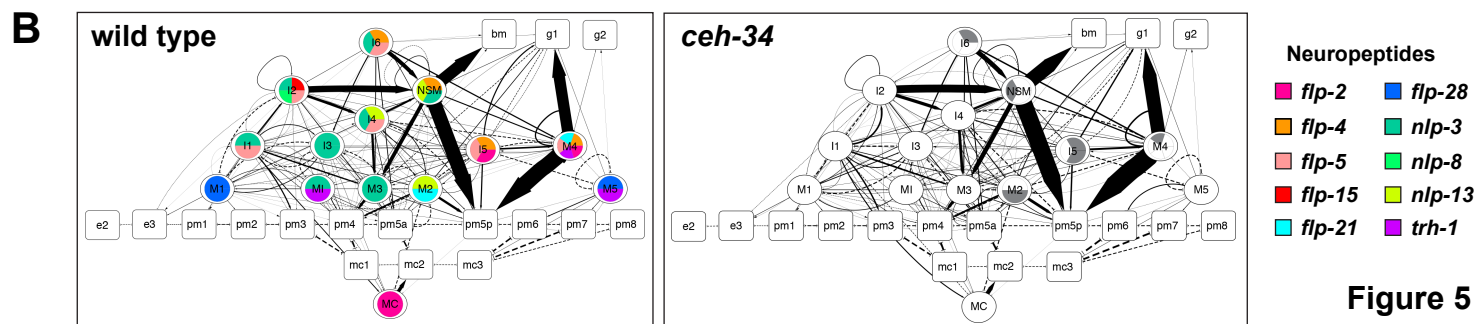
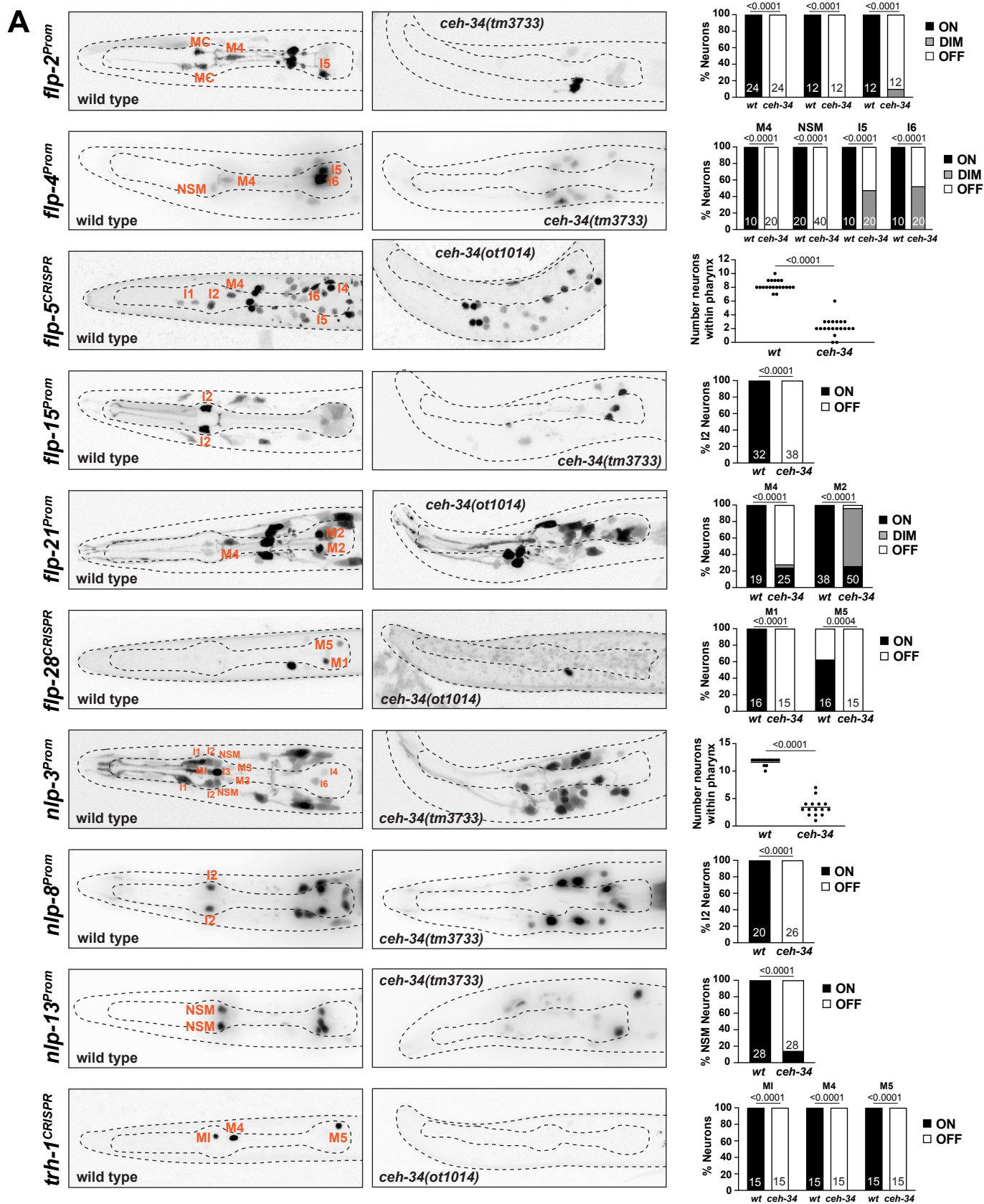
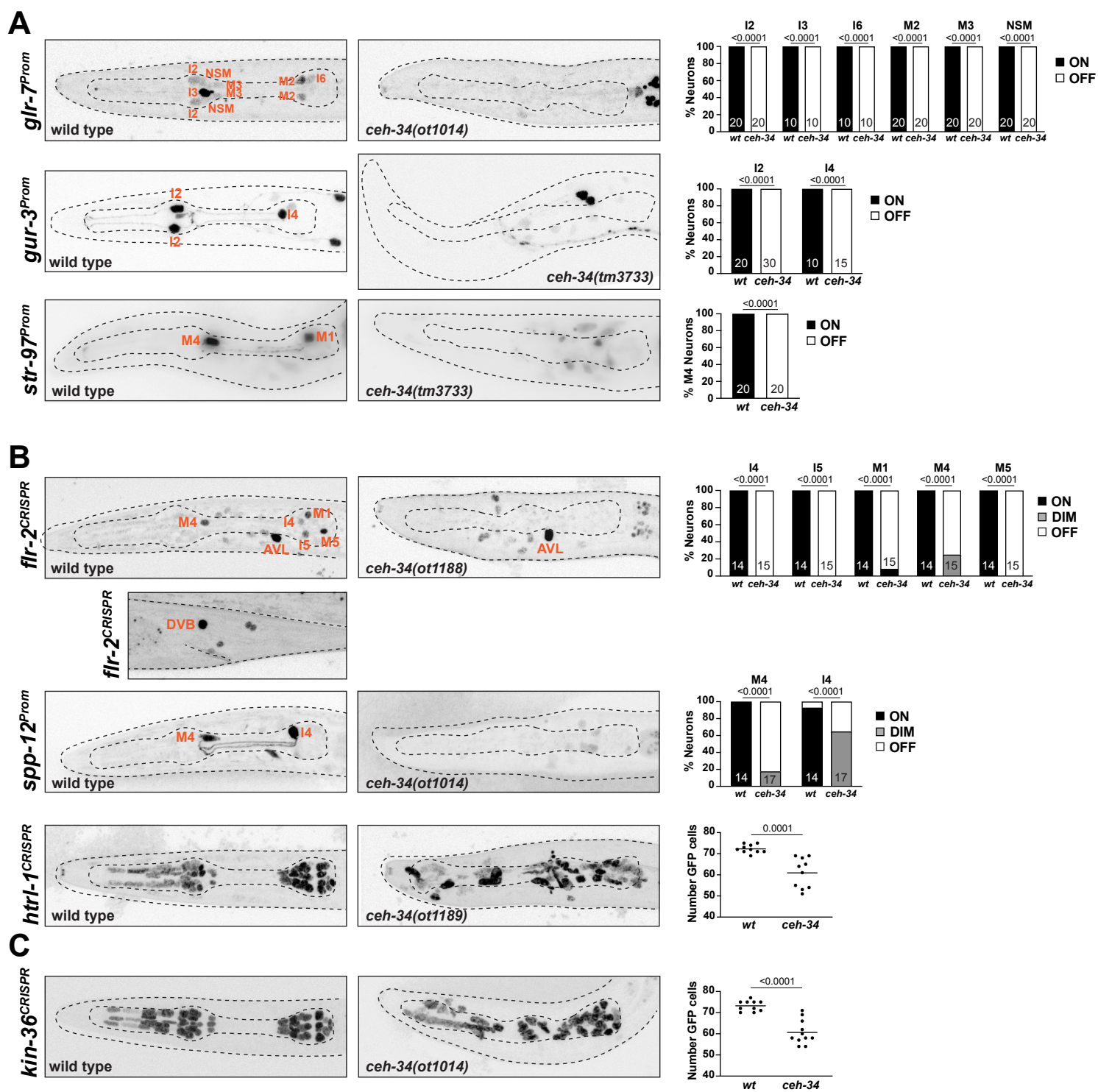


Figure 4







## Figure 6

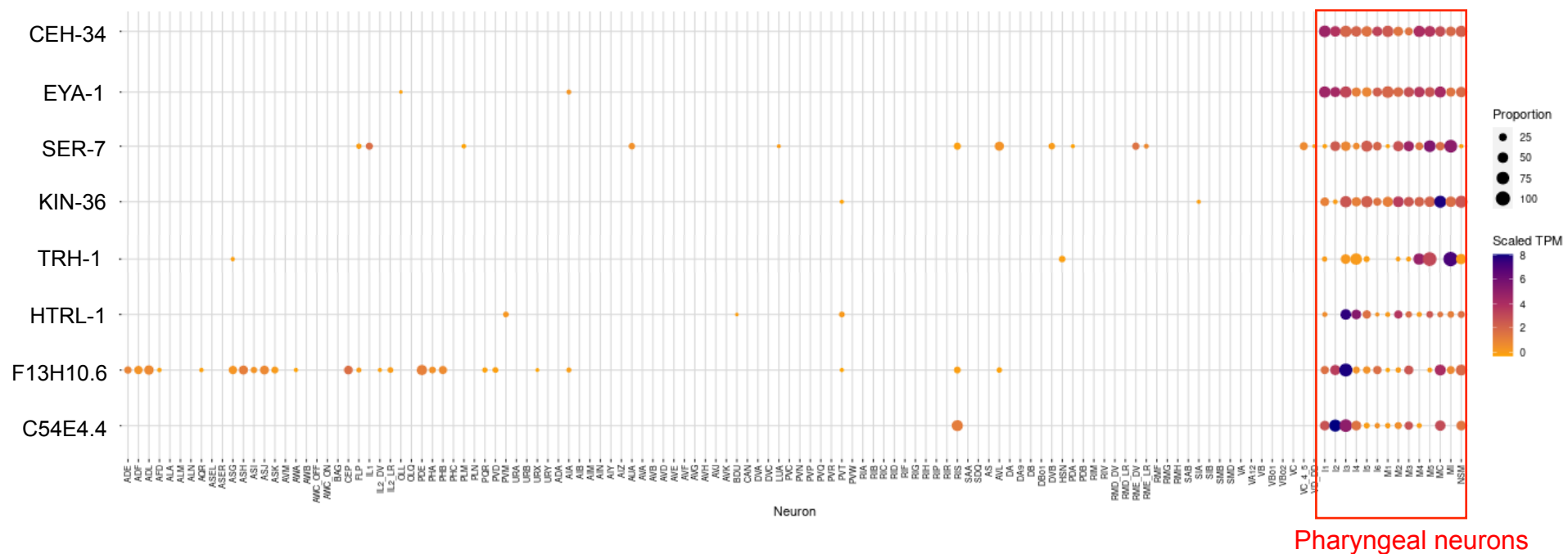
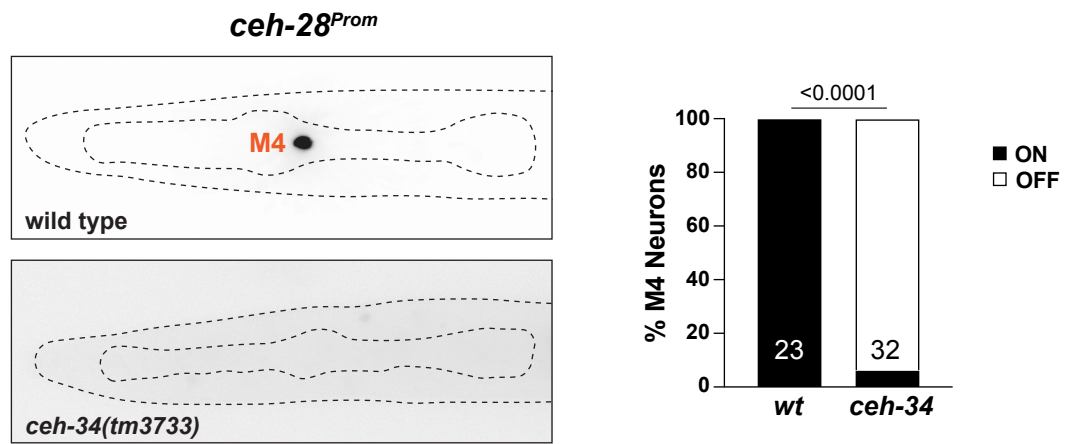


Fig.6 – Supplement 1



**Fig. 6 - Supplement 2**

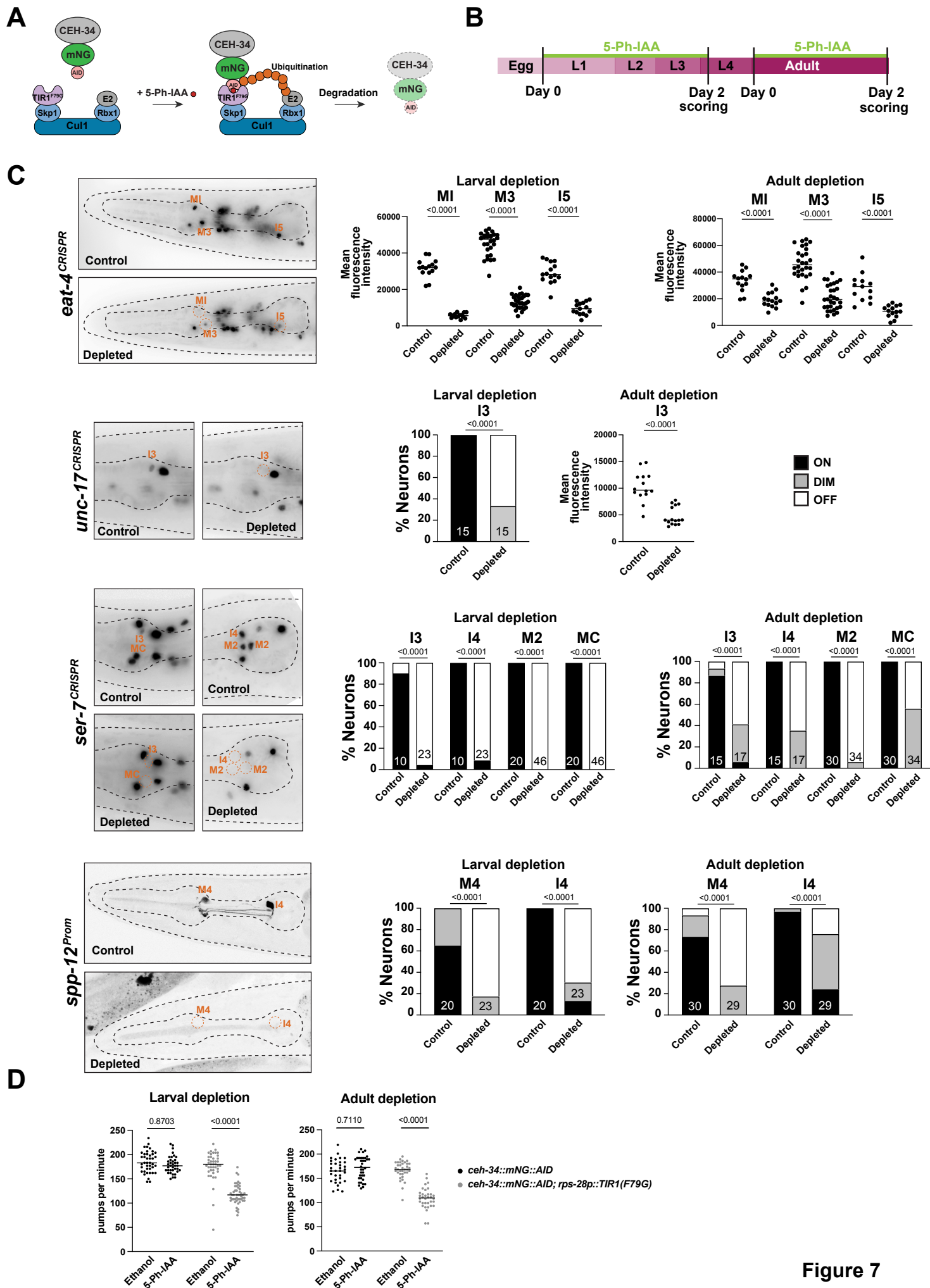


Figure 7



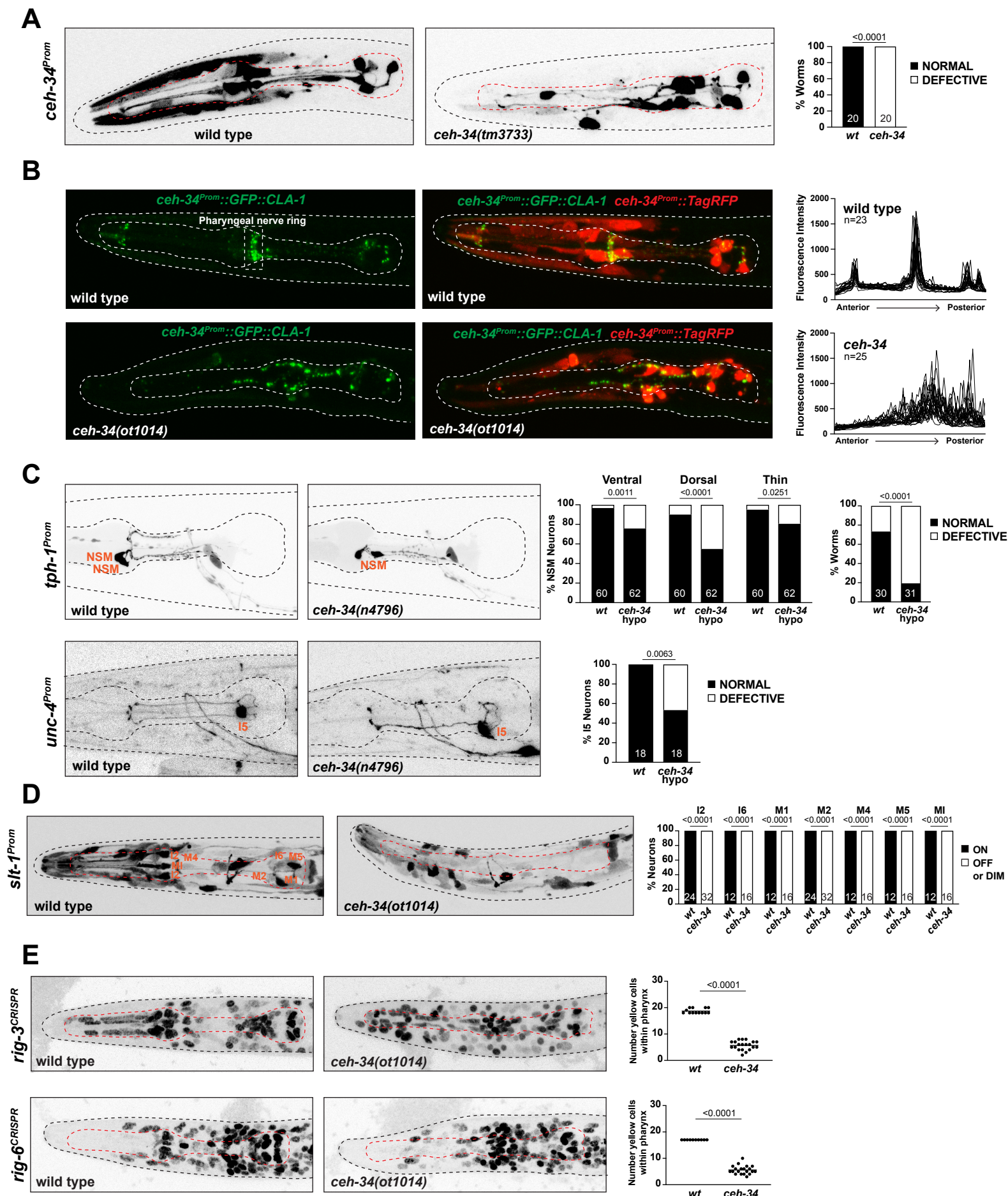
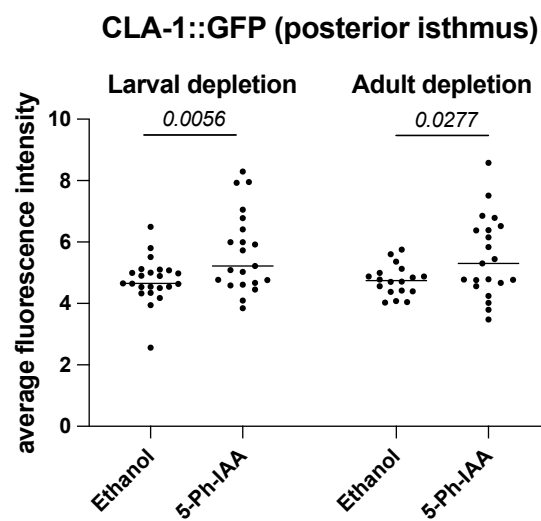
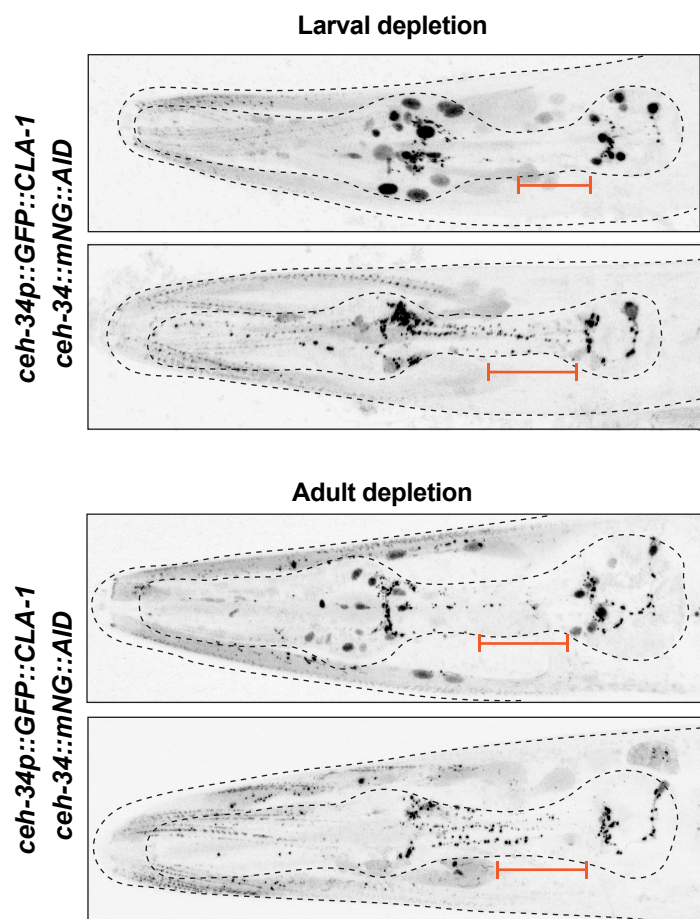


Figure 8



**Figure 8 Supplement 1**

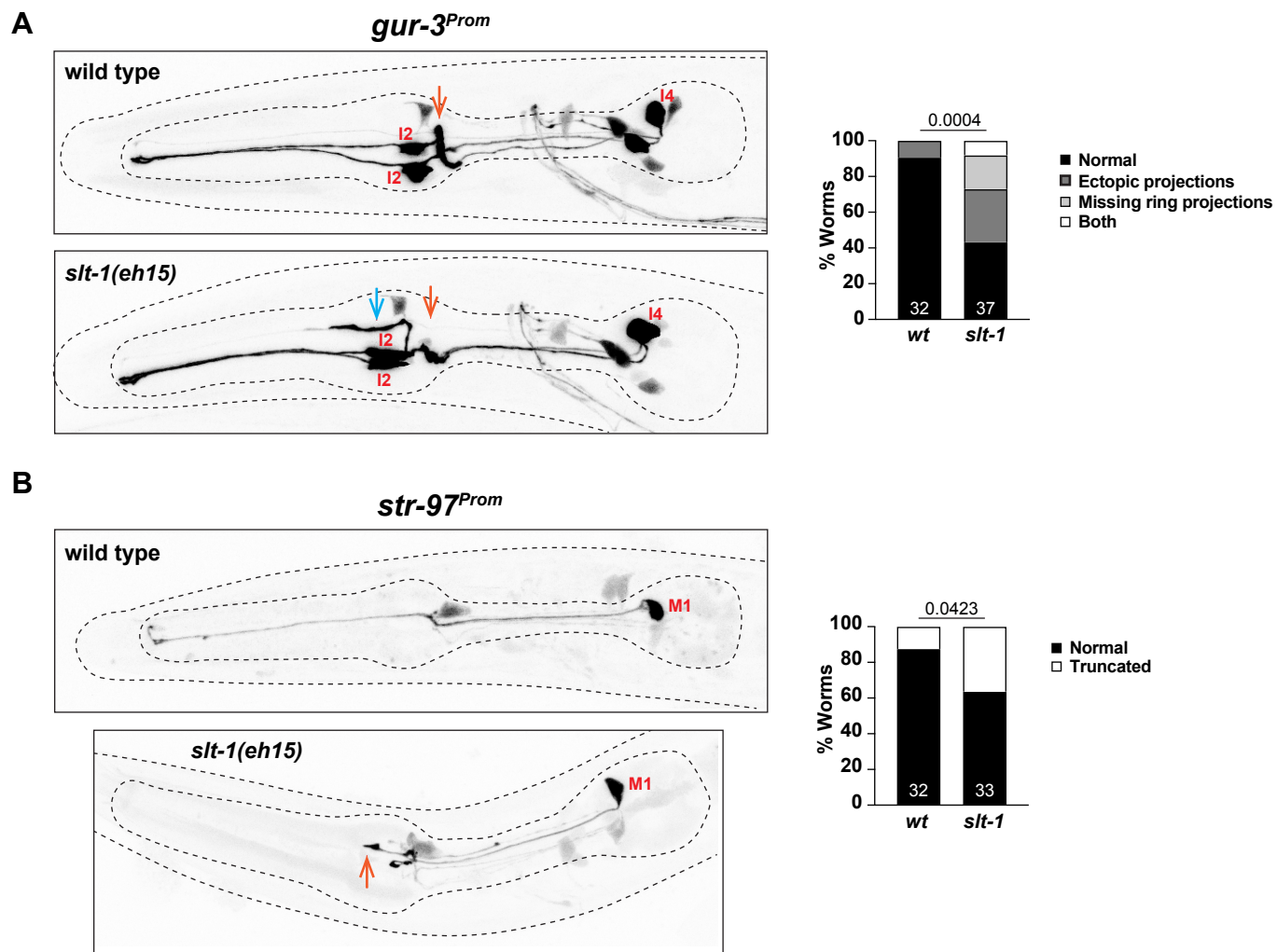
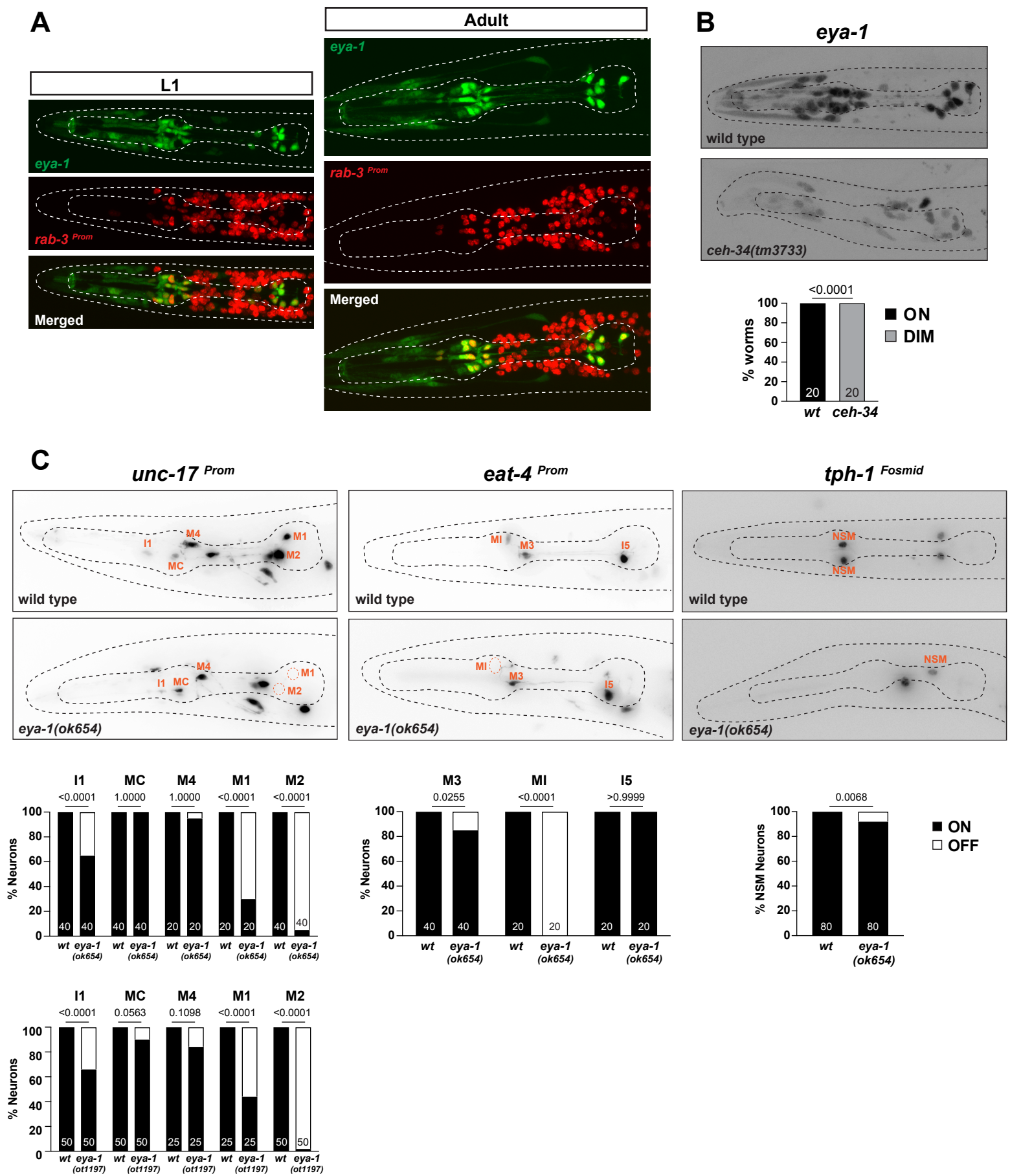


Figure 8 - Supplement 1





**Figure 9**

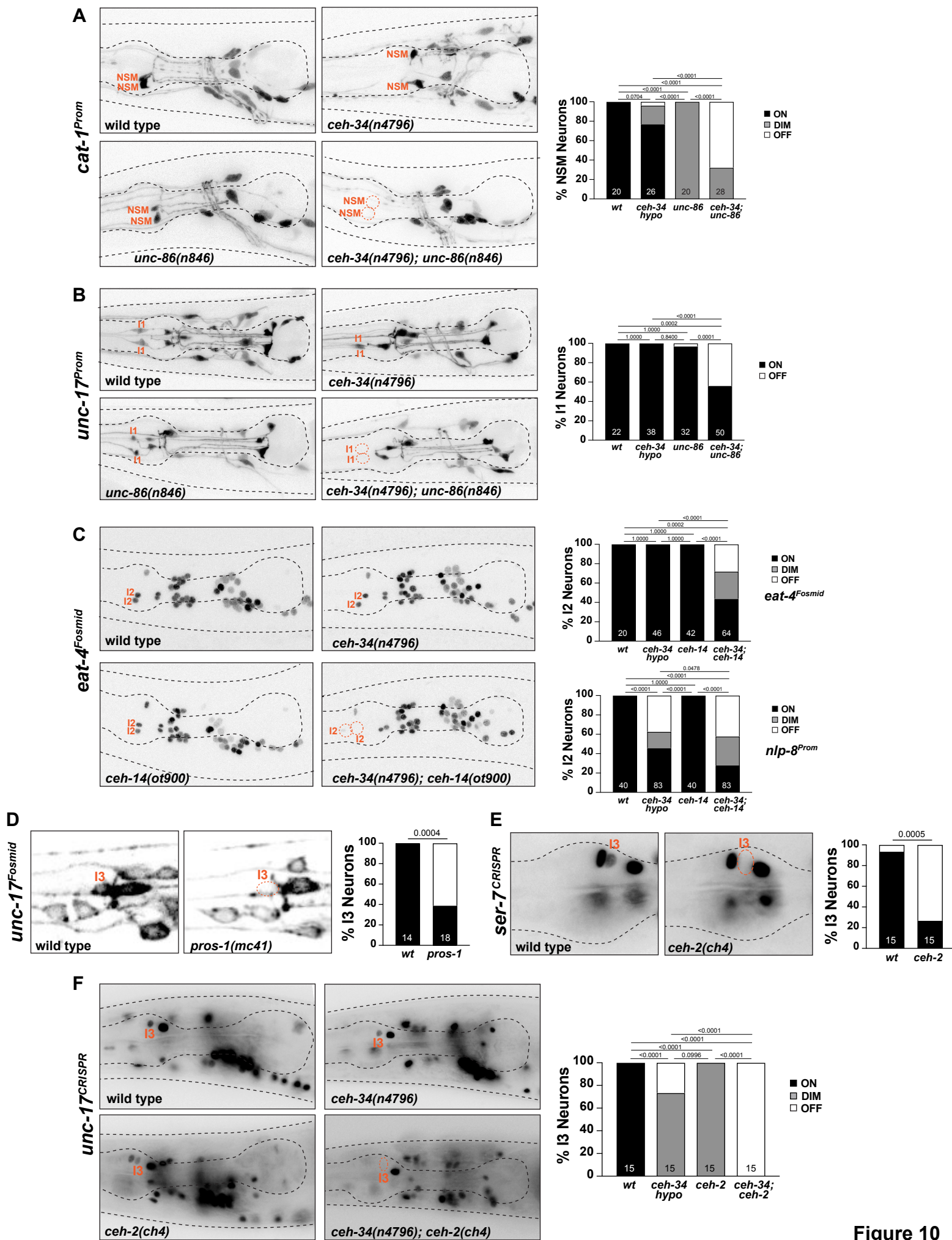


Figure 10

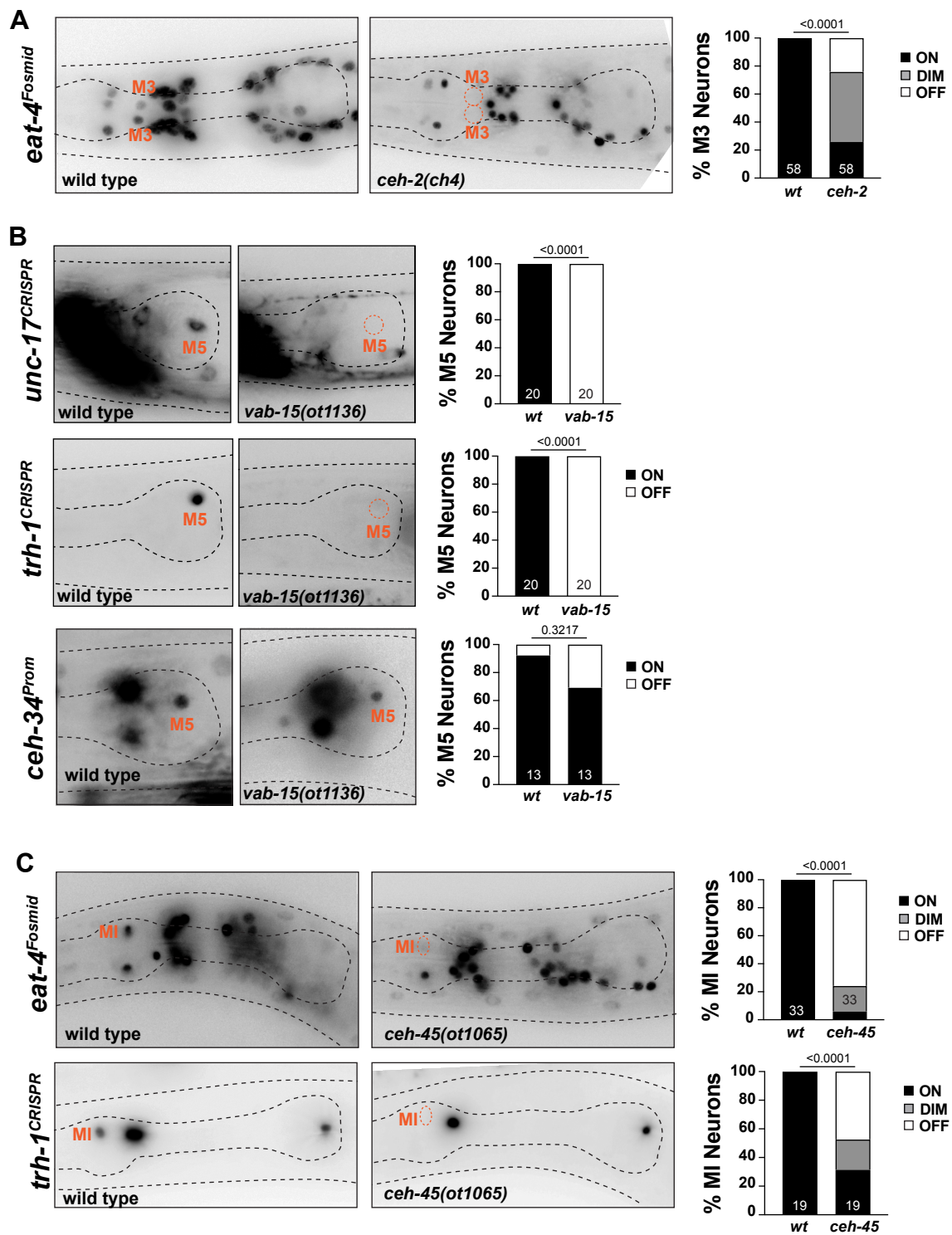


Figure 11

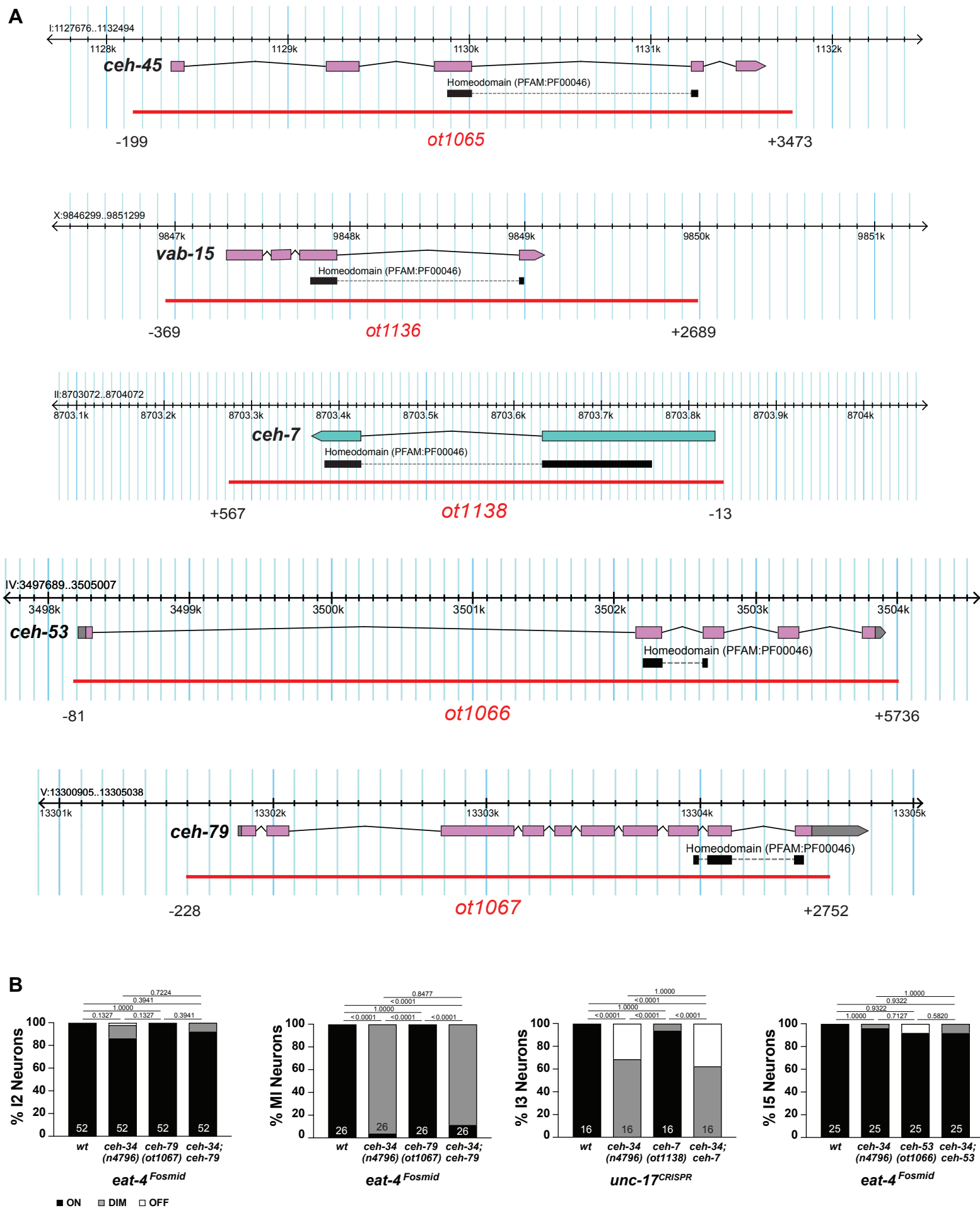


Figure 11 - Supplement 1



*Ex [ehs-1p::ttx-3 genomic, ehs-1p::unc-86 genomic, rol-6(d)]*

*tph-1p::gfp*

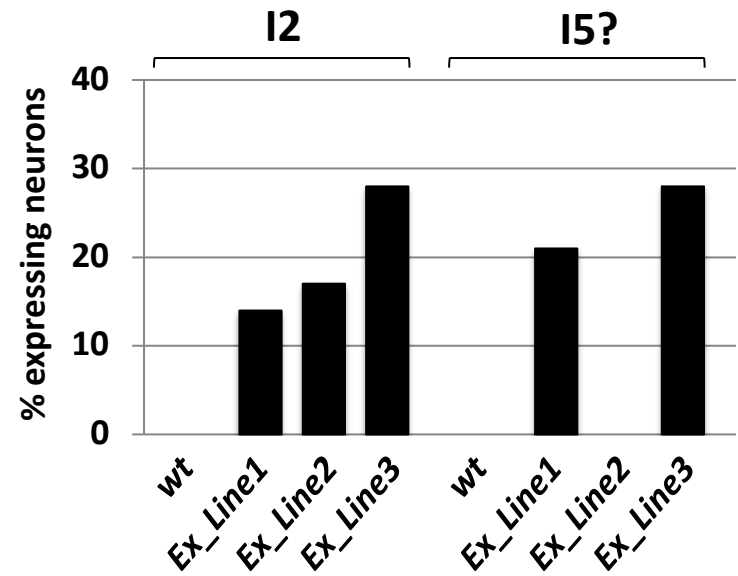
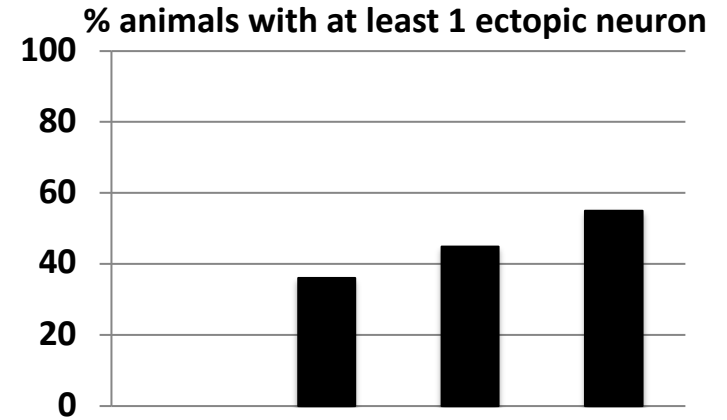
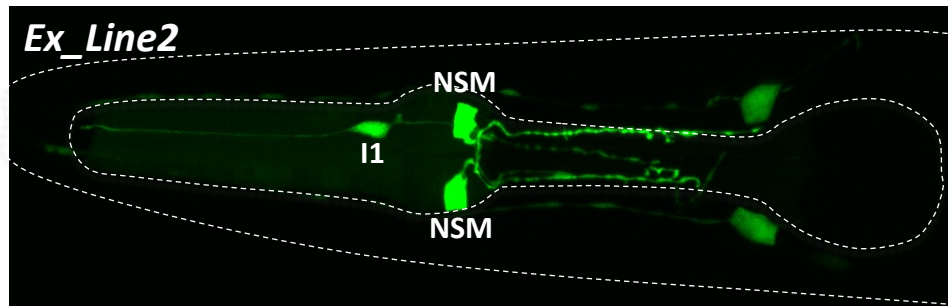
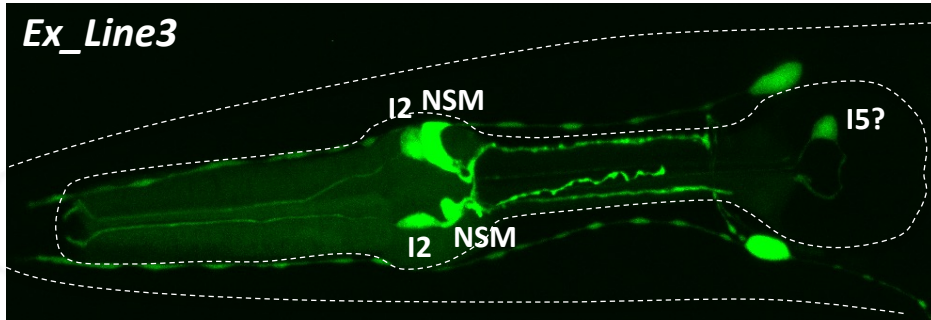
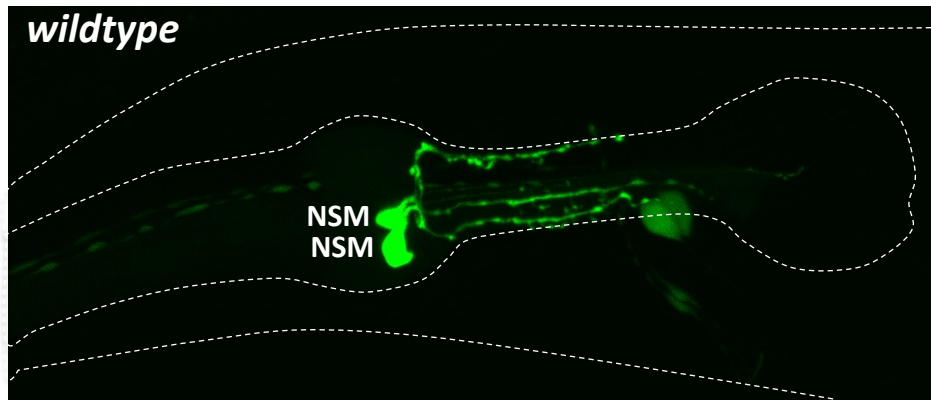


Figure 11 – Supplement 2

homeobox gene		enteric neuron class							
<i>C. elegans</i>	Vertebrate homolog	I1	I2	I3	M3	M4	M5	MI	NSM
<i>ceh-34</i>	SIX1/2								
<i>unc-86</i>	BRN3								
<i>ttx-3</i>	LHX2/9								
<i>ceh-2</i>	EMX1/2								
<i>ceh-14</i>	LHX3/4								
<i>ceh-45</i>	GSC								
<i>ceh-28</i>	NKX2								
<i>zag-1</i>	ZEB1/2								
<i>vab-15</i>	MSX1/2								
<i>pros-1</i>	PROX1/2								

Figure 12